A NUCLEAR MAGNETIC RESONANCE STUDY OF MOLECULAR DISORDER IN THE SOLID STATE OF SOME MEDIUM RING HYDROCARBONS

James R. Brookeman

A Thesis Submitted for the Degree of PhD
at the
University of St Andrews

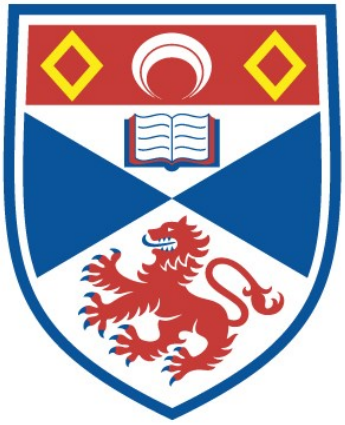

1968

A NUCLEAR MAGNETIC RESONANCE STUDY OF MOLECULAR DISORDER IN THE SOLID STATE OF SOME MEDIUM RING HYDROCARBONS

A Thesis

presented by

James R. Brookeman, B.Sc.

to the

University of St. Andrews

in application for the Degree

of Doctor of Philosophy.

ProQuest LLC.
789 East Eisenhower Parkway
P.O. Box 1346
Ann Arbor, MI 48106 – 1346

DECLARATION

I hereby declare that this thesis has been composed by me, is a record of work done by me, and has not previously been presented for a Higher Degree.

The work was carried out in the research laboratories of the Physics Department, St. Salvator's College, University of St. Andrews, under the supervision of Dr. F. A. Rushworth.

James R. Brookeman

CERTIFICATE

I certify that James R. Brookeman, B.Sc., has spent nine terms at research work in the Physical Laboratory of St. Salvator's College, University of St. Andrews, under my direction, that he has fulfilled the conditions of Ordinance No. 16 (St. Andrews) and that he is qualified to submit the accompanying thesis in application for the Degree of Doctor of Philosophy.

Research Supervisor.

CAREER

In July 1964 I graduated with 2nd class 1st division B.Sc. honours in Physics at St. Salvator's College, University of St. Andrews. In October 1964 with the award of a Science Research Council studentship I was enrolled under general Ordinance 12 as a research student in the Physics Department, University of St. Andrews. In October 1965 I was transferred to Ordinance 16 as a candidate for the degree of Ph.D.

ACKNOWLEDGEMENTS

The author wishes to express his sincere thanks to Dr. F. A. Rushworth for suggesting this investigation and for his advice and help during the course of the work, to Dr. D. P. Tunstall for interesting discussions, to Professor J. F. Allen, F.R.S. for his encouragement and the extensive facilities of the research laboratories, and to the technical staff for their help and co-operation.

Contents

Section		Page
1.	INTRODUCTION	1
2.	THEORY	
	2.1 Introduction	3
	2.2 Resonance line shape of a Rigid Lattice	3
	2.3 Line shape in the presence of motion of the spins	9
	2.4 Spin Lattice Relaxation	17
	2.5 Saturation	20
3.	EXPERIMENTAL APPARATUS AND TECHNIQUES	
	3.1 The N.M.R. Spectrometer	23
	3.2 The Cryostat	27
	3.3 Temperature Control	33
	3.4 Experimental Measurements and Calibrations ..	36
4.	THE EXPERIMENTAL PROGRAMME	42
5.	CYCLOHEPTANE	
	5.1 The Sample	44
	5.2 Physical Data	44
	5.3 Results	47
	5.4 Discussion	48
6.	CYCLO-OCTANE	
	6.1 The Sample	57
	6.2 Physical Data	57
	6.3 Results	60
	6.4 Discussion	62

Contents

Section		Page
7.	CYCLOHEPTATRIENE	
	7.1 The Sample	72
	7.2 Physical Data	73
	7.3 Results	76
	7.4 Discussion	77
8.	SUMMARY OF RESULTS AND COMPARISON WITH THE BEHAVIOUR OF OTHER CYCLIC HYDROCARBONS	92
	APPENDICES	
	REFERENCES	

1. INTRODUCTION

Since the discovery of nuclear magnetic resonance in bulk matter in 1945, n.m.r. studies of molecular motion in solids have provided a powerful insight into the details of molecular reorientation processes that occur in solids. By studying the variation of the n.m.r. parameters as a function of temperature it is usually possible to obtain information regarding such phenomena as solid-solid phase transitions, including the anomalous behaviour of heat capacity associated with order-disorder and co-operative processes, rotational disorder and self-diffusion. In suitable cases it is possible to estimate the origin and magnitude of the potential barriers of the crystalline field which hinder the various reorientation processes.

The cycloalkane ring series $(CH_2)_n$ from cyclopropane n = 3 to cyclohexane n = 6 have all previously been studied in the solid state by n.m.r. (Hoch and Rushworth 1964, Rushworth 1954, Andrew and Eades 1953). The results indicate that considerable molecular mobility occurs in the solid state of these substances and that in general the solid-solid phase transitions detected by heat capacity measurements are associated with the onset of molecular reorientation and in some cases self-diffusion. The current interest in the molecular configuration of the medium ring hydrocarbons, and the extensive study by Finke et al. (1956) of the low temperature thermal properties of cycloheptane n = 7, and cyclooctane n = 8, showing three and two solid-solid phase transitions respectively, prompted an n.m.r.

study of cycloheptane and cyclooctane.

The results of this investigation together with those of a related seven membered ring hydrocarbon 1,3,5 cycloheptatriene C_7H_8 are presented in this thesis, and show that extensive molecular motion exists well below the melting points of all three substances, and information is given regarding the form of the motion in the various crystalline phases.

2. THEORY

2.1 Introduction

Although the discovery of Nuclear Magnetic Resonance in bulk matter is relatively recent there now exist several excellent books and review articles which treat the general theory of nuclear magnetic resonance in bulk matter in detail, e.g. Andrew (1955), Pake (1956), Slichter (1964) and in particular the comprehensive treatment of Abragam (1961). For this reason only the theory necessary for the interpretation of the experiments described in this thesis will be given.

The hydrocarbon samples were studied in polycrystalline form, and measurements were made of the nuclear magnetic resonance of the hydrogen protons, which were effectively the only magnetic nuclei present. Measurements of absorption spectra and spin-lattice relaxation times were made with a wide line continuous wave n.m.r. spectrometer.

2.2 Resonance line-shape of a Rigid Lattice

2.2.1 Basic interaction

When a system such as an array of nuclei with spin I possessing a magnetic moment μ and angular momentum J (where $\gamma = \frac{\mu}{J}$ is the gyromagnetic ratio) is placed in a large external magnetic field H_o, the nuclei will gyroscopically precess with a characteristic frequency $\omega = \gamma H_o$ about the field H_o, and in general the nuclear magnetic resonance spectrum of this system will show a finite linewidth. If

the nuclei are rigidly fixed in a lattice and $I = \frac{1}{2}$, then the linewidth is determined by the dipolar interactions between the nuclei, provided H_o is sufficiently homogeneous and diamagnetic screening effects of the electronic environment are negligible (Andrew 1963).

The Hamiltonian for a system of identical interacting spins in a large external field H_o along the Z axis may be written as the sum of two terms

$$\mathcal{H} = \mathcal{H}_{Zeeman} + \mathcal{H}_{Dipolar}$$

$$= -\gamma\hbar H_o \sum_j I_{j,Z} + \sum_{j>k} \frac{\hbar^2\gamma^2}{r_{jk}^3}\left[\bar{I}_j\cdot\bar{I}_k - 3(\bar{I}_j\cdot\bar{r}_{jk})(\bar{I}_k\cdot\bar{r}_{jk})\right] \qquad (2.1)$$

where r_{jk} is the internuclear distance in a direction $\bar{r}_{jk}$ and I the operator of angular momentum.

The Zeeman term represents the dominant interaction of the nuclei with the external field H_o, and the dipolar term is treated as a small perturbation on this interaction.

A solution of this problem in terms of the eigenvalues of the system is only possible for very simple systems of spins. Pake (1948) has treated the problem of an isolated pair of spins with $I = \frac{1}{2}$, which approximates to the situation in crystal hydrates where the protons of the water molecules exist in relatively isolated pairs. From a first-order perturbation calculation he found that a pair of resonances peaks is predicted with positions in field units given by

$$H = H_o \pm \frac{3}{4} \frac{\gamma\hbar}{r^3} (3\cos^2\theta - 1) \qquad (2.2)$$

where θ is the angle between the internuclear vector r and the applied field H_o. The neglected small interactions between the isolated pairs can be allowed for in a qualitative manner by assuming a gaussian broadening of the two discrete peaks. If the sample is polycrystalline then the isotropic average of the term $(3\cos^2\theta - 1)$ must be taken, since the internuclear vectors will be randomly orientated. For this situation a double humped curve is predicted with a peak separation of $\frac{3}{2} \frac{\gamma\hbar}{r^3}$. This shape of resonance curve was found for the proton resonance spectrum of the water molecules in powdered gypsum $CaSO_4.2H_2O$.

In suitable cases it is possible to use this peak separation for an accurate determination of the inter proton distance r, and if single crystals are used, the orientation of the vector r in the crystal through the term $(3\cos^2\theta - 1)$ may be obtained.

2.2.2 Spin systems greater than two

The perturbation problem for isolated groups of three and four spin systems has been studied by a number of workers Andrew and Bersohn (1950), Waugh et al. (1953), Andrew and Finch (1957), Itoh et al. (1952), Bersohn and Gutowsky (1954) and reasonable agreement with experiment found. However the increasing complexity of the spectra expected for larger groups of interacting nuclei, and the fact that any fine structure is usually smeared out by the interaction

with neighbouring groups, makes further studies in this direction unrewarding.

Fortunately an alternative technique due to Van Vleck (1948) exists whereby the properties of the resonance line shape may be obtained without solving explicitly for the eigenstates of the system. This approach is known as the method of moments.

2.2.3 Method of Moments

Van Vleck (1948) has shown that if the resonance curve is described by a normalized shape function $g(\omega)$ centred at a frequency ω_o, then the n'th moment about the point ω_o can be defined as

$$M_n = \int_{-\infty}^{\infty} (\omega - \omega_o)^n \, g(\omega) d\omega \qquad (2.3)$$

or alternatively expressed in units of magnetic field by the relation $\omega = \gamma H$ and setting $h = H - H_o$

$$M_n = \int_{-\infty}^{\infty} h^n \, g(h) dH \qquad (2.4)$$

By use of the diagonal sum method, Van Vleck obtained rigorous expressions for the second and fourth moments of the resonance curve in terms of simple parameters of the spin system. The most useful of these is the expression for the second moment, which is just the mean square width of the experimental resonance curve about its centre. For a single crystal containing only one species of magnetic nuclei

with spin I, the theoretical expression obtained is

$$M_2 = \frac{3}{2} I(I+1) \frac{\gamma^2 \hbar^2}{N} \sum_{j>k} (1 - 3\cos^2\theta_{jk})^2 . r_{jk}^{-6} \qquad (2.5)$$

where r_{jk} is the distance between nuclei j and k

θ_{jk} is the angle r_{jk} makes with the applied field

N is the number of nuclei over which the sum is taken, it is usually sufficient to consider only the nuclei within a short distance since the dependence on the term r_{jk}^{-6} causes the summation to converge rapidly. This expression has been given ample experimental verification, and in certain cases has provided useful information on the structure of the crystals studied; in particular the positions of Hydrogen atoms, a feature often absent from X-ray and electron diffraction structure determinations.

For a polycrystalline sample all values of θ_{jk} are equally probable and so the term $(1 - 3\cos^2\theta_{jk})^2$ must be replaced by its isotropic average, $\frac{4}{5}$.

$$M_2 = \frac{6}{5} I(I+1) \frac{\gamma^2 \hbar^2}{N} \sum_{j>k} r_{jk}^{-6} \qquad (2.6)$$

The calculation of the theoretical second moment for a given sample is conveniently separated into two contributions, the intramolecular and the inter-molecular. The intra contribution depends on the molecular structure, and only includes interactions between

nuclei within the molecule. The inter contribution is determined by the crystal structure and corresponds to interactions between nuclei in neighbouring molecules. Various approximation methods have been developed to reduce the amount of computation required for calculating the inter contribution. If the crystal structure is known, it may be separated into two terms; an exact calculation for all nuclei up to a cut off radius L, and a term obtained from an integral over all the remaining nuclei, assumed to exist as a continuous distribution beyond L.

$$M_2 = 358.1 \sum_{j>k}^{r<L} r_{jk}^{-6} + 358.1 \ (4\pi N_p / 3L^3 V) \qquad 2.7$$

where N_p is the number of protons per unit cell

V is the volume of the unit cell. (L^3, V in cubic angstroms).

If the crystal structure is unknown the following methods can be used. A comparison can be made with molecules having similar proton configurations whose n.m.r. results are known. Andrew and Eades (1953) have also suggested that the lattice energy may serve as a semi-quantitative basis for comparison of inter contributions, the lattice energy taken as the sum of the heats of transition, fusion, and vapourisation.

Finally Smith (1965) has suggested that if in the second term of 2.7, L is taken as equal to the maximum proton radius R from the

centre of the molecule, the inter contribution may be written as,

$$M_2^{inter} \simeq 358.1\ (4\pi N_p/3R^3V)$$

$$= 358.1\ (4\pi N_o\rho/3R^3M) \qquad 2.8$$

where N_o is the number of protons per molecule

ρ is the density in g/cc

and M is the molecular weight in grams x 10^{24}

Since the second moment is the mean square width of the experimental absorption curve, significant contributions come from the wings of the curve, where the signal height may be comparable to the noise level of the spectrometer. For this reason it is important that the signal to noise ratio should always be as high as possible.

2.3 Line shape in the presence of motion of the spins

2.3.1 Variation of Line width

If at any temperature the nuclei are not rigidly fixed in the crystal lattice, then any random relative motion that occurs will modulate the dipolar interaction between the nuclear spins. The usual model considered for the dynamics of crystals whose molecules, like those considered in this thesis, possess orientational freedom is due to Frenkel (1935). This model, recently extended by Darmon and Brot (1967), assumes that each molecule spends most of its time in one of a set of allowed orientations in the crystalline field of

its nearest neighbours. Rapid jumps between allowed orientations are caused by thermal fluctuations in the lattice energy, which enable the molecules to obtain sufficient energy to overcome the periodic potential barriers of the local crystalline field. At a given lattice temperature there will be a mean frequency of reorientation ν, with an associated correlation time between jumps of $\tau_c = 1/2\pi\nu$. In general the rate at which the molecules reorientate will increase with temperature in a manner described by the Arhennius relation:

$$\nu = \nu_o \exp(-E/RT) \qquad 2.9$$

where E is the activation energy for the reorientation process

R is the gas constant, and T the absolute temperature.

The theory of Bloembergen, Purcell and Pound (1948, hereafter referred to as BPP) relating the line width of the resonance curve and the correlation frequency has been modified by Gutowsky and Pake (1950) and Kubo and Tomita (1954). This theory shows that when the frequency of reorientation becomes comparable with the line width expressed in frequency units i.e. $\nu \leq 10^4$-10^5 c/s, there will be a reduction in the observed line width described by the relation:

$$\tau_c = \frac{1}{2\pi\nu} = \frac{\tan\left[\pi(\delta H^2 - B^2)/2(c^2 - B^2)\right]}{\alpha\ \gamma\ \delta H} \qquad 2.10$$

where δH is the line width (for definition see 3.4.2) of the resonance

curve at a temperature T.

C is the rigid lattice line width i.e. for $\gamma \delta H \gg 2\pi\nu$

B is the line width for $2\pi\nu \quad \gamma \delta H$

$\alpha = (8 \ln 2)^{-1}$

By following the variation of the line width with temperature, it is possible with use of 2.9 and 2.10 to obtain a value for the activation energy E for a reorientation process causing a reduction in the line width.

Waugh and Fedin (1963) have approached the same problem from a different aspect and have obtained the approximate formula

$$E \leq 2.5 \, KT_o \log \frac{n}{C - B} \cdot \sqrt{\frac{kT_o}{2I}} \qquad 2.11$$

where T_o is the temperature where the line width begins to narrow

k is the Boltzmann factor

n is the number of orientations available to the molecule

and I is the molecule's moment of inertia.

For qualitative calculations they suggest 2.11 may be simplified to

$$E \leq 37 \, T_o \, (^\circ K) \qquad 2.12$$

Although the line width has proved a useful parameter for studying many aspects of molecular motion, it does not have such a firm theoretical relationship to the details of the spin system as does the second moment. For this reason it is usually necessary to

complement line width measurements with those of second moments, particularly the plateau values on either side of a transition region. In suitable cases it is possible to use these values to positively identify the form of the reorientation process.

2.3.2 Variation of Second Moment

It can be shown on general theoretical grounds that the second moment should be invariant with respect to motion of the magnetic nuclei. However the observed experimental reductions in the second moment can be explained by the results of an experiment by Andrew, Bradbury and Eades (1958), where a single crystal of sodium chloride was macroscopically rotated about a suitable axis. The observed spectrum consisted of a narrowed central curve flanked by sidebands at integral multiples of the rotation rate. When the sidebands were included in the second moment, its value was found to be the same as for the stationary crystal.

In the case of the random molecular motion in a solid, these sidebands are distributed over a range of frequencies, and the average intensity of the sidebands is so small that it is lost in the noise level of the spectrometer, and so only the narrowed central curve contributes to the experimentally observed second moment.

The second moment of the narrowed curve can be related to the rigid lattice expression 2.5 by replacing the terms $(1 - 3\cos^2\theta_{jk})$ and r_{jk}^{-3} by their averages over the molecular motion modulating the

dipolar interaction. The various types of motion that modify the observed second moment are considered in the following sections.

Lattice vibrations and torsional oscillations

In general at very low temperatures one might expect that the only motion of the nuclei remaining is that due to lattice vibrations. Deeley and Richards (1954) have shown that these vibrations, which modify the term r_{jk}^{-3}, have a negligible effect on the second moment (a 10% change in r_{jk} gives a 3% change in the second moment). Pedersen (1964) however has pointed out that this effect must be considered in the accurate determination of interproton distances by the Pake doublet peak separation.

For molecules with small moments of inertia Andrew (1950) and Das (1957) have shown that torsional oscillations can cause an appreciable reduction in the second moment. The molecules considered in this thesis are all quite large, and so a reduction due to this type of motion is not to be expected. However, because of the very flexible nature of these large ring compounds it is possible that certain segments of the rings may be affected.

Molecular reorientation

A molecule possessing an n-fold symmetry axis may reorientate about that axis. The motion of the molecule will usually be restricted by a potential barrier. Clough (1968) has shown that the narrowed spectrum observed at very low temperatures with molecules containing methyl groups can be explained by the coherent zero-point motion of

the methyl group about their three-fold symmetry axis. At higher temperatures the increased lattice vibrations break down the coherence of the motion, and the random reorientation model of Frenkel is then applicable. Gutowsky and Pake (1950) have shown that provided this reorientation is sufficiently rapid, the effect on the intra-molecular second moment for a polycrystalline sample can be calculated by multiplying each term in the summation of 2.6 by the reduction factor

$$\rho_3 = (3 \cos^2 \gamma_{jk} - 1)^2/4 \qquad 2.13$$

where γ_{jk} is the angle the internuclear vector makes with the axis of reorientation. This reduction factor applies for both reorientation about an n-fold symmetry axis when $n \geq 3$ and for classical rotation.

In the case of reorientation about a two-fold axis the reduction factor is, (Eades, 1952)

$$\rho_2 = (1 - 3 \sin^2 \gamma_{jk} \cos^2 \gamma_{jk}) \qquad 2.14$$

These reduction factors are only applicable for the intra-molecular contribution to the second moment, where for a rigid molecule r_{jk} is constant. To calculate the effect of this motion on the inter-molecular contribution, or the intra for a non-rigid molecule, it is necessary to use the more general expression of Andrew and Eades (1953), which considers the variation of both θ_{jk} and r_{jk} (see

Appendix A6).

Hendrickson (1964) has suggested that because of the flexible nature of the large ring cycloalkanes it is possible for pseudo-rotation of the molecule to occur. This may be described as the concerted change of position of each ring atom so that every atom sequentially takes up each of the possible ring positions. Anet and Jacques (1966) have examined the high resolution n.m.r. spectra of dilute solutions of cyclo-octane at low temperatures, and report that the simple spectra they obtain is consistent with rapid pseudo-rotation of the molecule. Similar studies of cycloheptatriene by Anet (1964) suggest that rapid ring inversion is responsible for the observed equivalence of the methylene protons.

When motion occurs about more than one molecular axis, then each term of 2.6 is multiplied by a combination of reduction factors. If the resultant motion sufficiently approximates to the situation of quasi-isotropic reorientation, i.e. all orientations of the molecule equally probable, then the intra-molecular second moment will be effectively reduced to zero. The effect on the inter-molecular part will be less drastic, a calculation originally conceived as an approximation by Andrew and Eades (1953) and subsequently shown to be exact for quasi-isotropic reorientation by Dimitrieva and Moskalev (1964), gives the following expression for the second moment

$$M_2 = 358.1\ N_o \sum_{i=1} N_i\ R_i^{-6} \qquad 2.15$$

where N_o is the number of protons per molecule

N_i is the number of i'th nearest neighbours

R_i is the centre to centre distance (in angstroms) between a molecule and its i'th nearest neighbour.

This expression is equivalent to concentrating all the protons at their molecular centres. The summation $\sum N_i R_i^{-6}$ is known for various regular lattice structures, such as b.c.c., f.c.c. Gutowsky and McGarvey (1952), so that provided the crystal unit cell constants are known the calculation is relatively simple. An example of a Fortran computer programme to calculate this summation for the unit cell of cyclo-octane is given in Appendix A12. If the crystal structure is not known then various approximate calculations are possible, Smith (1965).

Self Diffusion

In a number of experimental situations, it is found that the measured value of the second moment is smaller by more than an order of magnitude than the value given by equation 2.15. Since the molecules have now obtained all their rotational degrees of freedom, for further averaging to occur, it is necessary to postulate that they now obtain translational freedom as well. This suggestion for molecular solids has received support from the radioactive tracer studies of Hood and Sherwood (1966), which show conclusively that self-diffusion does occur in these cases, probably by a vacancy jump mechanism. Further quantitive support has come from the n.m.r.

experiments of Resing et al. (1968), employing the ultra-slow motion technique of Allion and Slichter (1965), to measure $T_{1\rho}$ the relaxation time in the rotating frame for solid adamantane, caused by self-diffusion of the molecules.

2.4 Spin Lattice Relaxation

In an applied magnetic field H_o each nucleus of spin I in a weakly coupled array will occupy one of $2I + 1$ energy levels, corresponding to different orientations of the nuclear spins to the applied field. For protons with $I = \frac{1}{2}$ the relative population of the two levels is given by the Boltzmann factor $\exp(-\gamma\hbar H_o/kT_s)$, where T_s may be thought of as a characteristic temperature of the spin system. If there exists a coupling between the spin system and the lattice, then at equilibrium, T_s will correspond to the lattice temperature.

Should the relative populations for any reason be disturbed, such as irradiation with a radio frequency field satisfying the Larmor condition $\omega_o = \gamma H_o$, then the rate at which the spin system relaxes to the lattice temperature is called the spin lattice relaxation time T_1. If the bulk alignment of the nuclear spins at equilibrium with the lattice corresponds to a magnetisation M_o, then after the disturbance, the magnetisation will recover exponentially at a rate described by the equation

$$M_t = M_o\ (1 - \exp(-t/T_1)) \qquad 2.16$$

This rate is determined by the strength of the coupling between the

spins and the lattice, so that a measurement of T_1 provides information about this coupling.

In non-metallic fluids the coupling is the Brownian motion of the molecules which causes fluctuations in the dipolar interaction between the spins. These fluctuations have components at the Larmor frequency ω_o, which induce transitions between the energy levels. The theory for this mechanism was first developed by Bloembergen, Purcell, and Pound (BPP, 1948) who employed the method of random functions, it has since been modified by Kubo and Tomita (1954) and Solomon (1955). This theory was originally developed to describe the relaxation contribution of the interaction between the proton pairs in the H_2O molecule. However the treatment has been found to apply to the molecular motion in many solids, where the dominant contribution to the relaxation is provided by the modulation of the interaction between a pair or other small groups of nuclei.

The BPP theory gives an expression of the form

$$\frac{1}{T_1} = C_1\left[\frac{\tau_c}{1 + \omega_o^2\tau_c^2} + \frac{4\tau_c}{1 + 4\omega_o^2\tau_c^2}\right] \qquad 2.17$$

where C_1 is a constant characteristic of the form of the interaction which for proton pairs is

$$C_1 = \frac{2}{5}\gamma^4 h^2 I(I+1)\sum_j b_j^{-6}$$

and b_j is the inter proton separation. The correlation time τ_c has been discussed in 2.3, and is the average time between significant changes in the nuclear positions. Besides lattice fluctuations at ω_o, equation 2.17 includes contributions at $2\omega_o$, since it is possible for suitable motions of one nucleus at $2\omega_o$ to reverse the sense of the previously ineffective circularly polarised fluctuating field experienced by a neighbouring nucleus. In this situation a double transition occurs.

From equation 2.17 three cases may be distinguished:

(1) For slow motion, $\omega_o^2\tau_c^2 \gg 1$ $\quad \frac{1}{T_1} = \frac{2C_1}{\omega_o^2\tau_c}$

(2) For rapid motion, $\omega_o^2\tau_c^2 \ll 1$ $\quad \frac{1}{T_1} = 5C_1\tau_c$

(3) and a minimum value for T_1 $\quad \frac{1}{T_1} = 1.42C_1/\omega_o$
when $\omega_o\tau_c \doteq 0.62$

It is found experimentally that a plot of the logarithm of T_1 versus reciprocal temperature $1/T^\circ K$ in many cases yields a straight line for points removed from the minimum. This corresponds to the similar situation described in section 2.3.1 for the line width analysis, and supports the suggestion that the correlation time depends on temperature as

$$\tau_c = \tau_o \exp(E/RT)$$

enabling the activation energy E for the motion to be determined. If a minimum value of T_1 is observed then it is possible to draw conclusions regarding the value of C_1, and the nature of the interaction causing the relaxation.

At low temperatures the presence of small traces of paramagnetic impurity can provide the dominant relaxation mechanism, and a similar situation can prevail in organic solids at higher temperatures Sandu et al. (1960), due to dissolved oxygen. For this reason it is important to degas samples used for relaxation studies, see Appendix B for details.

2.5 Saturation

In the previous sections the absorption of radiofrequency energy by a system of spins situated in a large external field H_o has been introduced as a source of information regarding the nature of the environment of the spins. The possible disturbance of this probing r.f. field on the spin system has so far been assumed to be negligible. The circumstances under which this assumption is valid will now be discussed.

It has already been mentioned that in the simple case of a weakly coupled array of N spins each with $I = \frac{1}{2}$, fluctuations due to the molecular motions can induce transitions between the two spin states, and that this provides a thermal coupling between the spins and the lattice. Since at ordinary temperatures the heat capacity

of the lattice is very much greater than that of the spin system, this coupling will tend to keep the two systems at the common temperature of the lattice. The application of a radio frequency field satisfying the Larmor condition $\omega_o = \gamma H_o$ will also induce transitions at a certain rate W which will tend to "heat up" the spin system. The combined effect of the two processes will give an absorption of r.f. energy $\delta E/\delta t$ described by the equation

$$\delta E/\delta t = N h\omega_o W(1 + 2WT_1)^{-1} \qquad 2.18$$

where the rate W is proportional to the square of the amplitude of the r.f. field H_1. Two cases can be distinguished:

(1) for small H_1, $\delta E/\delta t \propto W$

(2) for large H_1, $\delta E/\delta t \propto 1/T_1$

In the latter case when T_1 is long, the absorption rate can be very small, and this situation is termed saturation.

Provided H_1 is small the effect of a finite r.f. field on the absorption line shape is negligible, but it is important to test for the condition $\delta E/\delta t \propto W$ before recording the absorption spectra.

The effect on the measurement of the relaxation time T_1 is to cause the magnetisation to recover with an apparent time constant τ where

$$\tau = T_1 Z = T_1(1 + 2WT_1)^{-1} \qquad 2.19$$

so that provided $2WT_1 \ll 1$, $T_1 \simeq \tau$.

Although the above theory strictly only applies to systems with a weak coupling between the spins such as occurs in liquids, its general conclusions have been found to apply to many situations in solids, particularly when molecular motion is present. This will be true for the substances studied in this work, where both reorientation and self diffusion have been found to occur in the solid state.

In general of course in solids there exists a tight coupling between the spins, and if one wishes to inquire into the details of the saturation behaviour of such a system, the above simple picture is no longer adequate. Redfield (1955) has introduced the concept of a spin temperature in the rotating frame to describe this situation. However since the saturation behaviour was not a topic of interest in the present work, the wider ramifications of this more general approach will not be discussed.

N. M. R. SPECTROMETER

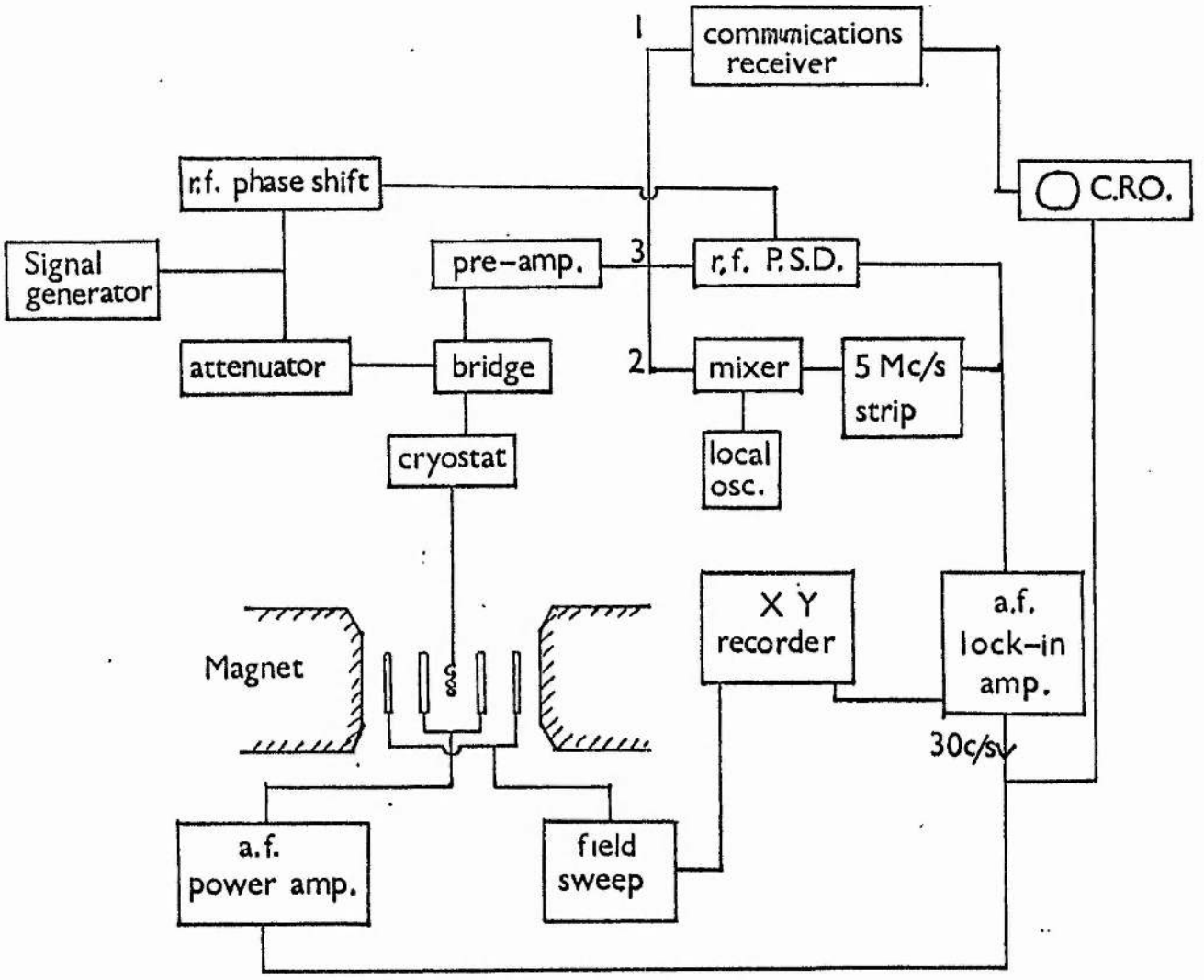

fig. 1

3. Experimental Apparatus and Techniques

3.1 The N.M.R. Spectrometer

The proton magnetic resonance experiments were performed using a broad line continuous wave spectrometer, incorporating a single coil radio frequency bridge system. A block diagram of the equipment is given in figure 1. To improve the signal to noise ratio, the conventional procedure of audio frequency field modulation with subsequent phase sensitive detection was employed, thus the derivative of the n.m.r. absorption curve was plotted on the X-Y recorder.

Two magnets were used with this spectrometer, a permanent magnet designed for broad line n.m.r. work and described by Andrew and Rushworth (1955), and a Mullard electromagnet. The permanent magnet had a field of 5,300 gauss, a pole face diameter of 8 inches with a pole gap of 2 inches, and the field homogeneity was approximately 0.25 gauss/cm^3. The Mullard electromagnet could be operated with fields up to 12,000 gauss, had a pole face diameter of 12 inches with a pole gap of 2.5 inches, and the field homogeneity at 5,300 gauss was approximately 0.1 gauss/cm^3. Both magnets had an electronic linear field sweep with provision for driving the X axis of the X-Y recorder. Modulation of both magnet fields by several gauss in the range 20 to 300 c/s was accomplished with modulation coils wound on formers attached to the pole faces. A low distortion audio frequency 25 watt power amplifier (Radford MA25) supplied the

modulation current to these coils.

The signal generator was a Schlumberger type D01001, with a quartz crystal locked output frequency, stable to 1 part in 10^8, and capable of delivering 1 volt rms into 50 ohms in the range 50 kc/s to 50 Mc/s. The proton resonance frequency for a field of 5,300 gauss is 22.6 Mc/s, and this frequency was fed from the signal generator via a calibrated 50 ohm attenuator to the r.f. bridge. This was of the twin-T type (Anderson, 1949) and was housed in a rigid 1/16" gauge copper box. The values of the components within the bridge were adjusted for optimum signal to noise ratio in the manner suggested by Gheorghiu and Valeriu (1962). The twin-T bridge has the advantage of orthogonality of adjustment for resistive and reactive balance, and in practice was adjusted for exact phase balance and approximately 40 db down in amplitude balance so that the absorption rather than the dispersion curve could be recorded. The sample coil is located in the tail of the cryostat, and a short length of low loss coaxial cable connected the bridge to the cryostat.

A low noise pre-amplifier provided the first stage of radio frequency amplification. For some of the early experiments a cascode circuit employing a Mullard E88CC special quality twin-triode was used (Hoch 1963). This pre-amplifier had a narrow bandwidth (1 Mc/s approx.) and high gain, and gave a measured noise factor of 1.5 db when suitably matched to the bridge. The tuning

of the pre-amplifier was rather temperature dependent, and this unit was later replaced by a Decca Radar solid state pre-amplifier. This had a bandwidth of 3 Mc/s, a 63 db gain, and a noise factor of 3 db with an input impedance of 50 ohms and negligible temperature variation of gain.

As shown in figure 1 three systems were used for the demodulation of the radio-frequency signal. System 1 was a conventional communications receiver, an Eddystone "680" model; it had a bandwidth of 10 kc/s and was employed for the oscilloscope display of narrow lines for relaxation studies, see section 3.4.3. Well smoothed external H.T. and L.T. power supplies were used to run both the cascode pre-amplifier and the communications receiver to avoid any spurious 50 c/s modulation of the r.f. carrier. This precaution also applied to the power units for the solid state amplifiers.

Unfortunately the tuning of the communications receiver was also prone to temperature drift, and so the receiver was unsuitable for use while recording the derivatives of the broad lines, since it is necessary to sweep very slowly (~10 mins.) through a broad line resonance if full advantage is to be taken of the integrating characteristics of the a.f. phase sensitive detector output. However, Robinson (1962) has shown that provided an amplifying system does not pass harmonics of the carrier frequency, the effective noise bandwidth after phase sensitive detection is determined only by the time constant of the integrating circuit following the phase sensitive

detector. For this reason systems 2 and 3 were used when tracing out the derivative curves on the X-Y recorder, and for relaxation studies by the direct recovery method, see section 3.4.3. Both systems had bandwidths greater than 3 Mc/s, and negligible temperature drift of gain.

System 2 comprises a Hatfield MD3 wide band mixer, 17.6 Mc/s local oscillator, and Decca Radar solid state 5 Mc/s i.f. strip with a detector output. These units were part of a variable frequency n.m.r. receiver system that was designed to operate at 22.6 Mc/s, 35 Mc/s and 45 Mc/s. The majority of recordings of the absorption derivative lineshapes were made with system 2, feeding the output into the a.f. phase detector, here its gain stability was a decided advantage over system 1. Although the wide bandwidth, 3.2 Mc/s, meant that it was not as suitable as system 1 for oscilloscope display, this was no disadvantage when followed by the a.f. phase sensitive detector as Robinson's analysis shows. The extra noise components were never sufficient to overload the a.f. stages, a situation where a narrower bandwidth would have been necessary.

System 3 was a simplified version of 2 and was only available for some of the later experiments, when it was used to check lineshapes at particular temperatures. It consists of a radio frequency phase shift unit and Hatfield MD3 wide band mixer, with the internal connections suitably modified to operate as a radio frequency phase sensitive detector. This arrangement is similar to the receiver systems

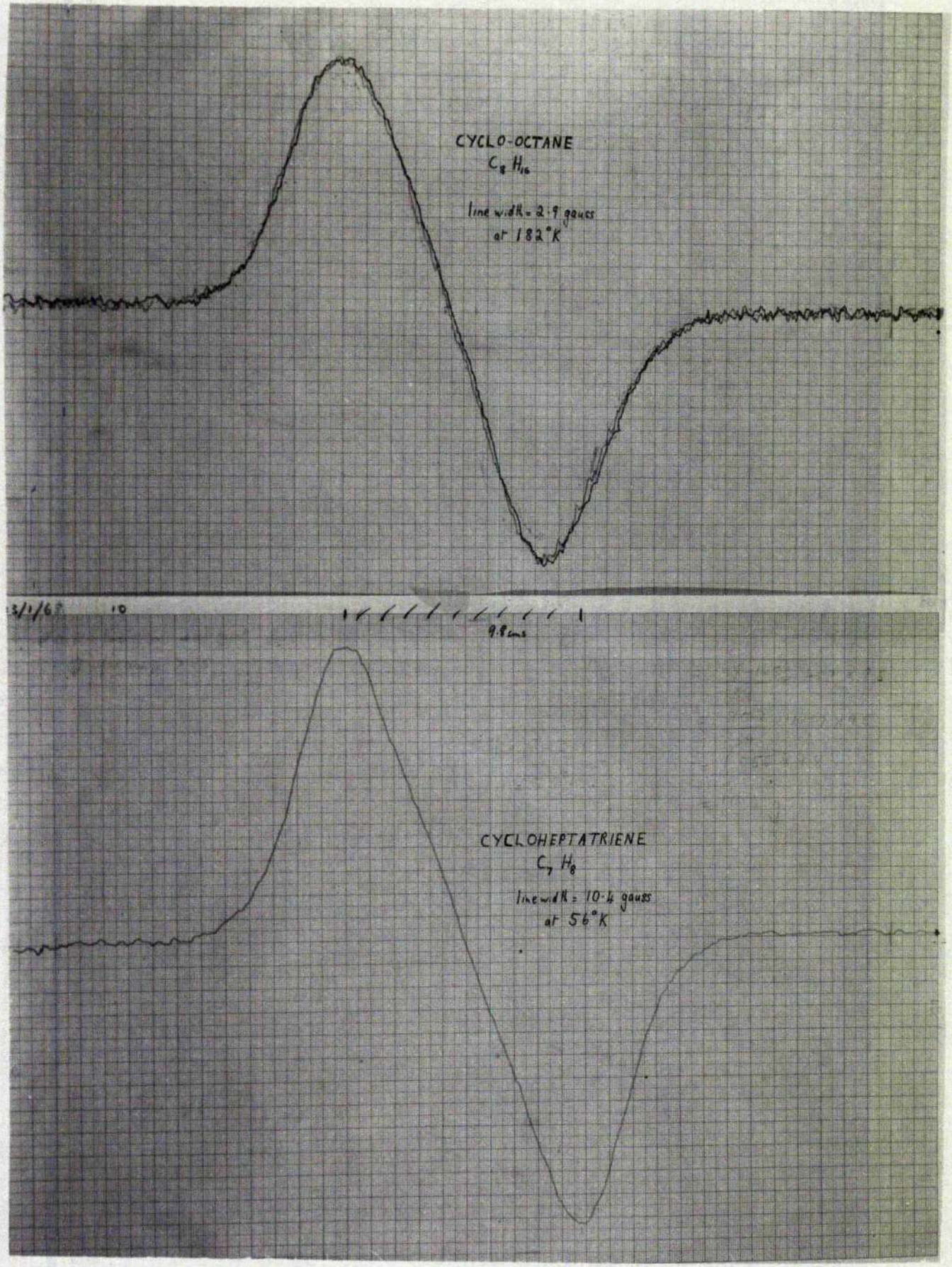
CYCLO-OCTANE
$C_8 H_{16}$
line width = 2·9 gauss
at 182°K
3/1/68
10
9.8 cms
CYCLOHEPTATRIENE
$C_7 H_8$
line width = 10·4 gauss
at 56°K

fig 2

described by Richards and White (1962) and Hansen, Grimes and Libchaber (1967). Its performance when used with the a.f. units for recording the derivative curves was comparable with system 2, but it had the advantage of being composed of fewer units.

When recording the derivative curves the field was modulated at a frequency of 30 c/s, derived from the internal oscillator of a Princeton Applied Research JB-4 lock-in amplifier. This amplifier also provided the narrow band a.f. amplifier with a $Q \simeq 25$, the a.f. phase sensitive detector, and phase shifter. The DC output of the JB-4, available through a time constant network with switch selectable values of .001, .01, 1, 3, 10 secs, was fed on to the Y axis of a Varian F80 X-Y recorder, with the X axis driven by the field sweep unit. The equivalent noise bandwidth of the JB-4 with a 10 sec time constant is quoted as 0.024 c/s, and it was found in practice to give satisfactory performance provided that careful attention was paid to the alignment procedure given in the manual.

The overall performance of the spectrometer was satisfactory with adequate signal-to-noise ratio for all the samples studied, and the fact that the spectrometer was situated in an electrically screened room with a filtered AC supply reduced outside interference to a minimum. An example of the absorption derivative lineshapes obtained is given in figure 2.

3.2 Liquid Nitrogen Cryostat

The basic design of this cryostat is similar to previous nitrogen

CRYOSTAT

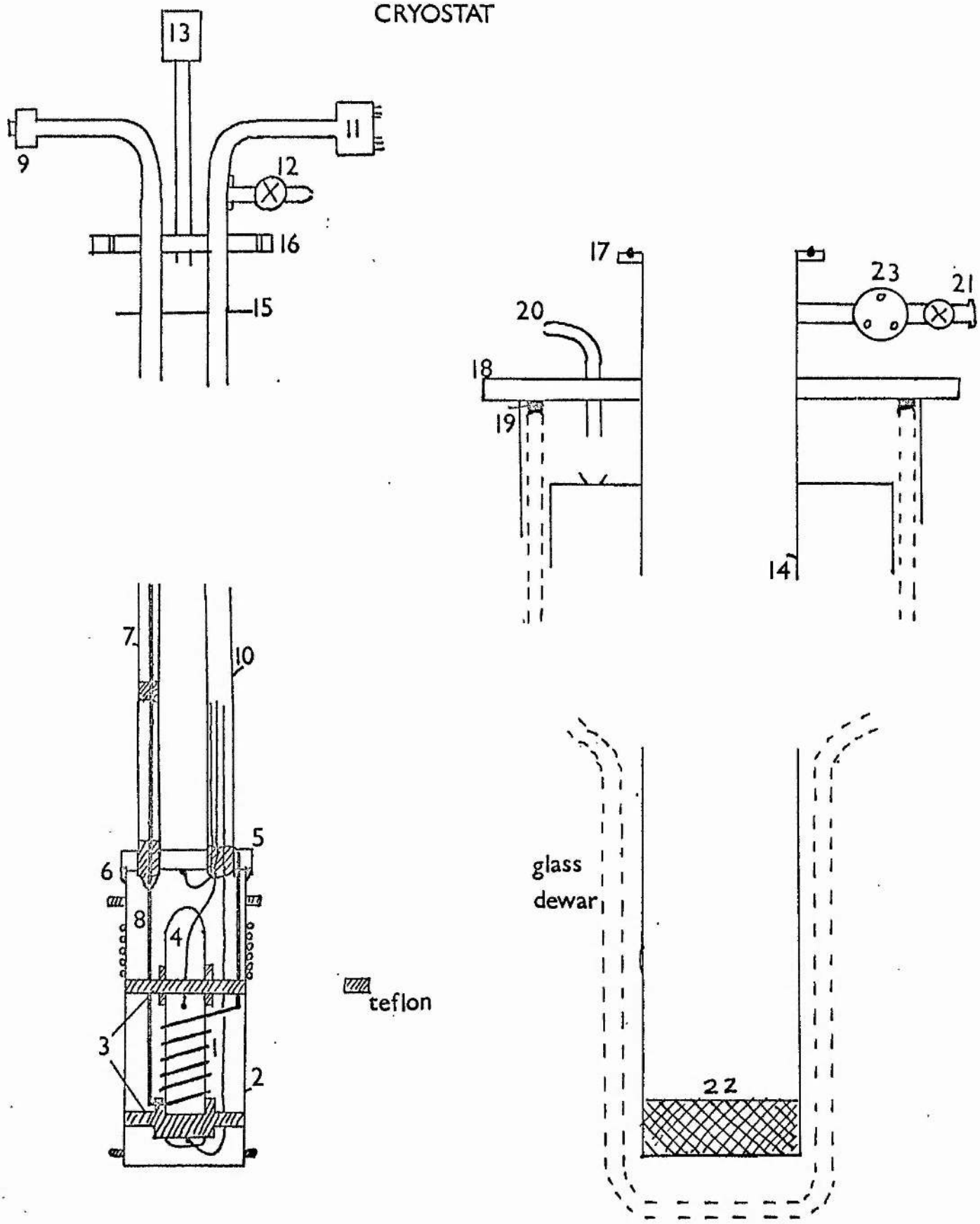

fig 3

cryostats used in this laboratory Hoch (1963); a schematic diagram of the cryostat is shown in figure 3 and a photograph in figure 4. Four improvements were incorporated which were considered important. These were:-

1. The elimination of temperature gradients greater than .1 deg over the length of the sample tube by surrounding the sample area at all times with a helium exchange gas at a pressure of approximately 10 cms Hg.

2. Rigid construction of all the radio frequency components within the cryostat, and in particular the use of electrolytically copper plated 1 mm stainless steel tubing as the inner conductor of the coaxial r.f. down feed. The use of thin walled hollow tubing has the advantage of reducing the heat leak to the sample coil, while at the same time not increasing the resistance of the conductor, since the current at 22 Mc/s is restricted to the surface of the conductor by the "skin effect".

3. The use of a zeolite sorption pump consisting of Union Carbide 13X molecular sieve pellets situated at the lower end of the tail of the cryostat. This maintained a vacuum better than 10^{-5} torr in a metal walled vacuum space for a period of up to 3 weeks, without the use of any external pumps.

4. A facility for pumping on the liquid nitrogen to obtain sample temperatures down to~50°K.

Referring to figure 3 the details of the cryostat are as follows:

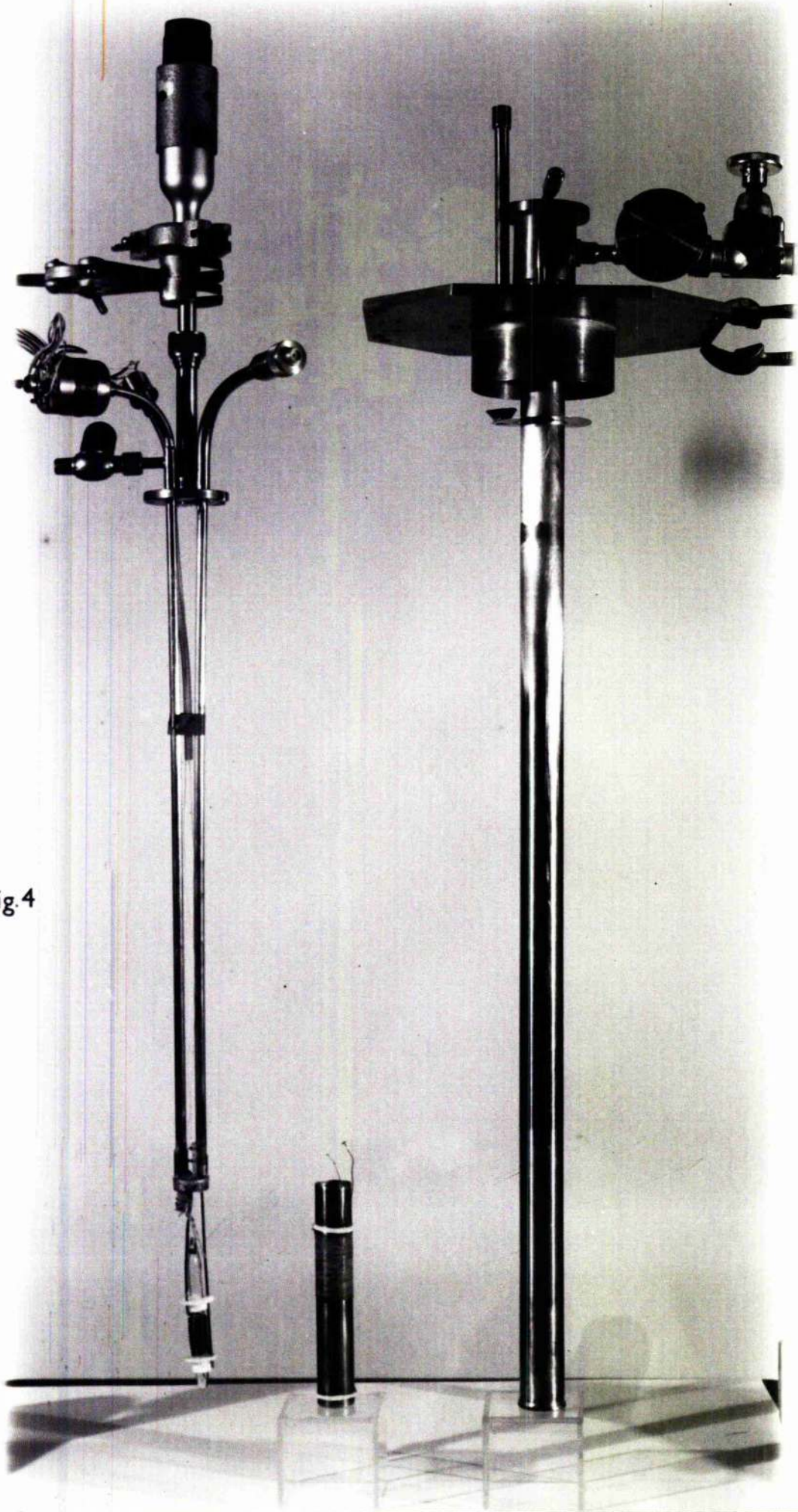

fig. 4

the resonance coil (1), which consisted of 12 turns of 18 swg copper wire, was rigidly mounted inside the copper isothermal shield (2) by the teflon spacers (3). The n.m.r. sample tube (4) was also firmly held by split sleeves in the teflon spacers (3). This tube was made with thin walled Monax glass to improve the sample filling factor of the coil. The isothermal shield (2) was secured to the copper flange (5) by the vacuum tight soft soldered circular joint (6). A heater of 32 swg Eureka wire was non-inductively wound on the outside of the copper shield. R.f. power was fed to the resonance coil through a coaxial lead consisting of an outer conductor of 5 mm cupro-nickel tubing (7), and an inner conductor (8) of 1 mm copper plated stainless steel tubing. The inner conductor was rigidly held in the straight length of tubing by the teflon spacers as shown, and in the curved portion by a short length of the inner sleeving of a standard low loss coaxial cable threaded over the 1 mm tubing. The vacuum tight r.f. feed-through (9), was a modified Transradio pressure tight, 50 ohm r.f. connector.

The 5 mm stainless steel tube (10) contained three pairs of copper constantan thermocouple leads, these were threaded inside the six parallel channels of the inner sleeving of a length of low loss coaxial cable, from which the outer braiding and central conductor had been stripped. Two of these thermocouples measured the temperature at each end of the sample tube and were secured to the glass tube by G.E. low temperature varnish. The third was attached to the flange (5), and

provided the temperature indication for the automatic temperature control system described in section 3.3. The thermocouples entered the cryostat through vacuum tight seals in the flange (11). The valve (12) permitted Helium exchange gas to be admitted to the copper isothermal shield (2). A Penning vacuum gauge (13) monitored the vacuum in the space between the Helium filled enclosure of the copper isothermal shield (2) and the thin walled stainless steel jacket (14). A thin cupro-nickel disc (15) attached to the 5 mm tubes served as a radiation shield.

The assembly below the flange (16) could be inserted into the stainless steel jacket (14), with the flanges (16) and (17) coupled together with an O-ring. Thermal isolation between the copper isothermal shield (2) and the stainless steel jacket (14) was aided by small teflon guides attached to the outside of the copper shield. The top plate of the cryostat (18) was supported by four levelling screws which facilitated adjustment of the sample position in the magnet pole gap. A stepped glass dewar of $1\frac{1}{2}$ litres capacity, could be fitted tightly against the rubber seal (19) on the under side of the top plate, so that when a rotary oil pump was connected at (20), the liquid Nitrogen within the dewar could be pumped until it solidified at approximately 66°K and with further pumping of the solid Nitrogen until its vapour pressure was of the order of 1 torr it would reach a temperature of approximately 50°K.

When operating the cryostat with sample temperatures very much

above that of liquid Nitrogen, it was necessary to maintain a large temperature gradient in the small space between the copper shield (2) and the stainless steel jacket (14). Unless excessive heater current inputs with a consequent rapid boil off rate of the coolant could be tolerated, this space must be evacuated to a very low pressure $\simeq 10^{-5}$ torr. This was achieved in two ways, either by connecting a mercury diffusion pump with a rotary oil backing pump to the valve (21), or by the use of about 25 grms of zeolite pellets (22) located at the bottom of the stainless steel jacket (14). With the latter scheme the zeolite would pump the vacuum space to about 10^{-3} torr when liquid nitrogen was introduced into the dewar, or alternatively, if the space was pre-evacuated with a rotary oil pump to about 10^{-1} torr, the zeolite would achieve an ultimate vacuum of 10^{-5} torr. The use of sorption pumps to obtain high and ultra-high vacua is described by Read (1963). Provided that the system was free from leaks, these low pressures would be attained each time liquid Nitrogen was introduced into the dewar without further external pumping. The circular flange (23) was a spring loaded over pressure release valve, a necessary safety feature with sorption pumps.

For temperatures below 77°K an exchange gas of Helium at a pressure of 10^{-2} torr was introduced into the vacuum space to provide thermal contact between the copper isothermal shield (2), and the stainless steel jacket (14). With this arrangement it was possible to obtain an indicated sample temperature of 53°K, after

pumping on the liquid Nitrogen for 30 mins.

The lowest temperature obtainable with previous Nitrogen cryostats used in this laboratory was about 70°K, and from some preliminary measurements with cycloheptatriene it appeared desirable to take the sample to temperatures well below 70°K. In view of the extensive Helium facilities available in a new laboratory occupied during the course of this work it was decided to construct a liquid Helium n.m.r. cryostat. A considerable time was spent in the design and testing of this cryostat, which was made by The Oxford Instrument Company. The design was a Nitrogen shielded liquid Helium metal cryostat with a 16" by 2" diameter cylindrical tail. The Helium reservoir capacity was 2 litres, and the evaporation rate permitted 8 hours of experiment for each fill. The n.m.r. probe assembly was very similar in design to the Nitrogen probe described earlier. Chromel Gold (.03% Iron) thermocouples were used to measure the sample temperature, and a heater, exchange gas system was employed to obtain temperatures between 4.2 and 77°K. An initial problem arose from an inability to get liquid Helium into the narrow tail with the probe in position. This was solved by altering the probe attachment at the cryostat top plate to a double O-ring sliding piston arrangement. This enabled the tail of the Helium reservoir to be filled with the probe suspended above, in the body of the reservoir. When the liquid Helium transfer was complete, the probe was slid

back into the tail. In the course of these alterations it was found that modifications to the Nitrogen cryostat had extended the lower temperature range from 70°K to 53°K. The results obtained with cycloheptatriene at this temperature showed that measurements at temperatures below 53°K were now unnecessary, and so further work on the Helium cryostat was postponed to later experiments.

Temperature control

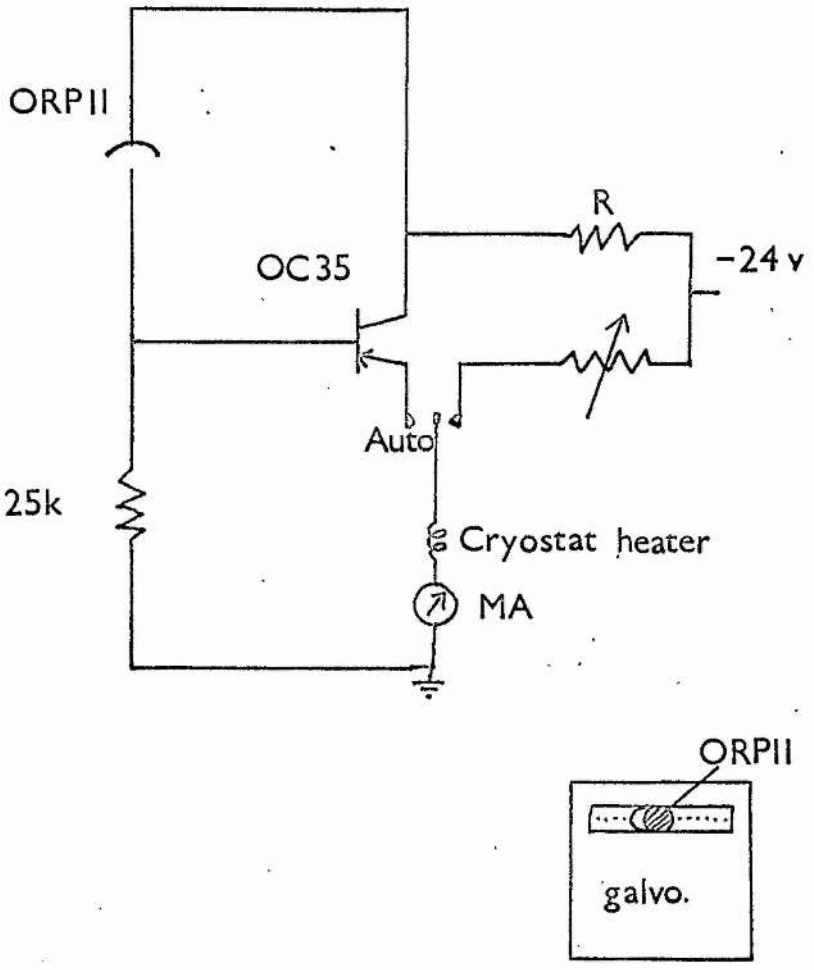

fig. 5

3.3 Sample Temperature Control

Automatic control of the sample temperature in the cryostat was achieved by a galvanometer light spot and photo-conductive cell amplifying system. The circuit is given in figure 5, and is based on a scheme of Woodhams, Carlow and Meads (1966). It has the advantages of proportional control, with no switching circuits; it is entirely D.C., and driven by small currents from storage batteries, and can be used in the range 20 deg. K. to 300 deg. K. with Copper Constantan thermocouples, and down to 4.2 deg. K. with Chromel Gold/Iron thermocouples.

The galvanometer deflection is proportional to the out of balance voltage between the setting of the potentiometer and the thermocouple e.m.f. An ORP 11 Cadmium Sulphide photo-conductive cell is positioned slightly off centre of the galvanometer scale. When the light spot shines directly on the cell, its resistance falls to 7 K., and returns to 700 K. when the light spot moves off the cell. For partial illumination, the cell resistance is intermediate between these two values.

The operating characteristics of the system were: 500 milliwatts heat input to sample heater for full illumination, and less than 10 milliwatts for no illumination; and a control range of 10 milliwatts per degree K. off balance, for small temperature excursions. Five hundred milliwatts heat input was sufficient to maintain a temperature difference of 230 degrees between the sample area and the liquid

nitrogen surround for an exchange gas pressure of less than 10^{-5} m.m. Hg.

Since the N.M.R. experiments were always performed as a series of increasing temperatures, it was important not to accidentally overheat the sample while the system was left unattended between measurements and prematurely pass it through a phase transition, or boil off all the liquid gas. For these reasons the system was of the "fail-safe" type, i.e. no heater input unless the cell was illuminated.

The amount of heat required to maintain a given temperature is a sensitive function of the exchange gas pressure, which was usually set at about 10^{-3} m.m. Hg for temperatures below 150 deg. K., and 10^{-5} m.m. Hg for temperatures above 150 deg. K. Hence the procedure for a given temperature was as follows:-

(1) The exchange gas pressure was set for the required temperature range.

(2) The null position of the galvanometer was set to illuminate the cell to give approximately the heater current for maintaining the sample at the required temperature.

(3) The potentiometer was set to the equivalent thermocouple e.m.f. for this temperature, the galvanometer would now be off null.

(4) Under manual control the sample was heated until the galvanometer light spot once more illuminated the cell.

(5) The system was now set to automatic control, and within five minutes, temperature stabilisation would occur to within 0.2 deg. K.

(6) For subsequent small temperature changes of about 5 degrees, the usual experimental case, it was sufficient merely to change the potentiometer setting.

The performance of the system was very satisfactory, and it could be left unattended for long periods. In fact the boil off rate of the liquid gas was the main limitation, this typically being about eight hours for each fill of liquid nitrogen. One critical arrangement for the proper operation of the system, was the position of the thermocouple relative to the heater windings. A suitable position to give correct feedback, without undue overshoot or oscillation, was found by experiment.

3.4 Experimental Measurements

3.4.1 Calibration

1. Field Sweep

The field sweep current for the permanent magnet was measured by a millivoltmeter shunted across a 0.2 ohm resistance in series with the magnet sweep coils. In the case of the Mullard electro-magnet, the sweep unit had an output voltage socket. This voltage was linearly proportional to the field sweep, and was monitored by a digital voltmeter.

Calibration of these meters in terms of the field variation of the magnets was accomplished by observing a strong proton signal from a Newport Mark II Magnetometer on an oscilloscope, and then measuring the frequency of zero beat between the magnetometer and the Schlumberger signal generator. The frequency of the signal generator could be read to $\pm$ 25 c/s and was stable to 1 part in 10^8. This was repeated for a series of discrete field increments, and the required calibrations obtained from a computer least squares analysis of the results.

2. Magnet field modulation

The amplitude of the field modulation was measured for both magnets by a milliammeter in series with the modulation coils. This meter was calibrated in a similar manner to the field sweep. For a series of modulation currents, the zero beat frequencies were measured for the two extreme positions of a strong proton signal on the oscil-

loscope. The required calibrations were then obtained by a computer least squares analysis of the modulation current versus frequency difference.

3. Copper-Constantan thermocouples

The interpolation of the thermocouple e.m.f. between six calibrated values, previously obtained from known melting points, was calculated by a computer least squares polynomial fit to these six data points. A good fit was found with the equation:

$$E = aT + bT^2 + cT^3$$

where E is the thermocouple e.m.f. in m.v., and T is the temperature in degrees centigrade of the measuring junction, with the reference junction at the melting point of ice. This was in agreement with general experience for the behaviour of copper constantan thermocouples below zero degrees centigrade, Herzfeld (1962).

The temperatures measured with the thermocouples calibrated by this method agreed to within 0.5 degree with the values measured using a commercial copper constantan thermocouple (British Standard 1828), in conjunction with a Comark 165CL thermocouple amplifier. The Comark 165CL thermocouple system was only available for some of the later experiments, mainly those with Cycloheptatriene, and had a specification of $\pm$ 0.5 deg. C. in the range -200 to + 30 deg. C., with a resolution of .1 deg. C.

3.4.2 Line Width and Second Moment

The line widths for all the absorption spectra were taken as the separation in gauss between the peaks of the absorption derivative curves. This corresponds to the points of maximum and minimum slope of the absorption curve.

From section 2.2.3 the second moment of the absorption curve is given by

$$M_2 = \frac{\int_{-\infty}^{\infty} h^2 g(h)dh}{\int_{-\infty}^{\infty} g(h)dh}$$

where the denominator is a normalizing factor. Integrating this expression by parts

$$M_2 = \frac{1}{3} \frac{\int_{-\infty}^{\infty} h^3 (dg(h)/dh)dh}{\int_{-\infty}^{\infty} h(dg(h)/dh)dh}$$

The output of the lock-in amplifier f(h) is the derivative of the absorption curve, so that the quantity dg(h)/dh is proportional to f(h). By applying the trapezium rule to perform the numerical integration, the expression for the experimental second moment may be written as:

$$M_2 = \frac{1}{3} \frac{\sum h^3 f(h)}{\sum h f(h)}$$

All second moment values were corrected for modulation broadening by subtracting the quantity $\frac{1}{4} h_m^2$, where h_m is the modulation amplitude Andrew (1955). To avoid distortion of the spectra, the modulation amplitude was always made less than one-sixth of the line width. The

radio frequency field was at all times kept below saturation level while recording the spectra. This was checked by measuring one of the derivative peaks as a function of the level of the radio frequency field and noting when the peak began to show saturation. The level used while recording the spectra was then set at about 10 db. below the saturation level.

The computer program given in appendix A13 was used to calculate the second moment from the experimental curves. On average twenty-five points were taken on each side of a derivative curve. For each temperature a series of derivative curves was plotted on the X-Y recorder, and the quoted experimental errors are the standard deviations for a set of curves.

3.4.3 Spin-Lattice Relaxation Time T_1

Two methods were used to measure the spin-lattice relaxation times. When the signal to noise ratio was poor, and the lock-in amplifier had to be used to monitor the signal, the direct recovery method was employed. This method was suited to the broad lines with long T_1's of a rigid lattice. With this method the signal at a peak of the derivative curve was initially saturated with a large r.f. field H_1, and then the exponential recovery with time was monitored with a much smaller r.f. field. The exponential recovery was plotted on the Y axis of the recorder, with the X axis acting as a linear time base. The value of T_1 was obtained from the exponential curve by the method of Mangelsdorf (1959), the details of which are given in appendix D.

Actually the time constant of the signal recovery is equal to T_1Z, where Z is the saturation factor mentioned in section 2.5. If Z, which is a function of the r.f. level H_1, is not close to unity the method of Andrew, Swanson and Williams, (1961) can be used to obtain T_1. With this method, the quantity T_1Z is measured for a series of r.f. power levels, and the true value of T_1 obtained by extrapolating the data to zero power. This method was employed for some of the experiments, but the correction was generally negligible.

When the absorption line was sufficiently strong for oscilloscope display, an alternative method was used to measure T_1. This method was similar to the "adiabatic passage with sampling" technique described by Anderson, Steele and Warnick (1967). With this method the oscilloscope signal is observed with a field modulation amplitude greater than the line width, and an r.f. level well below saturation. Then by switching an attenuator, the r.f. level is made sufficient to saturate the signal, and then switched to the lower level once more. The subsequent exponential recovery of the signal was recorded on a storage oscilloscope as a series of increasing peaks; two peaks for each cycle of the field modulation. The linear time base of the storage oscilloscope was set at a suitable calibrated speed, and was triggered by the switching of the attenuator. Different values of modulation frequency in the range 30-300 c/s were used, depending on the value of T_1 to be measured.

The actual value of T_1 was again calculated from a Mangelsdorf

plot, using the height of the signal at intervals of 1 cm. on the storage oscilloscope screen. Usually eight points on the recovery curve were taken to calculate each value of T_1, and for each temperature a series of T_1 measurements were made using at least two oscilloscope sweep speeds. As mentioned in appendix D, an accuracy of $\pm$ 7% was indicated in the values of T_1 obtained by this method. However for the shortest values of T_1 ($T_1 < .02$ sec), there is a possibility of a systematic error in the measured values owing to the finite recovery time of the receiver system from the switching transients. Further discussion of this point is given in section 7.

4. THE EXPERIMENTAL PROGRAMME

4. The Experimental Programme

As mentioned in the introduction it was decided to investigate the solid state behaviour of two medium ring hydrocarbons cycloheptane C_7H_{14} and cyclo-octane C_8H_{16}. These compounds are members of the cycloalkane ring series $(CH_2)_n$, which consists of a ring of n carbon atoms with two hydrogen atoms bonded to each carbon. The molecular conformation of both these compounds is at present unknown, and it was hoped that the n.m.r. results might provide some indication of the molecular structure and possible motion present in the various solid state phases.

An important part of this investigation has been the development of suitable Fortran computer programmes to calculate rapidly the necessary inter-nuclear distances and angles required for comparing the experimental results with suggested molecular conformations. The complexity of these calculations for the $(CH_2)_n$ series increases as a factor $n(2n - 1)$, and can involve several days of manual calculation for each conformation. A further complication is presented by the possibility of appreciable departures from regular tetrahedral bond angles (109.47°) in the cycloheptane and cyclo-octane rings. This tends to reduce the symmetry of the molecule and adds further to the labour involved in calculating the co-ordinates of the hydrogen atoms. Since it is now known that the chair form of cyclohexane C_6H_{12} has appreciable departures from tetrahedral bond angles (Eliel et al.

1965), it was felt important to consider the non-tetrahedral forms of cycloheptane and cyclo-octane. It is obvious that the second moment, which is a sensitive function of the inter-proton separation, will depend strongly on the H-C-H angle, and the results obtained have amply justified the inclusion of the non-tetrahedral forms. The details of the computer programme are given in Appendix A, and the computer output listings of the results obtained for each conformation are shown in the tables in the respective experimental sections.

The third compound studied was 1,3,5-cycloheptatriene, a partially saturated seven-membered ring hydrocarbon. This compound exhibits a thermal transition in the solid state very similar to the λ-type transition of cyclobutane, C_4H_8. It was hoped that a study of the solid state behaviour of cycloheptatriene would explain why cyclobutane, in contrast to all the other cycloalkanes, should have this type of transition rather than a normal first order transition.

5. CYCLOHEPTANE C_7H_{14}

5. Cycloheptane C_7H_{14}

5.1 The Sample

The sample of cycloheptane studied was supplied by the Shell Thornton Research Centre. A gas chromatography analysis indicated a purity of 99.8%, and the reasonable separations of the impurity peaks from the main peak suggested further purification by gas chromatography. This was carried out as indicated in Appendix C and a sample purity of better than 99.96% was achieved. This pure sample was degassed and distilled under vacuo into three thin walled Monax glass specimen tubes as described in Appendix B.

5.2 Physical Data

5.2.1 Molecular Structure

There has been considerable interest in the molecular conformation of cycloheptane, but owing to the highly flexible nature of the ring, a fact born out by the results presented here, there is at present no definitive conclusion regarding the most stable molecular configuration. Hendrickson (1961) has made a detailed theoretical study of the various possible molecular configurations by considering the total strain energy of each conformation. This analysis predicted the chair form to be more stable than the boat, and that a particular arrangement of the chair, referred to as a twist-chair, gave a lower energy than all the other forms. Hendrickson included in his investigation the effect of permitting

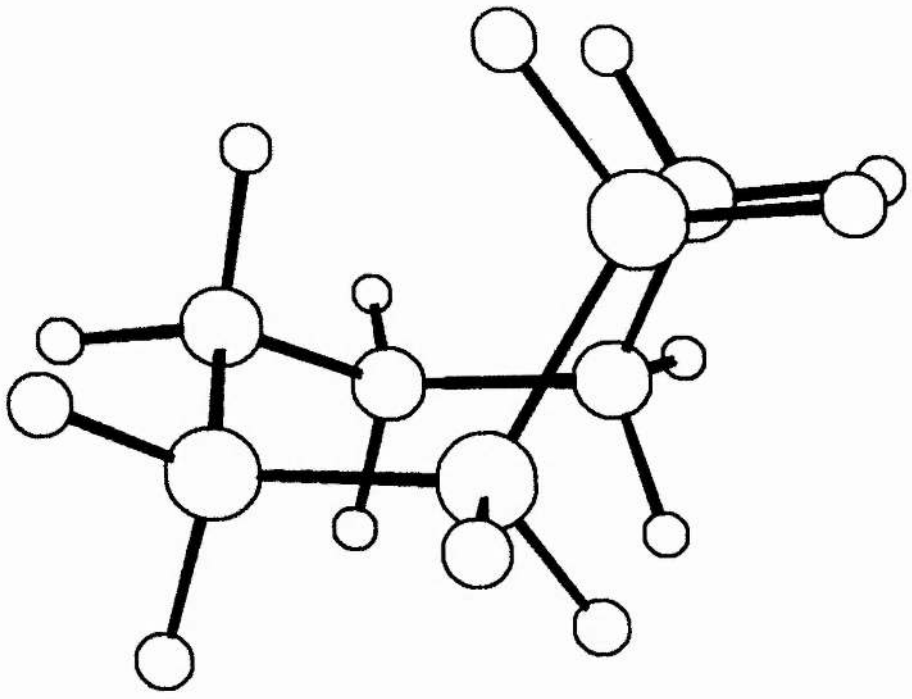

CYCLOHEPTANE BOAT

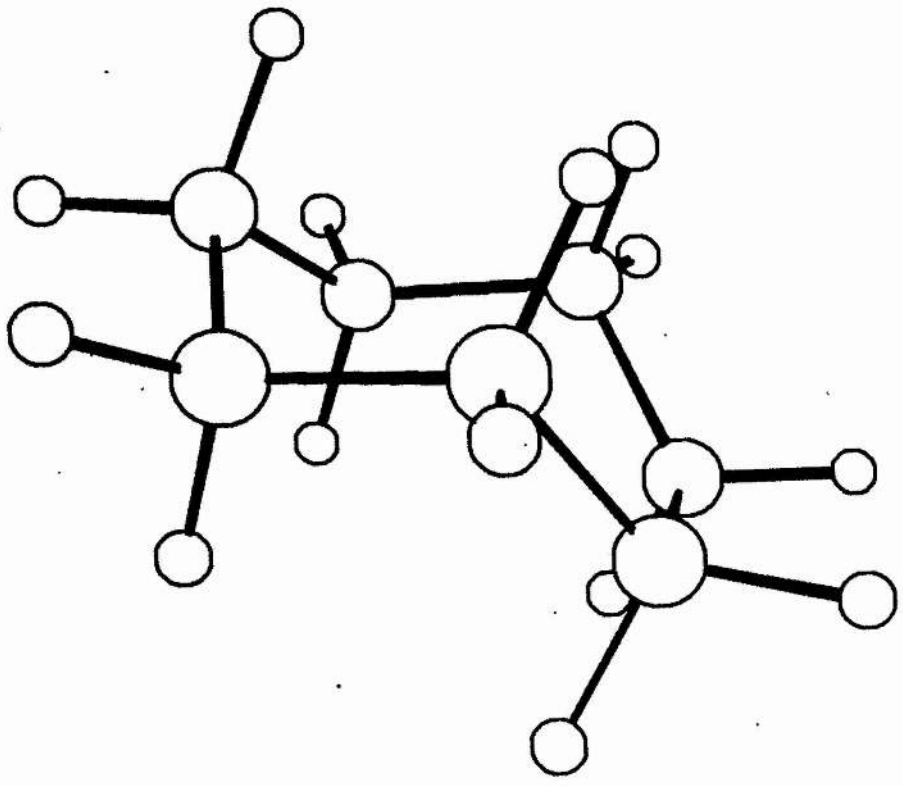

CYCLOHEPTANE CHAIR

fig. 5·1

CYCLO-HEPTANE BOAT HENDRICKSON MODEL NO.IV

****

ORIGIN=1 DUMMY ATOMS =1,2
FIRST CARBON = 3 AND 10 LAST CARBON = 9

NO	DATA INPUT BOND LENGTH	BOND ANGLE	DIHEDRAL ANGLE	COMPUTED CARBON COORDINATES X	Y	Z
2	1.390	0.00	180.00	-1.390	0.000	0.000
3	0.000	90.00	0.00	-1.390	0.000	0.000
4	1.533	90.00	86.11	-1.286	0.000	-1.530
5	1.533	114.00	242.85	0.000	.639	-2.067
6	1.533	114.00	56.70	1.285	0.000	-1.530
7	1.533	114.00	303.30	1.390	0.000	0.000
8	1.533	114.00	325.60	.766	1.231	.667
9	1.533	114.00	73.70	-.767	1.232	.666
10	1.533	114.00	0.00	-1.390	.002	-.002

****

C-H = 1.108

BOND ANGLES CCC	HCH	NO.	COMPUTED HYDROGEN COORDINATES X	Y	Z	X	Y	Z
113.9	108.2	3	-2.460	-.052	.282	-.886	-.906	.389
114.0	108.2	4	-2.155	.550	-1.943	-1.338	-1.047	-1.888
114.0	108.2	5	-.001	1.714	-1.799	-.001	.559	-3.172
114.0	108.2	6	2.154	.550	-1.944	1.337	-1.047	-1.888
114.0	108.2	7	2.460	-.052	.282	.886	-.907	.389
114.0	108.2	8	1.121	2.138	.139	1.120	1.283	1.716
114.0	108.2	9	-1.120	2.139	.135	-1.122	1.286	1.714

****

INTRA-MOLECULAR SECOND MOMENT

= 19.83 GAUSS*2 FOR 14 PROTONS

table 5·1

CYCLO-HEPTANE CHAIR HENDRICKSON MODEL NO.III

****

ORIGIN=1 DUMMY ATOMS =1,2
FIRST CARBON = 3 AND 10 LAST CARBON = 9

NO	DATA INPUT BOND LENGTH	BOND ANGLE	DIHEDRAL ANGLE	COMPUTED CARBON COORDINATES X	Y	Z
2	1.438	0.00	180.00	-1.439	0.000	0.000
3	0.000	90.00	0.00	-1.439	0.000	0.000
4	1.533	90.00	83.00	-1.252	0.000	-1.522
5	1.533	112.00	236.90	0.000	.776	-1.947
6	1.533	109.47	69.90	1.252	-.001	-1.522
7	1.533	112.00	290.10	1.439	-.001	0.000
8	1.533	111.00	91.80	.767	-1.223	.636
9	1.533	116.00	289.40	-.766	-1.224	.636
10	1.533	116.00	0.00	-1.439	-.001	.001

****

C-H = 1.108

BOND ANGLES CCC	HCH	NO.	COMPUTED HYDROGEN COORDINATES X	Y	Z	X	Y	Z
111.0	109.0	3	-.992	.922	.422	-2.521	-.016	.234
112.0	108.7	4	-2.141	.462	-1.994	-1.165	-1.047	-1.875
109.5	109.5	5	0.000	1.772	-1.460	0.000	.903	-3.047
112.0	108.7	6	2.141	.461	-1.995	1.164	-1.047	-1.875
111.0	109.0	7	.992	.921	.422	2.522	-.017	.234
116.0	107.6	8	1.114	-1.303	1.685	1.114	-2.128	.099
116.0	107.6	9	-1.112	-1.304	1.686	-1.112	-2.129	.100

****

INTRA-MOLECULAR SECOND MOMENT

= 19.05 GAUSS*2 FOR 14 PROTONS

table 5·2

the ring carbon C-C-C bond angles to depart from regular tetrahedral values of 109.47°. In general this led to a lower minimum energy for each conformation through the relief of non-bonded hydrogen interactions. Computer drawn perspective views of these minimum energy forms are given in figures 5.1 and 5.2. The cartesian co-ordinates are given in tables 5.1, 5.2, 5.3, 5.4 together with their relevant molecular structure data as explained in chapter 4.

Hendrickson also predicted that the barrier to the interconversion of the chair and boat forms was quite low, 8.5 kcal./mole, and even lower, 2.16 kcal./mole, for the interconversion between the chair and the twist chair forms by pseudorotation of the ring. For this reason he suggested that at room temperature cycloheptane will exist as a mixture of conformations. This is strongly supported by the evidence from high resolution n.m.r. studies of dilute solutions of 1,1-difluoro-cycloheptane and 1,1,3,3-tetrafluoro-cycloheptane Roberts (1967). Both of these compounds show equivalence of the fluorine peaks down to -180°C, indicating rapid interconversion between the molecular forms even at low temperatures. This evidence of course does not preclude the presence of one preferred conformation in the pure solid, where inter-molecular effects might restrict the flexibility of the ring. However at present no studies of the crystal structure of cycloheptane have been reported to confirm or deny this possibility, so that in this investi-

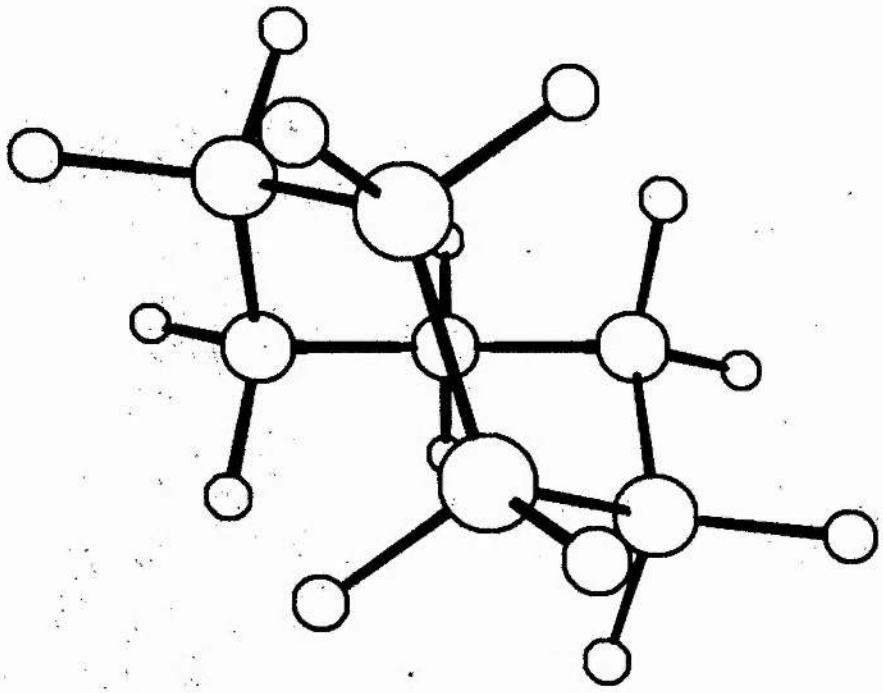

. CYCLOHEPTANE TWIST BOAT

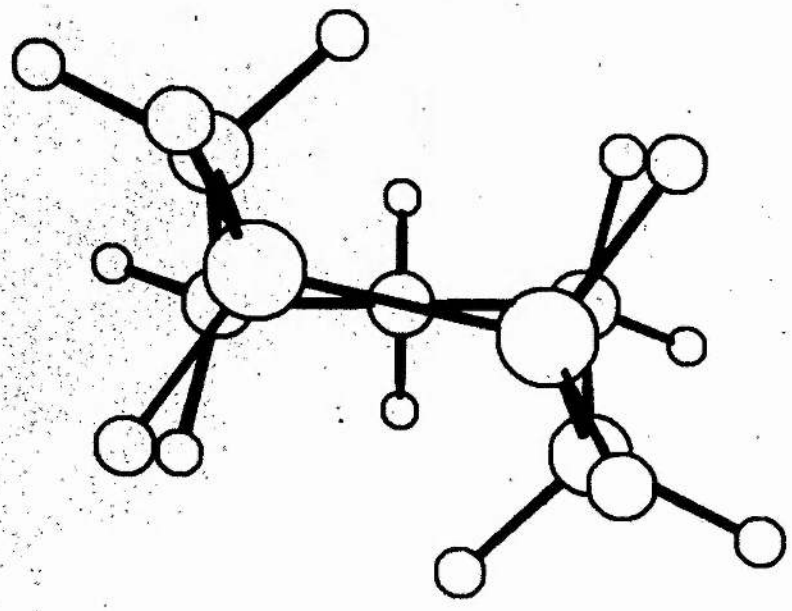

. CYCLOHEPTANE TWIST CHAIR

fig. 5·2

CYCLO-HEPTANE TWIST BOAT HENDRICKSON MODEL NO. VII

****

ORIGIN=1 DUMMY ATOMS =1,2
FIRST CARBON = 3 AND 10 LAST CARBON = 9

NO	DATA INPUT BOND LENGTH	BOND ANGLE	DIHEDRAL ANGLE	COMPUTED CARBON COORDINATES X	Y	Z
2	0.000	0.00	180.00	0.000	0.000	0.000
3	0.000	90.00	0.00	0.000	0.000	0.000
4	1.533	90.00	56.50	.846	0.000	-1.278
5	1.533	113.00	317.83	1.967	-1.046	-1.255
6	1.533	113.00	292.30	3.057	-.733	-.223
7	1.533	113.00	341.00	3.056	.734	.223
8	1.533	113.00	78.90	1.967	1.046	1.255
9	1.533	113.00	341.00	.847	-.001	1.279
10	1.533	113.00	292.30	0.000	-.001	.001

****

C-H = 1.108

BOND ANGLES CCC	HCH	NO.	COMPUTED HYDROGEN COORDINATES X	Y	Z	X	Y	Z
113.0	108.5	3	-.647	.899	0.000	-.648	-.899	-.001
113.0	108.4	4	1.297	1.004	-1.409	.186	-.203	-2.144
113.0	108.4	5	2.430	-1.096	-2.260	1.527	-2.036	-1.022
113.0	108.4	6	4.045	-.973	-.663	2.903	-1.377	.665
113.0	108.4	7	2.902	1.377	-.666	4.045	.974	.662
113.0	108.4	8	1.526	2.035	1.022	2.430	1.096	2.260
113.0	108.5	9	.187	.202	2.145	1.298	-1.004	1.409

****

INTRA-MOLECULAR SECOND MOMENT

= 20.44 GAUSS*2 FOR 14 PROTONS

table 5·3

CYCLO-HEPTANE TWIST CHAIR HENDRICKSON MODEL NO.V

****

ORIGIN=1 DUMMY ATOMS =1,2
FIRST CARBON = 3 AND 10 LAST CARBON = 9

NO	DATA INPUT BOND LENGTH	BOND ANGLE	DIHEDRAL ANGLE	COMPUTED CARBON COORDINATES X	Y	Z
2	0.000	0.00	180.00	0.000	0.000	0.000
3	0.000	90.00	0.00	0.000	0.000	0.000
4	1.533	90.00	56.00	.857	0.000	-1.271
5	1.533	112.00	311.25	2.064	-.937	-1.149
6	1.533	112.00	263.00	3.337	-.185	-.744
7	1.533	112.00	75.80	3.337	.185	.744
8	1.533	112.00	307.10	2.064	.938	1.148
9	1.533	112.00	75.80	.856	.001	1.269
10	1.533	112.00	263.00	0.000	.002	-.003

****

C-H = 1.108

BOND ANGLES CCC	HCH	NO.	COMPUTED HYDROGEN COORDINATES X	Y	Z	X	Y	Z
112.0	108.7	3	-.646	.900	0.000	-.645	-.901	.001
112.0	108.7	4	1.218	1.030	-1.463	.233	-.324	-2.127
112.0	108.7	5	2.234	-1.435	-2.125	1.845	-1.712	-.388
112.0	108.7	6	3.416	.742	-1.346	4.217	-.823	-.957
112.0	108.7	7	4.217	.822	.958	3.414	-.742	1.346
112.0	108.7	8	1.846	1.712	.387	2.234	1.436	2.123
112.1	108.7	9	.232	.326	2.125	1.216	-1.029	1.462

****

INTRA-MOLECULAR SECOND MOMENT

= 19.00 GAUSS*2 FOR 14 PROTONS

table 5·4

gation all four forms of chair, boat, twist-chair and twist-boat were considered as possible molecular configurations in the solid.

5.2.2 Thermal Data

Finke et al. (1956) have reported an extensive study of the low temperature thermal properties of cycloheptane. Their results are summarised in table 5.5 below, and the variation of heat capacity they obtain is shown as the continuous curves in figure 5.3. The dashed vertical lines in figure 5.3 are the transition temperatures given by Finke et al. (1956).

Table 5.5

Transition Type	Temperature °K	Entropy of Transition in e.u. (cal. deg.$^{-1}$ mole^{-1})
1st order solid-solid	134.8	8.806
1st order solid-solid	198.2	0.349
1st order solid-solid	212.4	0.506
Fusion	265.12	1.697
Vaporization	298.16	30.89

They report that cycloheptane exists in four different crystalline forms, and exhibits normal first order transitions between these forms, although they found that it was possible to supercool through the two lowest transitions. It is interesting to note that the entropy change associated with the lowest transition is very much greater than the entropy of fusion.

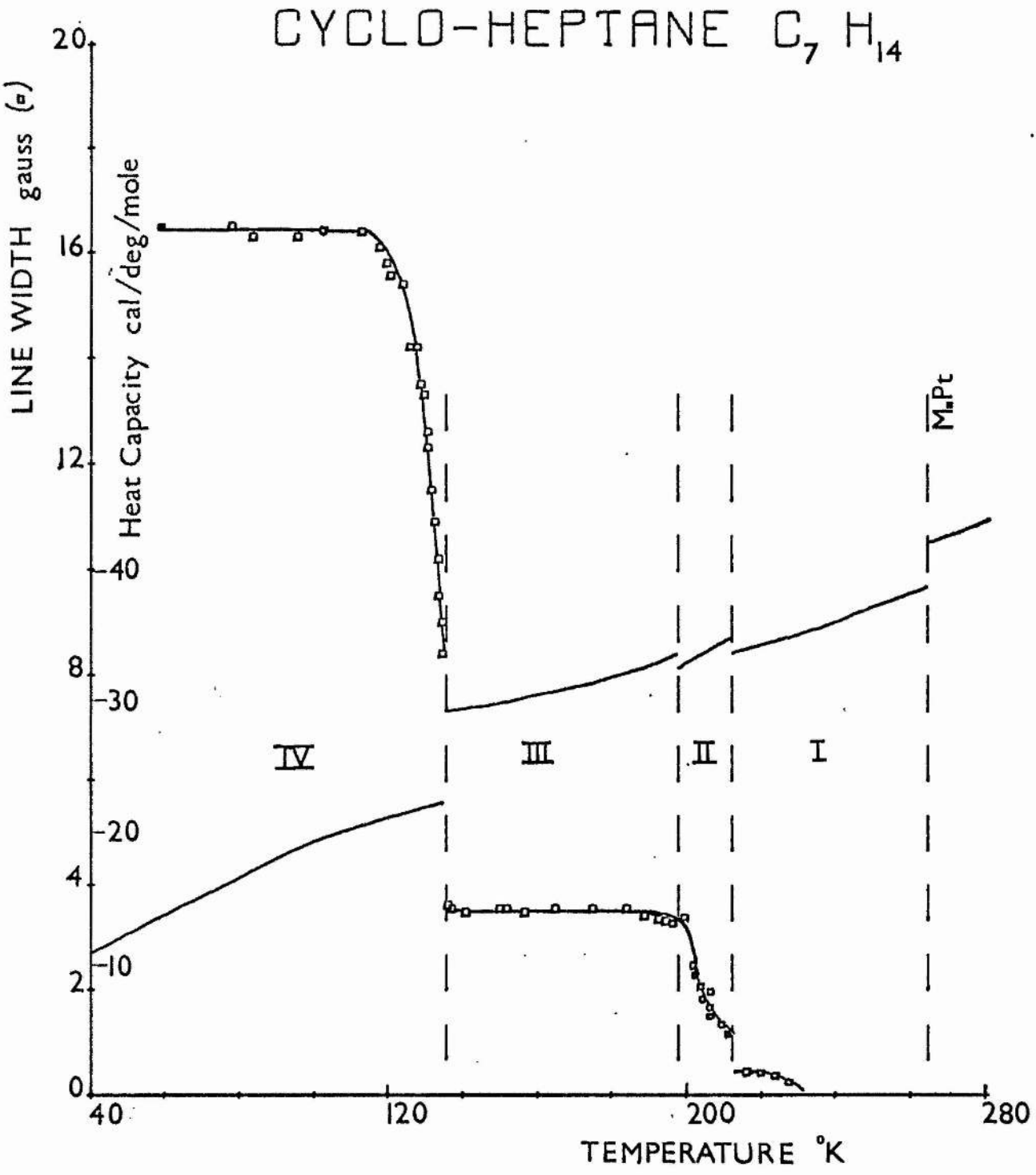
CYCLO-HEPTANE $C_7 H_{14}$
LINE WIDTH gauss (a)
Heat Capacity cal/deg/mole
20
16
12
8
4
2
0
40
30
20
10
IV
III
II
I
M.Pt
40
120
200
280
TEMPERATURE °K

fig.5·3

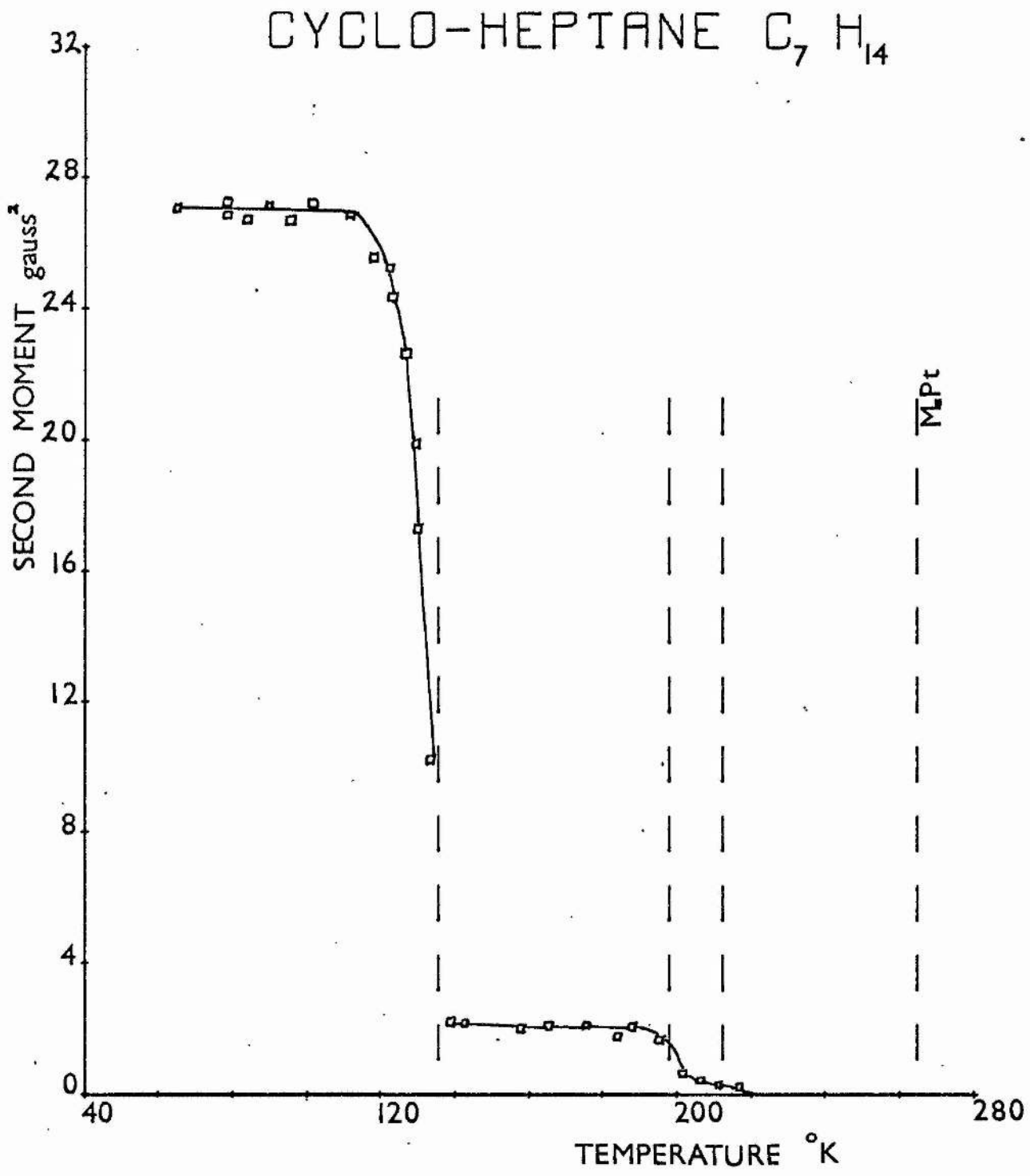
CYCLO-HEPTANE $C_7 H_{14}$
SECOND MOMENT gauss²
32
28
24
20
16
12
8
4
0
40
120
200
280
TEMPERATURE °K
T_{LPt}

fig. 5·4

5.3 Results

5.3.1 Temperature variation of Absorption Spectrum

The variation of the line width and second moment of cycloheptane are shown in figures 5.3 and 5.4. These measurements were taken as a series of increasing temperatures to avoid supercooling effects. Because the thermal conductivity of organic solids is very poor at low temperatures, the sample was always kept at the same temperature for about an hour before each measurement was made. This helped to ensure a uniform temperature over all the sample.

It was found easy to supercool the sample through the lowest transition, and in order to obtain phase IV it was usually necessary to thermally cycle the sample from 77°K up to about 140°K and then down again. This procedure always gave the very broad line of 16 gauss characteristic of phase IV. This behaviour was similar to the experience of Finke et al. (1956). The supercooled state could be maintained for many hours below the lowest transition at 134.8°K, and gave a strong resonance line of width 4.2 gauss which was easily observable on the oscilloscope.

Below 120°K the line width and second moment of phase IV attain steady values of $16.3 \pm .3$ gauss and $27.0 \pm .5$ gauss^2 respectively, and on warming to phase III they once more show steady values of $3.5 \pm .1$ gauss and $2.3 \pm .1$ gauss^2. On further warming to phase II there is a gradual reduction in the second moment from 2.3 to 2.1 gauss^2

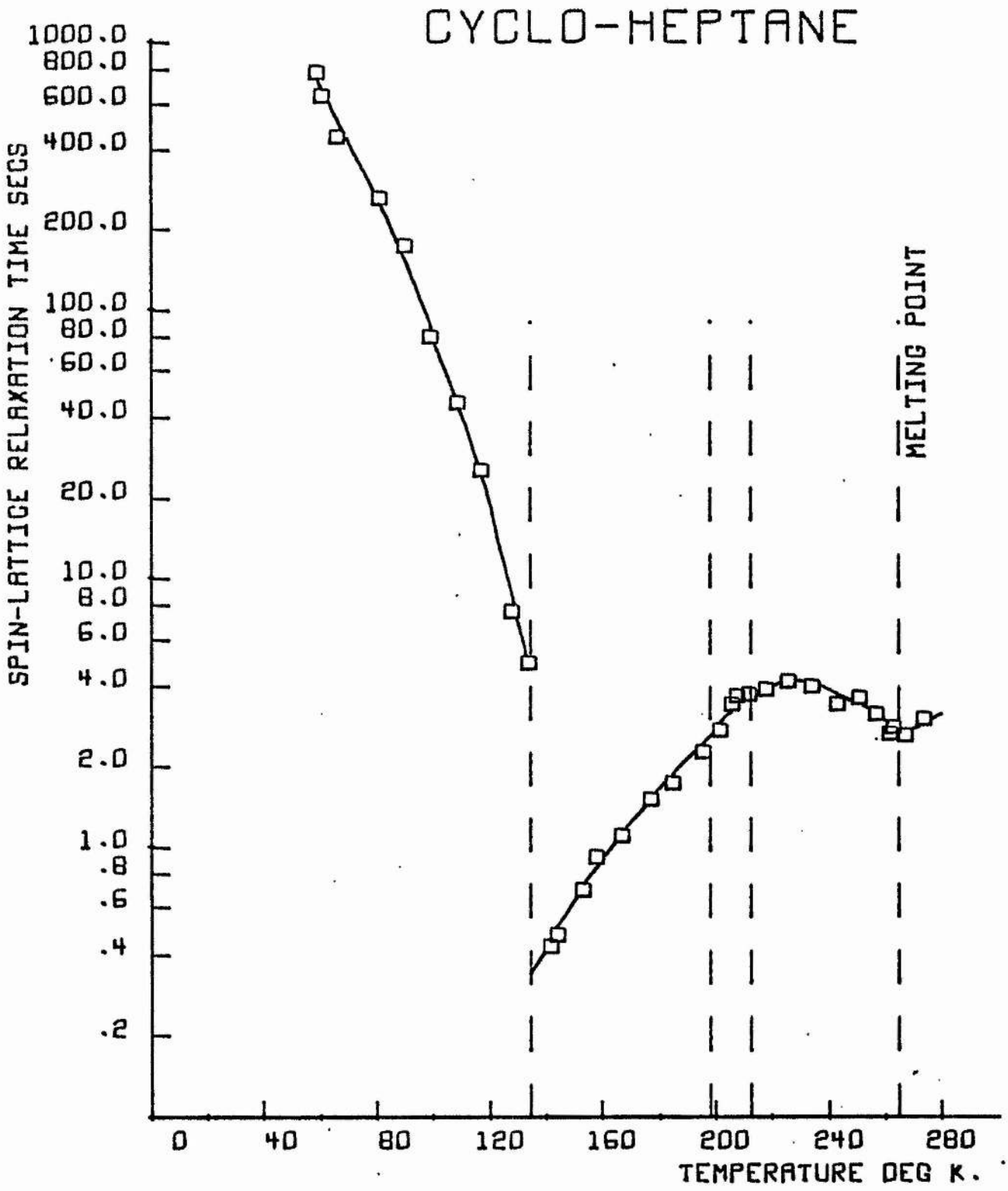
CYCLO-HEPTANE
SPIN-LATTICE RELAXATION TIME SECS
1000.0
800.0
600.0
400.0
200.0
100.0
80.0
60.0
40.0
20.0
10.0
8.0
6.0
4.0
2.0
1.0
.8
.6
.4
.2
0
40
80
120
160
200
240
280
TEMPERATURE DEG K.
MELTING POINT

fig.5·5

just below the III-II transition. In phase II the second moment is only of qualitative significance since no plateau value was obtained. It decreased from a value of approximately 1 gauss^2 to .3 gauss^2. At the II-I transition there was a further sharp reduction to a value largely determined by the magnet field inhomogeneity of approximately 0.05 gauss^2.

The line width in phase II was easier to follow than the second moment owing to significant contributions to the latter from the wings of the spectrum. The line width gradually decreased from 2 gauss at a temperature just above the III-II transition to a value of 1 gauss at the II-I transition. Above this transition there was a sharp reduction to a value determined by the magnet field inhomogeneity of about 0.2 gauss. From figures 5.3 and 5.4 it can be seen that these reductions were closely related to the thermal transitions found by Finke et al. (1956).

5.3.2 Spin Lattice Relaxation

The temperature variation of the spin lattice relaxation time T_1 is shown in figure 5.5. The values below 134.8°K were measured by the direct recovery method on the Y-T plotter. Above 134.8°K the absorption signals were strong and the storage oscilloscope method could be employed.

5.4 Discussion

5.4.1 Absorption Spectrum

(a) Rigid Lattice. Theoretical values for the rigid lattice intra-

Table 5.6

Cycloheptane: Rigid Lattice intra-molecular second moment for various minimum energy molecular conformations

	All bond angles tetrahedral (109.47°)	Variable bond angles (see tables 5.1 to 5.4)	
	C-H = 1.108 A°	C-H = 1.108 A°	C-H = 1.09 A°
chair	31.36	19.05	20.34
boat	32.23	19.83	21.10
twist-chair	20.45	19.00	20.28
twist-boat	28.23	20.44	21.66

(all values in gauss^2)

Table 5.7

Comparison of lattice energy and rigid lattice inter-molecular second moment for the cycloalkanes $(CH_2)_n$

	Lattice energy in kcal./mole	M_2 rigid lattice in gauss^2
Cyclopropane C_3H_6	6.1	6.5 ± 1
Cyclobutane C_4H_8	7.5	6.9 ± 1
Cyclopentane C_5H_{10}	8.4	7.2 ± 1.5
Cyclohexane C_6H_{12}	10.2	8.7 ± 0.5
Cycloheptane C_7H_{14}	11.4	$[9 \pm 1]$
Cyclo-octane C_8H_{16}	11.7	$[9.5 \pm 1]$

(results for n = 3 to n = 6 obtained from previous n.m.r. investigations)

molecular second moment for the four molecular forms of cycloheptane are given in table 5.6. These values were obtained with the computer programme described in appendix A using the structural parameters from Hendrickson (1961) listed in tables 5.1 to 5.4. In the first column the values for the tetrahedral bond angle forms are given for comparison. Two values with different C-H bond lengths are given for each of the latter. Hendrickson favours a length of 1.108 angstroms, which is supported by the recent electron diffraction studies of cyclo-octane by Almenningen et al. (1966). The results obtained with the more usual value of 1.09 angstroms are shown for comparison.

Since the crystal structure of cycloheptane is not known it is not possible to calculate the inter-molecular contribution to the second moment exactly. However by comparison with other members of the cycloalkane ring series, whose results are already known, see table 5.7, and noting the variation of the inter contribution with lattice energy, a reasonable estimate can be made. Although the relationship with the lattice energy is obviously not a simple one, a value of 9 gauss^2 with an uncertainty of $\pm$ 1 gauss^2 would appear acceptable.

At temperatures below 120°K the experimental second moment appears constant at 27.0 $\pm$ 0.5 gauss^2, and in view of the size of the molecule and the variation of T_1 below 120°K this is assumed to be the rigid lattice value. If the estimated inter contribution of

9 ± 1 gauss is deducted from this value, an intra contribution of 19.0 ± 1.5 gauss^2 is obtained. This value quite clearly excludes all the tetrahedral forms except the twist-chair as possible molecular configurations of cycloheptane in the solid state below 120°K. However it permits no distinction to be made between the variable bond angle forms, although it does perhaps lend some support to Hendrickson's suggestion that the non-bonded hydrogen interactions in cycloheptane will cause appreciable departures from tetrahedral angles in the carbon ring. The experimental value is certainly consistent with all four of his preferred forms as possible conformations for cycloheptane in phase IV.

(b) Spectrum between 120°K and 198°K. It is difficult to postulate the exact nature of the motion responsible for the observed reductions in the line width and second moment between 120°K and the IV-III transition. The initial reduction was quite smooth and no fine structure was observed; but as soon as the transition temperature was passed a narrow component appeared and grew rapidly at the expense of the broader line in a manner characteristic of a first order transition. The values just before the transition were quite reproducible between experiments, and the two thermocouples on the sample tube gave no indication of temperature gradients over the sample, nor was there any significant change in the values with time for a given temperature. In view of the large entropy change, 8.806 cal. deg.$^{-1}$ mole^{-1}, associated with the IV-III, the crystalline field will obviously be

very different for the two phases, so that it is difficult to relate the molecular motion that might be occurring in phase IV with that occurring in phase III. This point will be returned to later in the section.

In phase III the experimental second moment has a steady value of $2.3 \pm .1$ gauss^2 with a slight reduction to $2.1 \pm .1$ gauss^2 just before the III-II transition. This value is somewhat larger than the usual value of 1 gauss^2 expected for quasi-isotropic reorientation in molecular solids. For this reason the possibility of reorientation about a preferred molecular axis has been investigated. The calculations involved in this are necessarily of an approximate nature, since neither the crystal structure nor the precise molecular structure is known for this phase of the solid. The results obtained for the intra contribution using Hendrickson's structural parameters are shown in table 5.8

Table 5.8

Cycloheptane: reduced intra-molecular second moment for molecular reorientation

	pseudo-reorientation	motion about a symmetry axis	
		2-fold jumps	free rotation
chair	1.79	-	-
boat	1.41	-	-
twist-chair	1.88	11.95	3.41
twist-boat	1.39	9.74	3.07

(values in gauss^2)

Only the twist-chair and the twist-boat models possess symmetry axes as may be seen from figures 5.1 and 5.2, and the results for 2-fold jumps and free rotation about these axes are given in the last two columns. In the first column the results are given for the type of molecular motion suggested by Hendrickson, namely pseudo-reorientation, described as the concerted change of position of each ring atom so that every atom sequentially takes up each of the possible ring positions. The method of calculating the values for this form of motion is described in Appendix A7. The inter-molecular contribution must be added to these values. It is immediately evident, even without knowledge of the value of the inter contribution, that motion about a single symmetry axis will not explain the observed value of the second moment in phase III.

It is possible that pseudo-reorientation of the molecules could explain the observed second moment, particularly as the intra values given in table 5.8 do not take account of possible 'rocking' of the molecules as they reorientate. However since a lack of knowledge of the crystal structure prevents any precise calculation of the inter contribution for this type of motion, further meaningful discussion of this suggestion is not possible. The large entropy change at the IV-III transition, almost six times the entropy of melting, and the low value of the second moment after the transition certainly suggest that considerable molecular motion exists in phase III. It can be concluded that the observed value of $2.3 \pm .1$ gauss^2

is consistent with either general flexing of the ring through pseudo-reorientation, or molecular motion about more than one axis, approaching the situation of quasi-isotropic reorientation.

Since the molecular motion is so general in phase III, it is possible that the reductions observed in the line width and second moment just below the IV-III transition are due to some form of 'pre-melting' effect, involving either a slight flexing of the methylene groups or even the onset of some form of restricted molecular reorientation.

(c) Spectrum above 198°K (phases II and I). In phases II and I the further reduction in the observed second moment to a value less than the magnet field inhomogeneity, approximately 0.05 gauss^2, is similar to the situation observed in the high temperature solid phase of cyclohexane C_6H_{12} (Andrew and Eades 1953). This low value, which implies averaging of the remaining inter contribution, (the intra contribution is already zero due to isotropic reorientation) was attributed to the self-diffusion of the molecules, through the crystal lattice. It was suggested that this diffusion occurred by a 'vacancy jump' mechanism at a rate greater than the line width in frequency units, i.e. greater than 10^4 jumps per second. This was subsequently confirmed by the radio-active tracer study of cyclohexane by Hood and Sherwood (1966). In view of the similarity in the molecular structure of cyclohexane and cycloheptane, it might be expected that self-diffusion would occur in the high temperature solid phases of

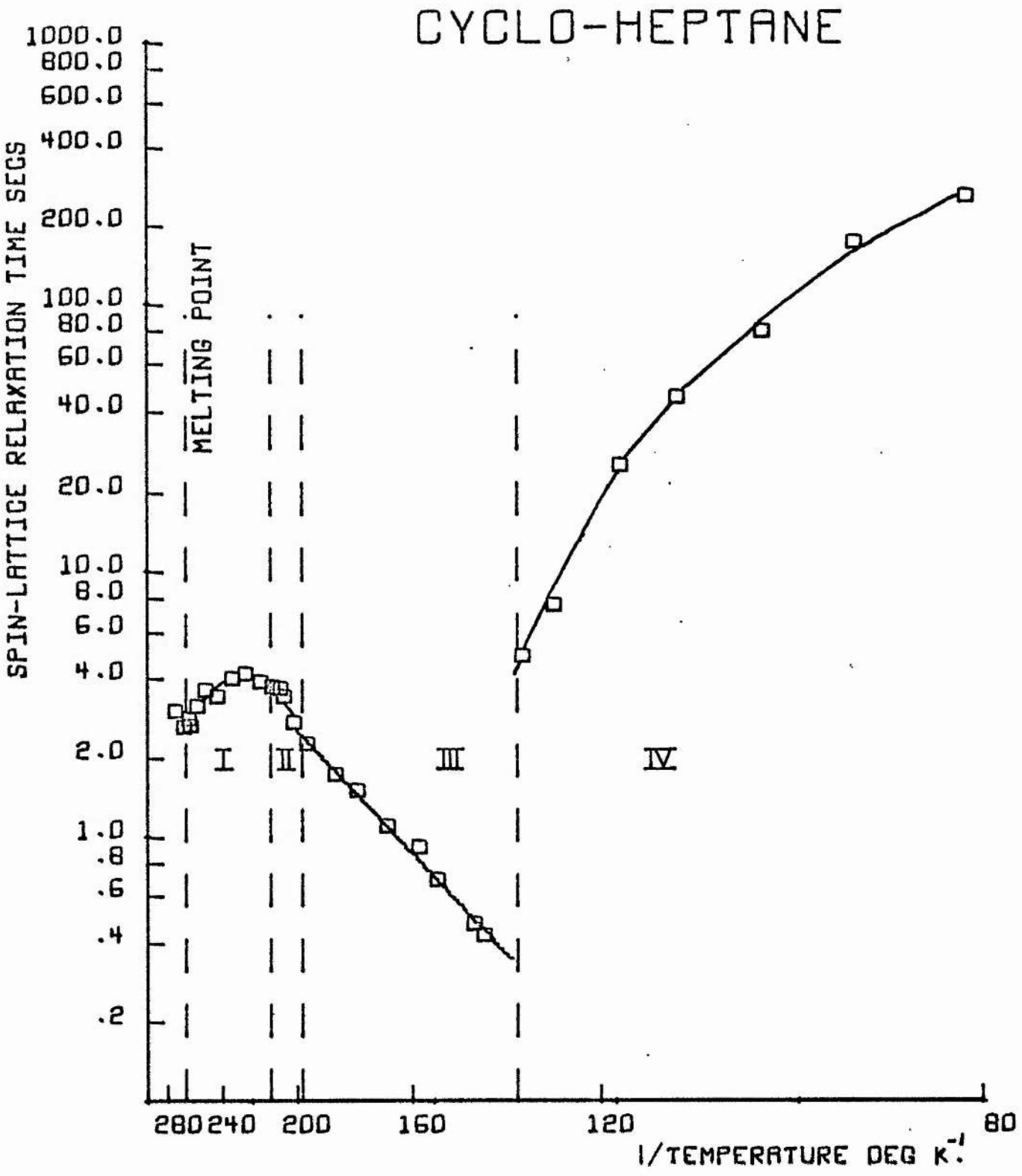
CYCLO-HEPTANE
SPIN-LATTICE RELAXATION TIME SECS
1000.0
800.0
600.0
400.0
200.0
100.0
80.0
60.0
40.0
20.0
10.0
8.0
6.0
4.0
2.0
1.0
.8
.6
.4
.2
MELTING POINT
I
II
III
IV
280
240
200
160
120
80
1/TEMPERATURE DEG K.-1

fig.5·6

cycloheptane. The very small value of the second moment in phase I strongly supports this contention. In phase II it is possible that self-diffusion does occur also, but at a rate too slow to completely average out the inter-molecular dipolar interaction (i.e. less than 10^4 jumps per second). The II-I transition might be expected to involve a modification of the crystal lattice structure making self-diffusion more facile.

5.4.2 Spin Lattice Relaxation time T_1

The graph of the logarithm of T_1 versus temperature given in figure 5.5 shows T_1 very long at low temperature. This supports the suggestion that the molecules are effectively stationary in phase IV below 120°K. The motion responsible for the reduced line width observed in phase IV above 120°K does not appear to modify the behaviour of T_1 greatly. A graph of the logarithm of T_1 versus reciprocal temperature shown in figure 5.6 gives no indication of a simple one-motion process dominating the relaxation in this temperature region. A straight line relationship would be expected for this type of motion, as given by case (1) $\omega_o^2 \tau_c^2 \ll 1$ of equation 2.17. It is probable that in this region the relaxation is controlled by a combination of factors such as lattice vibrations, torsional oscillations and paramagnetic impurities.

In phase III it would appear that the relaxation could be described by a simple one-motion process. A least squares calculation of the best straight line through the experimental points in this

region gives an activation energy of 1.7 $\pm$ 0.3 kcal./mole for this process. This calculation assumes case (2) $\omega_o^2\tau_c^2 \gg 1$ of equation 2.17, and the Arhennius relation of 2.9 for the variation of the mean frequency of the motion with temperature. The value obtained is similar to the energy barrier found for isotropic reorientation with other molecules, whose molecular envelopes, like cycloheptane, have a 'globular' shape. These barriers usually lie between 1 and 3 kcal./mole and originate in the inter-molecular forces of the lattice. In cyclohexane and cyclo-octane it is known from X-ray diffraction that the distances between the molecular centres, in similar solid phases, are appreciably less than the van der Waals diameters of the molecules. A similar situation can be expected to prevail in phase III of cycloheptane, and suggests that any reorientation process would necessarily be co-operative. The low barrier calculated by Hendrickson (1961) of 2.16 kcal./mole for pseudo-reorientation of the cycloheptane ring would also facilitate any molecular reorientation process.

In phase I the self-diffusion of the molecules gives an additional mechanism for spin lattice relaxation. Since the jumping frequency increases with temperature, and at 210°K is much less than the radio-frequency (22.6 Mc/s), the effect is to cause T_1 to decrease again with increase of temperature as shown in figure 5.5.

The small change observed in T_1 on melting suggests that the molecular freedom in phase I is very similar to that in the liquid,

and explains why the latent heat of fusion of cycloheptane should be so small.

6. CYCLO-OCTANE C_8H_{16}

6. Cyclo-octane C_8H_{16}

6.1 The Sample

The sample of cyclo-octane used in this investigation was supplied by the British Petroleum Company through the courtesy of Professor Cadogan of the Chemistry Department, St. Andrews University. This sample, which was understood to be at least 99% pure, was received sealed under vacuum in a small glass tube. Since this tube fitted the radio-frequency coil, it was used without further modification.

6.2 Physical Data

6.2.1 Molecular Structure

An early Raman and infra-red study of cyclo-octane by Bellis and Slowinski (1959) showed no change in the spectra from the solid at -50°C and the liquid at 120°C. This suggested that only one structural isomer of cyclo-octane was present under ordinary conditions. The authors found best agreement with their spectra on the basis of a tub model, but the agreement was not conclusive. A later electron diffraction investigation by Almenningen et al. (1966) showed that the assumption of any single conformation for cyclo-octane at 40°C was not compatible with their results. To fit the data it was necessary to assume a conformational mixture based on high flexibility of the ring. From the first two peaks of the experimental radial distribution curve they obtained the bond lengths as C-C = 1.540 Å, and C-H = 1.107 Å. High resolution n.m.r. studies of

dilute solutions of cyclo-octane, and deuterated cyclo-octane by Anet and Hartman (1963), and Anet and Jacques (1966), showed that the simple spectra obtained at room temperature separated into more complex spectra below -85°C. The low temperature spectra suggested that the major conformation of cyclo-octane was either the boat-chair or the twist boat-chair. However their data was also consistent with a rapid pseudo-rotation itinerary of crown forms (i.e. regular, stretched, and twisted, see below)

Crown forms of cyclo-octane

regular stretched twisted

Two extensive theoretical studies of the strain energy of the conformations of cyclo-octane by Hendrickson (1964), and Wiberg (1965), have given a more quantitative basis to the structure of the various models. Hendrickson's results favoured the twist-crown or the boat-chair as the minimum energy form; but he suggested that, because of the low transition barriers (< 3 kcal./mole) between these forms and the other crown and chair forms, cyclo-octane will exist at ordinary temperatures as a very mobile conformational mixture. Wiberg's results were very similar, he found three forms with approximately the same energy, the twist-crown and the boat-chair like Hendrickson, with the regular crown as a third possibility. His

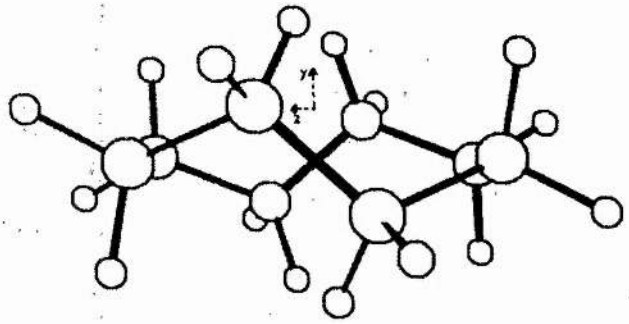

CYCLO-OCTANE TWIST CROWN

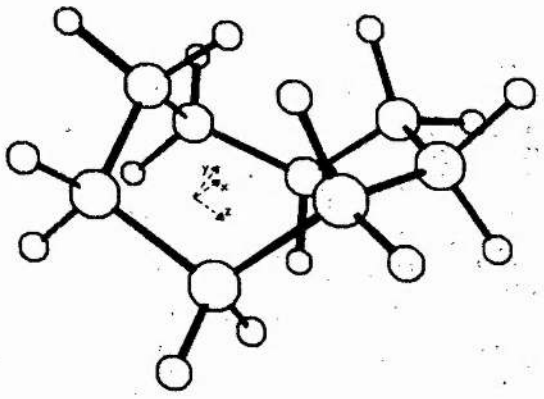

CYCLO-OCTANE BOAT CHAIR

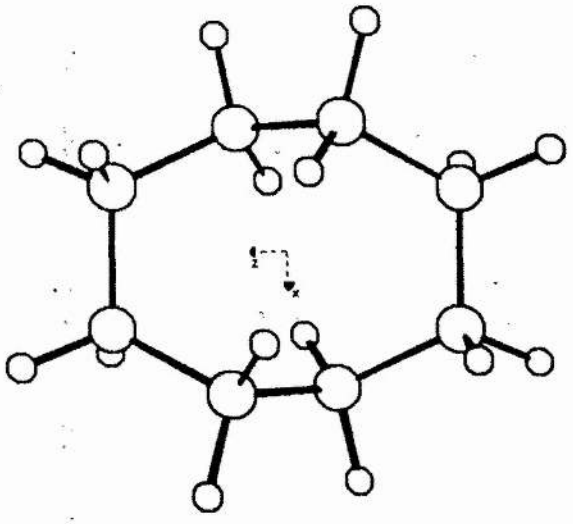

CYCLO-OCTANE TWIST CROWN

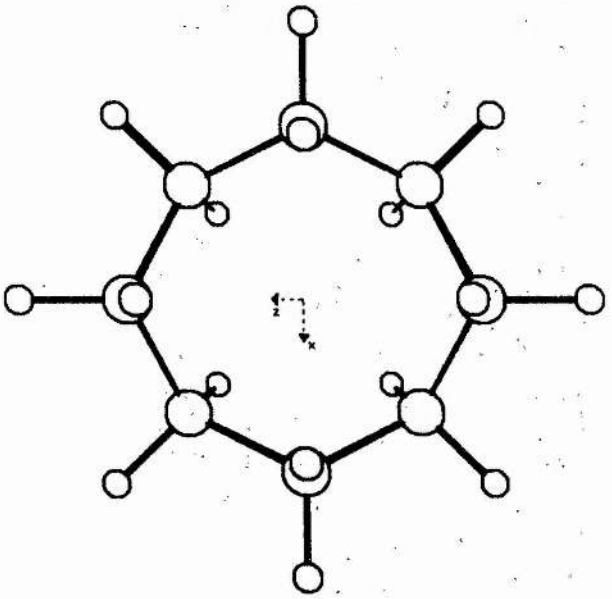

CYCLO-OCTANE CROWN

fig. 6.1

CYCLO-OCTANE CROWN WIBERG MODEL NO.I

****

ORIGIN=1 DUMMY ATOMS =1,2
FIRST CARBON = 3 AND 11 LAST CARBON =10

NO	DATA INPUT BOND LENGTH	BOND ANGLE	DIHEDRAL ANGLE	COMPUTED CARBON COORDINATES X	Y	Z
2	1.811	0.00	180.00	-1.811	0.000	0.000
3	.334	90.00	0.00	-1.811	.335	0.000
4	1.540	64.25	67.55	-1.281	-.335	-1.282
5	1.540	112.60	223.65	0.000	.335	-1.813
6	1.540	112.60	92.70	1.281	-.334	-1.282
7	1.540	112.60	267.30	1.811	.335	0.000
8	1.540	112.60	92.70	1.278	-.335	1.281
9	1.540	112.60	267.30	-.005	.334	1.809
10	1.540	112.60	92.70	-1.285	-.335	1.274
11	1.540	112.60	267.30	-1.811	.335	-.009

****

C-H = 1.108

BOND ANGLES CCC	HCH	NO.	COMPUTED HYDROGEN COORDINATES X	Y	Z	X	Y	Z
112.6	108.6	3	-1.505	1.400	.004	-2.918	.285	.002
112.6	108.6	4	-2.064	-.282	-2.064	-1.067	-1.401	-1.068
112.6	108.6	5	0.000	1.401	-1.510	0.000	.283	-2.920
112.6	108.6	6	2.064	-.282	-2.064	1.067	-1.400	-1.068
112.6	108.6	7	1.508	1.401	0.000	2.917	.282	.002
112.6	108.6	8	2.059	-.282	2.065	1.064	-1.401	1.066
112.6	108.6	9	-.004	1.400	1.506	-.008	.282	2.915
112.6	108.6	10	-2.071	-.286	2.054	-1.071	-1.400	1.055

****

INTRA-MOLECULAR SECOND MOMENT

= 19.97 GAUSS*2 FOR 16 PROTONS

table 6·I

CYCLO-OCTANE TWIST CROWN HENDRICKSON MODEL NO.III

****

ORIGIN=1 DUMMY ATOMS =1,2,3
FIRST CARBON = 4 AND 12 LAST CARBON =11

NO	DATA INPUT BOND LENGTH	BOND ANGLE	DIHEDRAL ANGLE	COMPUTED CARBON COORDINATES X	Y	Z
2	1.458	0.00	180.00	-1.458	0.000	0.000
3	0.000	90.00	0.00	-1.458	0.000	0.000
4	.766	51.75	90.00	-1.458	-.475	-.602
5	1.533	112.00	209.47	-.759	.142	-1.819
6	1.533	112.00	88.60	.747	-.148	-1.824
7	1.533	112.00	297.20	1.455	.474	-.615
8	1.533	112.00	88.60	1.464	-.470	.593
9	1.533	112.00	239.40	.763	.147	1.809
10	1.533	112.00	88.60	-.740	-.152	1.819
11	1.533	112.00	297.20	-1.455	.460	.609
12	1.533	112.00	88.60	-1.461	-.489	-.595

****

C-H = 1.108

BOND ANGLES CCC	HCH	NO.	COMPUTED HYDROGEN COORDINATES X	Y	Z	X	Y	Z
112.5	108.6	4	-2.507	-.711	-.870	-.943	-1.417	-.329
112.0	108.7	5	-.916	1.239	-1.808	-1.209	-.273	-2.743
112.0	108.7	6	1.190	.263	-2.752	.904	-1.244	-1.810
112.0	108.7	7	.936	1.412	-.336	2.500	.714	-.893
112.0	108.7	8	2.513	-.704	.861	.948	-1.412	.319
112.0	108.7	9	.913	1.245	1.794	1.218	-.261	2.734
112.0	108.7	10	-1.184	.260	2.747	-.890	-1.250	1.810
112.5	108.6	11	-.948	1.405	.331	-2.503	.690	.887

****

INTRA-MOLECULAR SECOND MOMENT

= 20.36 GAUSS*2 FOR 16 PROTONS

table 6·2

CYCLO-OCTANE TWIST CROWN WIBERG MODEL NO.V SET 1

****

ORIGIN=1 DUMMY ATOMS =1,2,3
FIRST CARBON = 4 AND 12 LAST CARBON =11

NO	DATA INPUT BOND LENGTH	BOND ANGLE	DIHEDRAL ANGLE	COMPUTED CARBON COORDINATES X	Y	Z
2	1.484	0.00	180.00	-1.484	0.000	0.000
3	0.000	90.00	0.00	-1.484	0.000	0.000
4	.770	133.33	90.00	-1.484	.528	-.560
5	1.540	110.10	330.45	-.771	-.024	-1.808
6	1.540	116.90	279.20	.769	.024	-1.809
7	1.540	116.90	49.40	1.483	-.529	-.562
8	1.540	110.10	279.20	1.485	.528	.558
9	1.540	110.10	120.80	.771	-.024	1.807
10	1.540	116.90	279.20	-.768	.026	1.808
11	1.540	116.90	49.40	-1.484	-.526	.561
12	1.540	110.10	279.20	-1.484	.531	-.560

****

C-H = 1.108

BOND ANGLES CCC	HCH	NO.	COMPUTED HYDROGEN COORDINATES X	Y	Z	X	Y	Z
110.2	109.3	4	-.958	1.438	-.208	-2.530	.788	-.819
116.9	107.3	5	-1.133	.543	-2.689	-1.082	-1.078	-1.944
116.9	107.3	6	1.080	1.079	-1.945	1.129	-.542	-2.691
110.1	109.3	7	2.528	-.789	-.823	.957	-1.438	-.210
110.1	109.3	8	.959	1.437	.206	2.531	.787	.818
116.9	107.3	9	1.134	.542	2.688	1.081	-1.079	1.942
116.9	107.3	10	-1.078	1.081	1.944	-1.129	-.540	2.689
110.2	109.3	11	-2.529	-.784	.821	-.959	-1.436	.208

****

INTRA-MOLECULAR SECOND MOMENT

= 20.08 GAUSS*2 FOR 16 PROTONS

table 6·3

CYCLO-OCTANE BOAT CHAIR HENDRICKSON MODEL NO. IV

****

ORIGIN=1 DUMMY ATOMS =1,2
FIRST CARBON = 3 AND 11 LAST CARBON =10

NO	DATA INPUT BOND LENGTH	BOND ANGLE	DIHEDRAL ANGLE	COMPUTED CARBON COORDINATES X	Y	Z
2	1.530	0.00	180.00	-1.530	0.000	0.000
3	0.000	90.00	0.00	-1.530	0.000	0.000
4	1.533	90.00	80.68	-1.282	0.000	-1.513
5	1.533	114.30	238.85	0.000	.723	-1.942
6	1.533	113.50	68.60	1.282	0.000	-1.512
7	1.533	114.30	291.40	1.530	0.000	0.000
8	1.533	115.20	315.60	1.294	1.343	.701
9	1.533	114.30	105.20	.001	1.409	1.521
10	1.533	113.50	291.40	-1.269	1.387	.662
11	1.533	114.30	68.60	-1.529	.052	-.046

****

C-H = 1.108

BOND ANGLES CCC	HCH	NO.	COMPUTED HYDROGEN COORDINATES X	Y	Z	X	Y	Z
113.1	108.4	3	-2.581	-.299	.183	-.866	-.756	.464
114.3	108.1	4	-2.144	.485	-2.012	-1.229	-1.050	-1.862
113.5	108.3	5	0.000	1.739	-1.501	.001	.822	-3.045
114.3	108.1	6	2.145	.485	-2.011	1.229	-1.050	-1.861
115.2	107.8	7	2.578	-.311	.183	.867	-.757	.464
114.3	108.1	8	1.266	2.141	-.067	2.150	1.545	1.375
113.5	108.3	9	.007	2.339	2.122	-.025	.546	2.215
112.9	108.5	10	-1.171	2.156	-.130	-2.132	1.652	1.304

****

INTRA-MOLECULAR SECOND MOMENT

= 21.43 GAUSS*2 FOR 16 PROTONS

table 6.4

CYCLO-OCTANE BOAT CHAIR WIBERG MODEL NO.II SET 1

****

ORIGIN=1 DUMMY ATOMS =1,2
FIRST CARBON = 3 AND 11 LAST CARBON =10

NO	DATA INPUT BOND LENGTH	BOND ANGLE	DIHEDRAL ANGLE	COMPUTED CARBON COORDINATES X	Y	Z
2	1.589	0.00	180.00	-1.589	0.000	0.000
3	.730	90.00	0.00	-1.589	.730	0.000
4	1.540	50.50	79.30	-1.368	-.250	-1.168
5	1.540	117.40	242.50	-.001	-.213	-1.874
6	1.540	125.30	49.40	1.367	-.249	-1.168
7	1.540	117.40	310.60	1.588	.730	0.000
8	1.540	109.60	95.20	1.280	.023	1.333
9	1.540	114.00	315.20	-.014	-.812	1.314
10	1.540	114.40	286.70	-1.309	.022	1.331
11	1.540	114.00	73.30	-1.616	.728	-.003

****

C-H = 1.108

BOND ANGLES CCC	HCH	NO.	COMPUTED HYDROGEN COORDINATES X	Y	Z	X	Y	Z
109.8	109.4	3	-.904	1.594	-.107	-2.637	1.089	-.011
117.4	107.2	4	-2.151	-.057	-1.928	-1.529	-1.277	-.786
125.3	104.9	5	-.001	.699	-2.504	-.001	-1.056	-2.594
117.4	107.2	6	2.150	-.057	-1.928	1.528	-1.277	-.787
109.6	109.4	7	.916	1.603	-.119	2.642	1.074	-.001
114.0	108.2	8	1.196	.789	2.129	2.128	-.644	1.584
114.4	108.0	9	-.013	-1.444	.404	-.014	-1.481	2.197
113.2	108.4	10	-1.234	.785	2.131	-2.162	-.646	1.564

****

INTRA-MOLECULAR SECOND MOMENT

= 20.79 GAUSS*2 FOR 16 PROTONS

table 6·5

results particularly favoured the twist-crown as the lowest energy conformation. Computer drawn perspective views of the three forms are shown in figure 6.1. Two projections of the twist-crown form are shown for clarity. The structural parameters and the computed co-ordinates for the various molecular models are shown in tables 6.1 to 6.5. All five of these minimum energy forms, together with their tetrahedral counterparts, have been considered as possible molecular configurations in the solid state of cyclo-octane for this investigation.

6.2.2 Thermal Data

Finke et al. (1956) have studied the low temperature thermal properties of cyclo-octane. They found three stable crystalline forms with the transitions between them occurring readily. The transition temperatures are given in table 6.6 below, and the temperature variation of the heat capacity is shown as the continuous curves in figure 6.3. The dashed vertical lines in figure 6.3 are the transition temperatures given by Finke.

Table 6.6

Transition Type	Temperature °K	Entropy of Transition in e.u. (cal. deg.$^{-1}$ mole^{-1})
1st order solid-solid	166.5	9.052
1st order solid-solid	183.8	0.622
Fusion	287.98	2.000
Vaporization	298.16	34.75

It is to be noted that the entropy change at 166.5°K is very

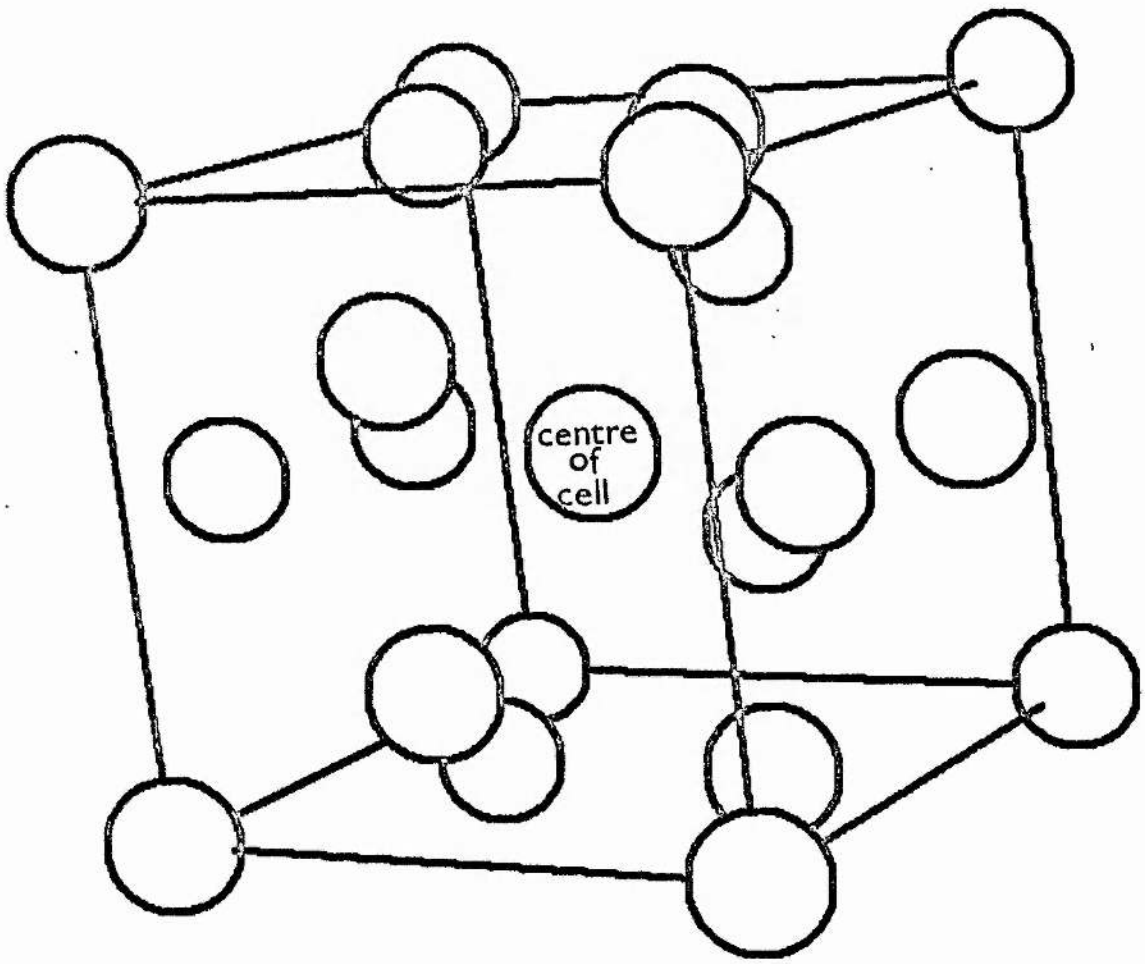

. CYCLO-OCTANE UNIT CELL

Pm3n

fig6·2

much greater than the entropy of fusion.

6.2.3 Crystal Structure

Sands and Day (1965) using X-ray diffraction determined the unit cell structure of the crystalline form I stable between 183.8°K and 287.98°K. The unit cell was cubic with edge a, where a = 11.90 ± 0.05 A° at 0°C and a = 11.82 A° at -64°C. From their limited data they were unable to determine the molecular structure directly. However their results were consistent with a crown form of cyclo-octane, with eight molecules per unit cell. The suggested dis-positions of the molecules within the cubic cell are shown in figure 6.2. This arrangement has six molecules in positions (.25, 0, .5; .5, .25, 0; 0, .5, .25; .75, 0, .5; .5, .75, 0; 0, .5, .75) and two molecules in positions (0, 0, 0; .5, .5, .5). This arrangement is similar to a body centred cubic lattice with the addition of two molecules on each face of the cube. The cubic symmetry of the cell implied disordering of the molecules on their lattice sites with the possibility of molecular over-crowding due to steric effects. This latter situation arises because a disordered crown requires a radius of 4.9 A°, whereas the cavity available in the lattice only has a radius of 4.0 A°.

6.3 Results

6.3.1 Temperature variation of Absorption Spectrum

The variation of the line width and second moment of cyclo-octane are shown in figures 6.3 and 6.4. The same precautions as for cyclo-

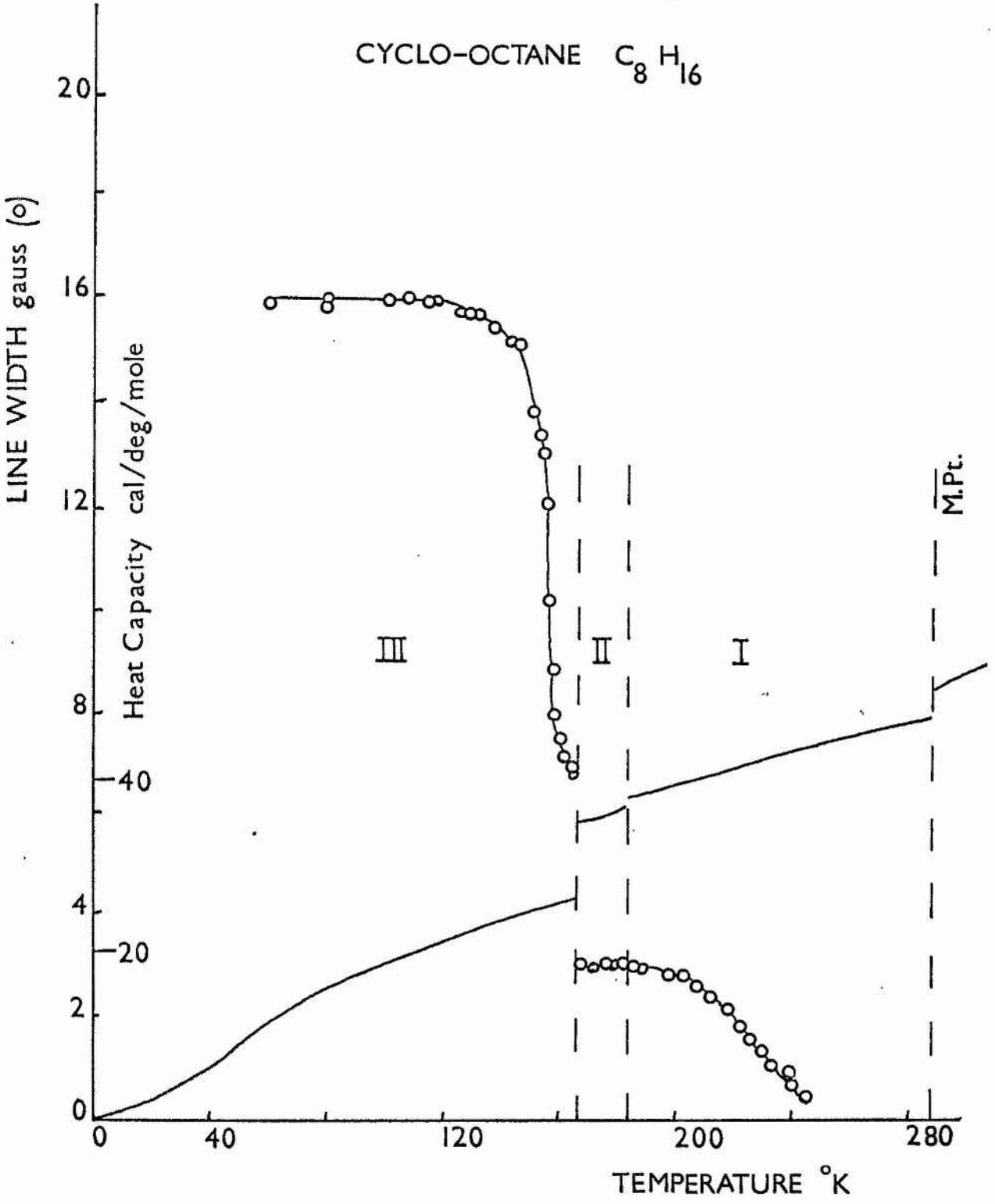
CYCLO-OCTANE $C_8 H_{16}$
LINE WIDTH gauss (o)
Heat Capacity cal/deg/mole
20
16
12
8
4
2
0
40
20
0
40
120
200
280
TEMPERATURE °K
III
II
I
M.Pt.

fig.6·3

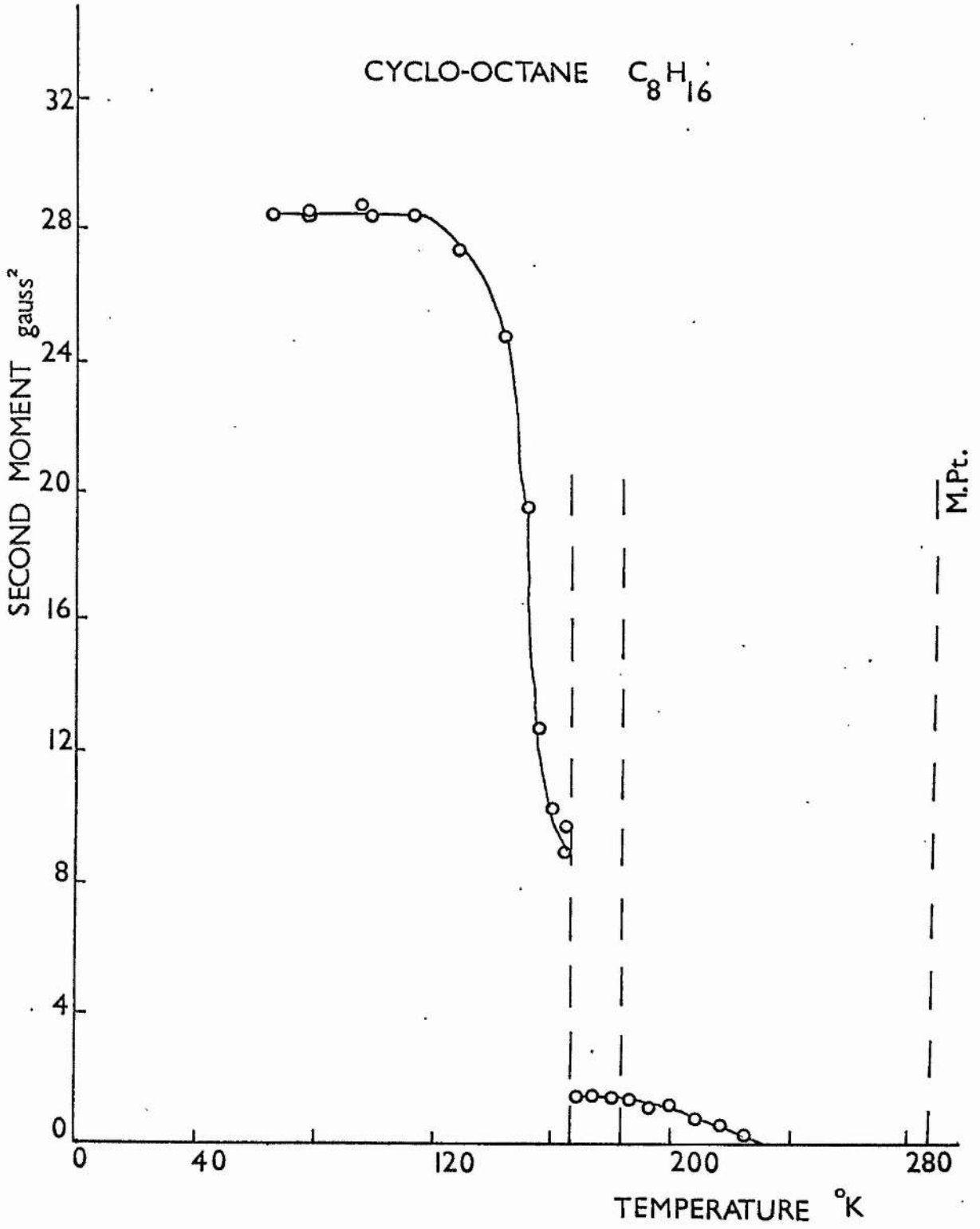
CYCLO-OCTANE C_8H_{16}
SECOND MOMENT gauss^2
32
28
24
20
16
12
8
4
0
0
40
120
200
280
TEMPERATURE °K
M.Pt.

fig 6·4

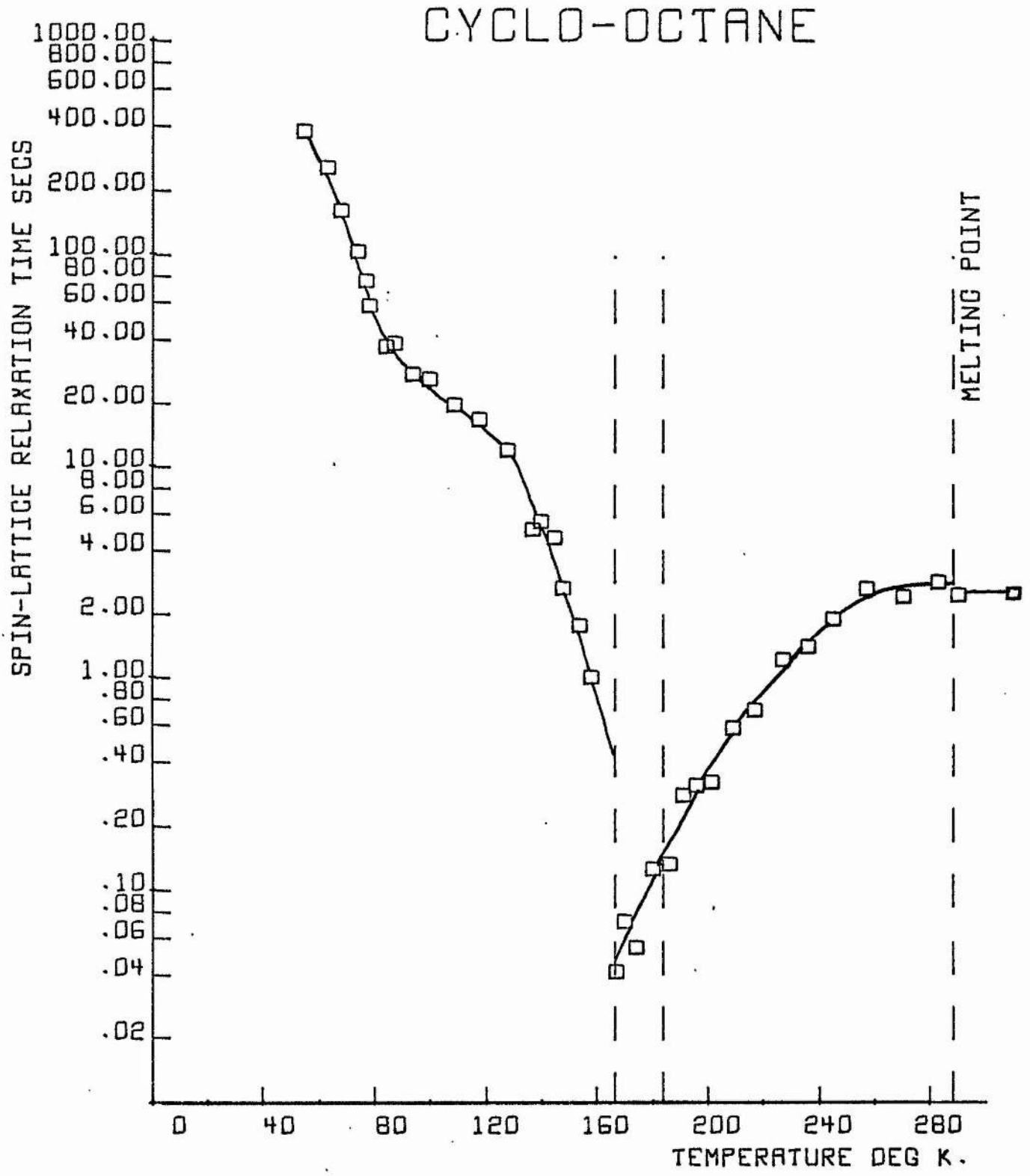
CYCLO-OCTANE
SPIN-LATTICE RELAXATION TIME SECS
1000.00
800.00
600.00
400.00
200.00
100.00
80.00
60.00
40.00
20.00
10.00
8.00
6.00
4.00
2.00
1.00
.80
.60
.40
.20
.10
.08
.06
.04
.02
MELTING POINT
0
40
80
120
160
200
240
280
TEMPERATURE DEG K.

fig.6·5

heptane were taken regarding supercooling and temperature gradients.

Below 120°K the line width and second moment of phase III attain steady values of 15.8 ± 0.3 gauss and 28.5 ± 0.5 gauss^2 respectively. Between 120°K and the III-II transition at 166.5°K there is a rapid reduction in the line width to 6.5 ± 0.3 gauss and the second moment to 9.5 ± 1.0 gauss^2. The larger uncertainty in the latter value is due to possible contributions to the second moment from the 'wings' of the absorption curve. This additional uncertainty is always present for second moment values in the intermediate region between plateaux values, (Abragam 1961). This reduction is similar to the situation observed at the IV-III transition in cyclo-heptane. In phase II they once more attain steady values of 2.9 ± 0.1 gauss and 1.5 ± 0.1 gauss^2, and at the II-I transition there is no significant change. Above a temperature of 200°K a gradual reduction is observed in both quantities to values of approximately 0.2 gauss and 0.05 gauss^2, governed by the magnet field inhomogeneity. No fine structure was apparent in the spectrum for any of the three solid phases.

6.3.2 Spin Lattice Relaxation

The temperature variation of the spin lattice relaxation time T_1 is shown in figure 6.5. The values below 166.5°K were measured by the direct recovery method on the Y-T plotter. Above 166.5°K, in phases II and I, the absorption signals were strong and the storage oscilloscope method could be employed.

6.4 Discussion

6.4.1 Absorption Spectrum

(a) Rigid Lattice.

Theoretical values for the rigid lattice intra-molecular second moment are given in table 6.7 for the three suggested molecular forms of cyclo-octane.

Table 6.7

Cyclo-octane: Rigid Lattice intra-molecular second moment for various minimum energy molecular conformations

		All bond angles tetrahedral (109.47)	Variable bond angles (see tables 6.1 to 6.5)	
		C-H = 1.108 A°	C-H = 1.108 A°	C-H = 1.09 A°
crown	(W)	21.51	19.97	21.21
twist-crown	(H)	21.40	20.36	21.57
	(W)	-	20.96	21.32
boat-chair	(H)	28.96	21.43	22.57
	(W)	-	20.79	22.03

(H, Hendrickson's data. W, Wiberg's data, no parameters for tetrahedral forms given. All values in gauss^2)

These values were obtained with the computer programme described in Appendix A using the structural parameters of Hendrickson (1964) and Wiberg (1965) given in tables 6.1 to 6.5. The difference between the values obtained by these two authors for the same molecular form can be attributed to their use of different base parameters. Hendrickson favours a C-C bond length of 1.533 angstroms and a C-H bond length of 1.108 angstroms, whereas Wiberg uses the values C-C =

1.54 angstroms and C-H = 1.100 angstroms. The second moment depends strongly on the C-H bond length, and the results obtained with two different values are shown for comparison.

The crystal structure of cyclo-octane in phase III is not known, and in view of the large entropy change at the III-II transition, it is expected to be very different from the structure found for phase I. An exact calculation for the inter contribution to the second moment therefore cannot be made. It would seem probable that the molecules will be effectively stationary at low temperatures in phase III, and so by comparing the lattice energy of this phase with the values for the other cycloalkanes, see table 5.7, an estimate of 9.5 ± 1 gauss^2 has been made for the rigid lattice inter-molecular second moment. At temperatures below 120°K the experimental second moment has a constant value of 28.5 ± 0.5 gauss^2. If the estimated inter contribution of 9.5 ± 1 gauss^2 is deducted, an intra value of 19.0 ± 1.5 gauss^2 is obtained. This is to be compared with the theoretical values given in table 6.7. All the values for the boat-chair model are greater than this value, particularly the tetrahedral form. However in view of the lack of knowledge of the crystal structure no clear distinction can be made between the various models, apart from excluding the tetrahedral boat-chair. The reasonable agreement with the other values supports the suggestion of an effective rigid lattice below 120°K, with the absence of any general motion at a rate sufficient to modify the

absorption spectrum, (i.e. greater than about 10^5 c/s).

(b) Spectrum between 120°K and 166.5°K.

The observed large reductions in the line width and second moment in this region suggest the onset of considerable molecular motion at a rate greater than 10^5 c/s. This situation is similar to the behaviour of cycloheptane. The variation just before the III-II transition suggests the beginning of a new plateau region which is interrupted by the transition. Any interpretation of the values observed in this region must be approached with some circumspection, since the second moment is only a well defined quantity for plateau values well removed from transition regions. In the transition regions the experimental values are very dependent on such factors as the modulation amplitude and spectrometer sensitivity. The most probable form of motion responsible for the observed reduction would be either general flexing of the ring through pseudo-reorientation, or rapid reorientation about a molecular symmetry axis. In table 6.8 the values are given for the effect of this motion on the intra contribution for the various models. These values were obtained using the computer programmes given in Appendices A7 and A1. The symmetry axes refer to the co-ordinate axes given in figure 6.1. Only reorientations between the 4-fold positions of the crown form gives a large reduction. Since no plateau value is established, implying incomplete averaging, this form of motion would be consistent with an estimated intra contribution of 1.9 $gauss^2$ or greater.

Table 6.8

Cyclo-octane: reduced intra-molecular second moment for molecular reorientation

	pseudo-reorientation (see Appendix A7)	Motion of the rigid molecule about an n-fold symmetry axis					
		x-axis		y-axis		z-axis	
		n = 2	free rotation	n = 4	free rotation	n = 2	free rotation
crown	0.8	10.9	3.7	1.9 (n = 2)	1.9	10.9	3.7
twist-crown	2.8	14.4	7.0	13.7	5.3	12.9	3.8
boat-chair	1.2	(No symmetry axis, only a plane of symmetry)					

(all values in gauss^2)

By comparison with other molecules for similar types of motion (e.g. reorientation of cyclohexane about its triad axis) a reduction of between a third and a quarter is expected in the estimated inter contribution i.e. to about 3 ± 1 gauss^2. Deducting this from the experimental value of 9.5 ± 1 gauss^2, an estimated intra contribution of 6.5 ± 2.0 gauss^2 is obtained. As mentioned previously any comparison of this value with the values given in table 6.8 is necessarily of qualitative significance only. Since free rotation of the molecules in this phase would appear unlikely, and the values for reorientations between the other symmetry positions of the various axes all appear too large, a form of pseudo-reorientation would be another possibility. This also would be occurring at a rate too slow to provide complete averaging of the dipolar interactions for the various positions of the reorientational itinerary. With com-

plete averaging for this type of motion a plateau region would be expected. Because no definite plateau value of the line width was observed, it was not possible to carry out a sensible analysis of the line width variation with the relations 2.9 and 2.10 to obtain an activation energy for the motion.

(c) Spectrum between 166.5°K and 183.8°K. (Phase II)

In phase II the line width and second moment show steady values of 2.9 ± 0.1 gauss and 1.5 ± 0.1 gauss^2 respectively. In view of the large entropy change at the III-II transition and the low value of the second moment, it is to be expected that more general motion occurs in phase II than that postulated for phase III. From table 6.8 it would appear that motion about any single symmetry axis would not explain the observed low value, particularly as the inter contribution must be added to these values for comparison with the experimental value. Lack of knowledge of the crystal structure of phase II prevents an exact calculation of the inter contribution for pseudo-reorientation, but in view of the drastic reduction of the intra contribution, a low inter value might be expected (~ 1 gauss^2). The reduced intra values given in table 6.8 do not take account of possible 'rocking' of the molecules in the pseudo-reorientational itinerary, so that even lower values might be expected. From these considerations, this form of motion in phase II would appear consistent with the observed second moment.

An alternative calculation for the second moment in phase II can

be made on the following assumptions:

(1) that the major contribution to the second moment is due to inter-molecular dipolar interactions.

(2) that whatever the details of the molecular motion, it sufficiently approximates to the situation of quasi-isotropic reorientation that the expression 2.15 of Dimitrieva and Moskalev (1964) can be applied to calculate the inter contribution.

(3) that the low entropy change at the II-I transition implies a similar crystal structure for phases II and I.

The unit cell crystal structure of phase I of cyclo-octane is known, see figure 6.2, and the value of the lattice summation $\sum_i N_i R_i^{-6}$ for this type of cell has been computed in Appendix A12. Using this value and making a reasonable assumption for the lattice contraction between -64°C (where the unit cell edge a = 11.82 Å) and phase II, it is possible to obtain from 2.15 a value for the second moment for quasi-isotropic reorientation of the molecules on their lattice sites. For a linear contraction of the unit cell with temperature, a value of 1.0 gauss^2 is obtained. This can be expected to be a lower limit, since the II-I transition would probably bring the molecular centres closer together by tighter packing of the molecules in phase II. The reasonable agreement between this estimated value and the experimental value of 1.5 $\pm$ 0.1 gauss^2 supports the proposal of quasi-isotropic reorientation in phase II. The small residual dis-

agreement could be attributed to a slight anisotropy of the motion.

Because of the uncertainty in the crystal structure parameters in phase II, the experimental results do not permit any clear distinction between the two alternatives for the motion i.e. between pseudo-reorientation of a flexible ring or isotropic reorientation of a rigid ring. It is of course equally probable that the motion is in fact a combination of the two alternatives. One consequence of the latter combined motion would be a lower activation energy for molecular reorientation.

(d) Spectrum above 183.3°K. (Phase I)

The lack of any significant change in the line width and second moment at the II-I transition suggests that the molecular motion present in phase I is very similar to that proposed for phase II. The reductions observed in both quantities above 200°K indicate the appearance of an additional form of motion with a mean rate greater than 10^4 c/s. This motion is sufficiently general to average the remaining inter contribution to the second moment, to a value less than that due to the inhomogeneity of the field over the sample (i.e. 0.05 gauss^2). By analogy with the behaviour of cyclohexane C_6H_{12} and cycloheptane C_7H_{14}, this motion is most likely to be self-diffusion of the molecules through the crystal lattice. In view of the closely packed structure of the unit cell found for phase I of cyclo-octane, this diffusion will be vacancy migration rather than interstitial. This diffusion probably begins at the II-I transition,

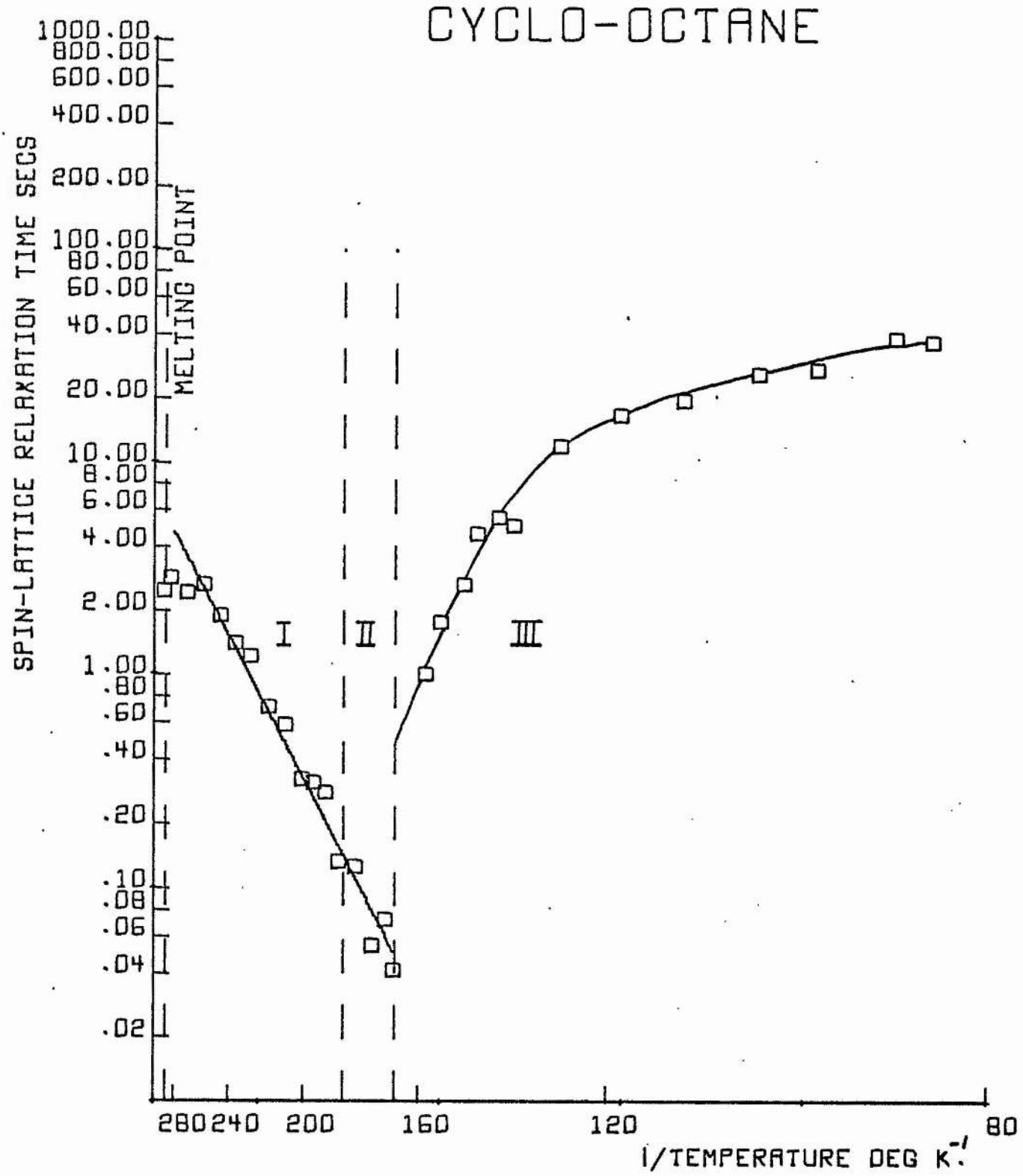
CYCLO-OCTANE
SPIN-LATTICE RELAXATION TIME SECS
1000.00
800.00
600.00
400.00
200.00
100.00
80.00
60.00
40.00
20.00
10.00
8.00
6.00
4.00
2.00
1.00
.80
.60
.40
.20
.10
.08
.06
.04
.02
MELTING POINT
I
II
III
280
240
200
160
120
80
1/TEMPERATURE DEG K.-1

fig.6-6

but at a rate too small ($< 10^4$ jumps per second) to affect the line width.

6.4.2 Spin Lattice Relaxation time T_1

The very long T_1 values observed at low temperatures supports the proposal that below 120°K in phase III the molecules are effectively stationary. It seems probable that below 120°K the relaxation is controlled by a combination of factors such as lattice vibrations, torsional oscillations and paramagnetic impurities. The type of motion suggested as responsible for the observed reductions in the line width and second moment above 120°K in 6.4.1 would be expected to contribute to the spin lattice relaxation. However it is only possible to distinguish the effect of one contribution if, by comparison with other contributions, it is so much more effective that it alone dominates the variation of T_1. In figure 6.6 the logarithm of T_1 is plotted against reciprocal temperature for the variation of T_1 above 80°K. A dominant one-motion process would show as a straight line on this graph. From the graph it is possible that above 120°K one contribution is beginning to dominate the variation of T_1, but any simple interpretation of the variation in this region would obviously be very speculative. Also there is a possibility of a systematic error in the values below about 2 seconds when the measured T_1's become comparable with the shortest usable time constant of the lock-in amplifier. This source of error places a lower limit on the T_1 values obtainable by the direct recovery method.

The T_1 values measured in phases II and I were obtained from strong 'liquid like' absorption signals by the storage oscilloscope technique, and so will not be subject to the same limitation as the low values obtained in phase III. In figure 6.6 it can be seen that the variation above the III-II transition is substantially a straight line relationship. The increase of T_1 with temperature indicates that whatever new motion began at the III-II transition, it commenced with a mean frequency greater than the resonance frequency (22.6 Mc/s). This is case (2) of equation 2.17, $\omega_o^2 \tau_c^2 \ll 1$. A least squares calculation of the best straight line through the experimental points yields an activation of 3.7 ± 0.3 kcal./mole from the Arhennius relation. The points that occur just below the melting point have been omitted from this calculation, since they are believed to be modified by another form of motion.

In view of the molecular chaos of the proposed motion present in phases II and I, quasi-isotropic reorientation of a flexible molecule, it is obviously a simplifying assumption to ascribe the calculated activation energy to any single relaxation mechanism. However it is of the same order of magnitude found for isotropic reorientation in similar molecules with a 'globular' molecular envelope, and this agreement gives further support to the proposed motion.

In phase I, the increasing rate of self-diffusion of the molecules with temperature will provide a further contribution to the

spin lattice relaxation. At 200°K this rate is less than the resonance frequency of 22.6 Mc/s. so that a decrease in T_1 for higher temperatures will be expected. The observed levelling of T_1 above 260°K in figure 6.5 can be explained on this basis. The two values of T_1 for the liquid state of cyclo-octane show that little change occurs in the molecular motion on melting. This is in agreement with the low value obtained for the entropy of fusion.

7. CYCLOHEPTATRIENE C_7H_8

7. Cycloheptatriene C_7H_8

7.1 The Sample

The sample of cycloheptatriene was kindly given by Mr. Lloyd of the Chemistry Department, St. Andrews University. This sample, which was a pale yellow liquid, was understood to have a purity of approximately 99 mole %. A 60 Mc/s high-resolution proton magnetic resonance spectrum of this specimen showed no bands other than those attributable to the pure substance. As a further precaution a spectrum of a small quantity of the specimen with approximately 5% of toluene added was obtained. Toluene was anticipated as a possible impurity, and because of the known persistence of methyl group reorientation at very low temperatures, it was important to be aware of its presence. Comparison of the two spectra revealed no detectable toluene bands in the spectrum of the pure substance.

A small quantity of the sample was degassed and distilled under vacuum into three thin walled Monax glass specimen tubes as described in Appendix B. A clear liquid was obtained from the third distillation into the specimen tubes. This clear liquid gave an identical high-resolution n.m.r. spectrum as that obtained from the original pale yellow sample. The colour of the original specimen was understood to be caused by the presence of small traces of a dimer of cycloheptatriene. The formation of this dimer is catalysed by the presence of oxygen, and this was confirmed by the gradual

CYCLOHEPTATRIENE C_7H_8

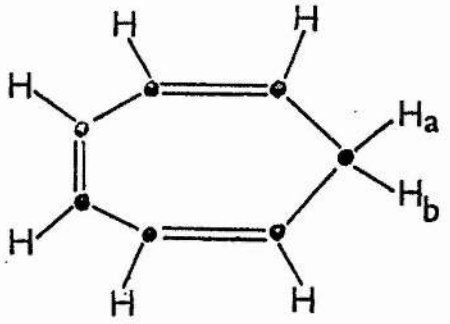

bond structure

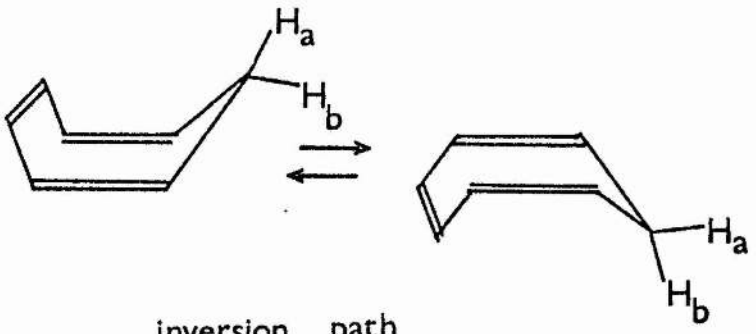

inversion path

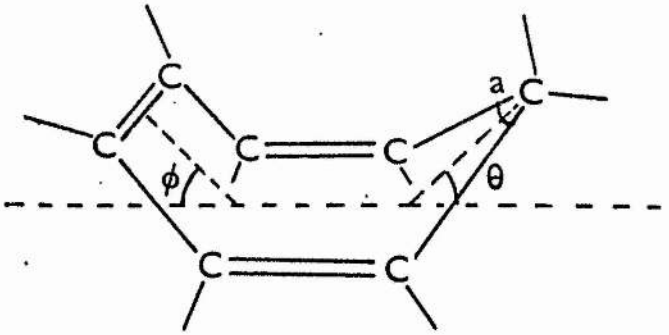

degree of non-planarity

fig. 7·1

darkening in the colour of a quantity of the sample kept in an ordinary stoppered bottle. The clear liquid sealed under vacuum in the specimen tubes showed no change in colour with time.

7.2 Physical Data

7.2.1 Molecular Structure

1,3,5-cycloheptatriene, hereafter called CHT, is a partially saturated seven-membered carbon ring compound with the bond structure shown in figure 7.1. Early Raman and infra-red spectral measurements by Evans and Lord (1960), were interpreted on the basis of a planar structure for CHT; but the possibility of the methylene carbon being slightly out of the plane of the other six carbon atoms could not be ruled out. Later infra-red studies by Lau and Ruyter (1963) of CHT and the monodeuterated CHT compound 7-D-CHT, confirmed the non-planarity of the carbon ring.

The non-planarity has received further support from the high-resolution n.m.r. studies of dilute solutions of CHT and 7-D-CHT by Anet (1964), and Jensen and Smith (1964). Both of these studies show that the methylene peaks of the spectrum separate into two distinct bands below -140°C. This separation indicates that the apparent equivalence of the peaks at room temperature is due to a rapidly inverting non-planar structure rather than the supposed planar structure (see figure 7.1). The activation energy for ring inversion was found to be 6.3 ± 0.5 kcal./mole. A subsequent investigation of the microwave spectrum of CHT by Butcher (1965) gave

the following parameters for the degree of non-planarity of the ring. (see figure 7.1) $\phi = 29.5° \pm 4°$, $\theta = 50° \pm 5°$, all C-C-C bond angles 124.5°, except methylene carbon angle a = 105°.

7.2.2 Thermal Data

Finke et al. (1956) have reported an extensive study of the low temperature thermal properties of CHT. Their results are summarised in table 7.1 below, and the variation of heat capacity they obtain is shown as the continuous curves in figure 7.2. The dashed vertical lines in figure 7.2 are the transition temperatures given by Finke.

Table 7.1

Transition Type	Temperature °K	Entropy of Transition in e.u. (cal. deg.$^{-1}$ mole^{-1})
λ-type	153.98	3.643
Fusion	197.92	1.402
Vaporization	298.16	31.02

They report that CHT exists in two crystalline forms, but the form stable at low temperatures has an anomalous curve of heat capacity versus temperature. In the range 82-92°K, the heat capacity changes to a higher level in a short temperature interval in a manner characteristic of organic glasses, see figure 7.2. The transition at 153.98°K to the form I, stable at higher temperatures, is preceded by a range of rapidly increasing heat capacity. This λ-type of transition has been classified as a type 2I transition under the

scheme given by McCullough (1963). Finke suggests it is unlikely that the 82-92°K anomaly involved "freezing in" of any disorder to produce residual entropy at very low temperatures. If the crystals did have residual entropy, then the observed calorimetric values of the entropy would be uncertain by more than the experimental errors. Although the entropy change at the solid-solid lambda transition for CHT is about half that found for cycloheptane and cyclo-octane, it is still very much greater than the entropy of fusion for CHT.

7.2.3 Crystal Structure

Reed and Lipscomb (1953) using X-ray diffraction attempted to determine the molecular structure of CHT by studying single crystals of the high temperature phase I. A cubic unit cell (edge $a = 10.6 \pm 0.1$ A°) was found, yielding only five reflections in a reciprocal lattice of O_h symmetry. The assumption of eight molecules in this unit cell gave a calculated density of 0.99 g. cm^{-3}. The paucity of reflections prevented any simple interpretation of this highly disordered phase. A major transition was found to occur at about -125°C, during which single crystals were transformed into a powder as the temperature was lowered. An inability to grow single crystals of this lower phase prevented any further studies.

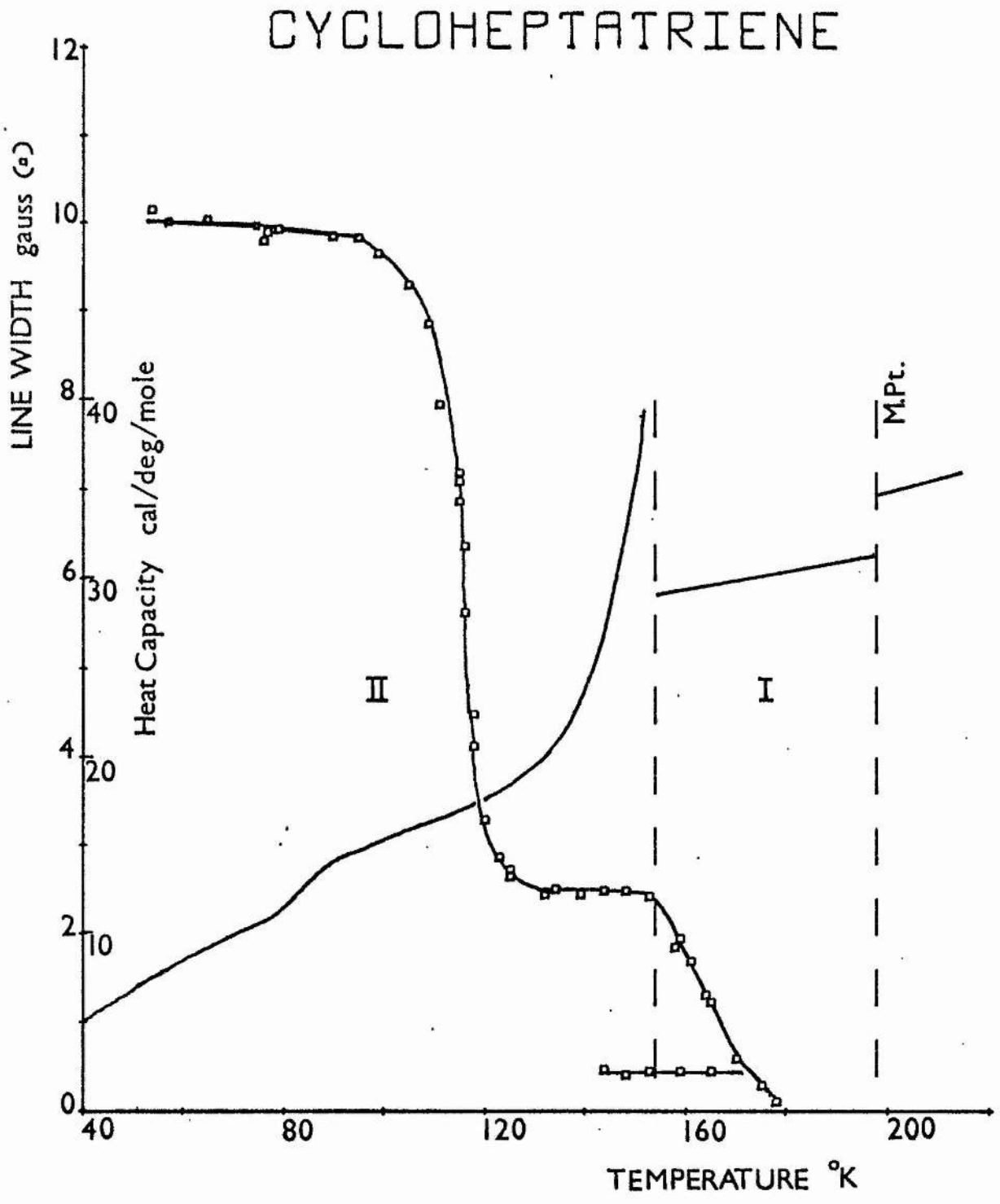
CYCLOHEPTATRIENE
LINE WIDTH gauss (a)
Heat Capacity cal/deg/mole
M.Pt.
II
I
TEMPERATURE °K
12
10
8
6
4
2
0
40
30
20
10
40
80
120
160
200

fig.7·2

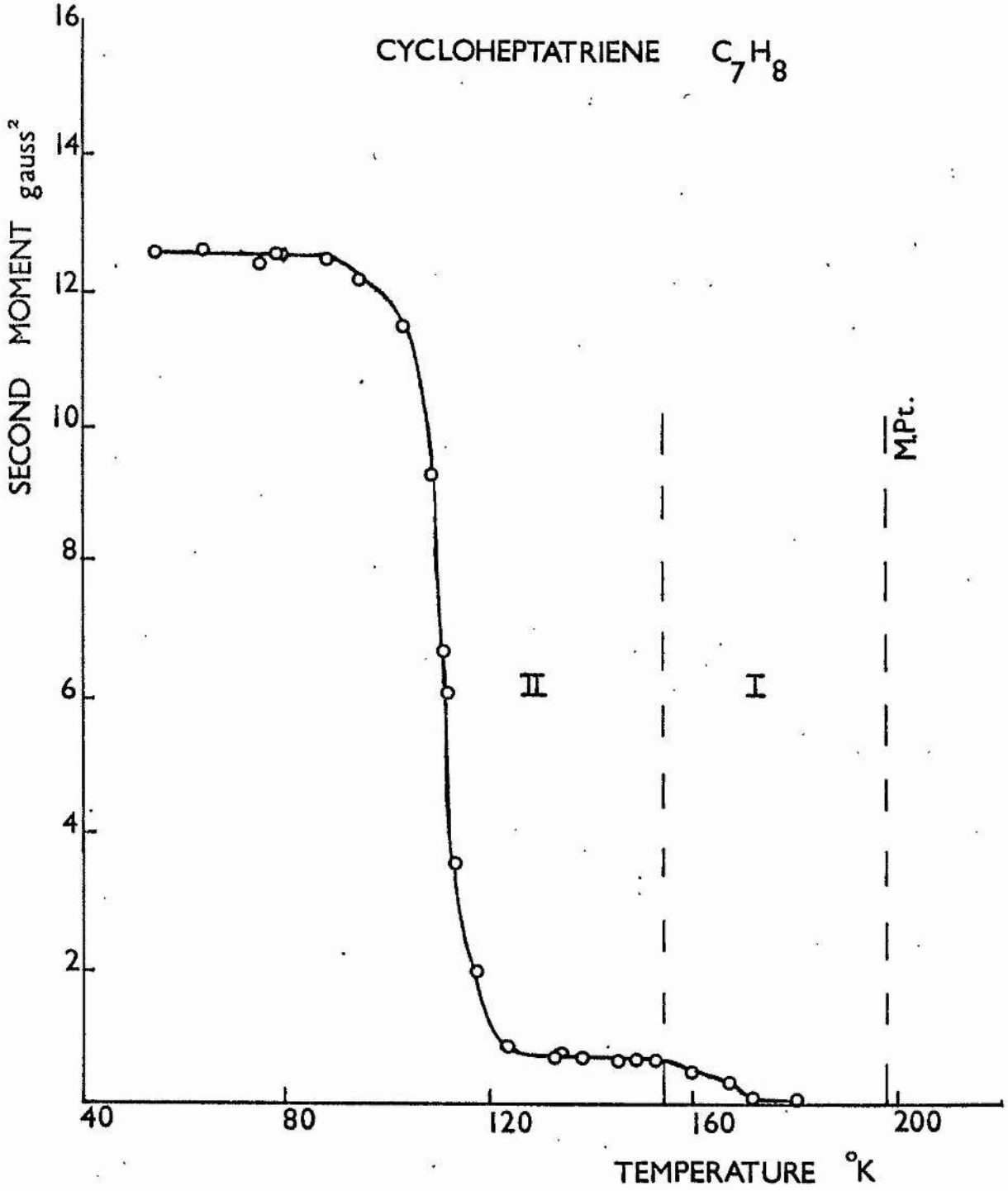
CYCLOHEPTATRIENE C_7H_8
SECOND MOMENT gauss^2
16
14
12
10
8
6
4
2
II
I
M.Pt.
40
80
120
160
200
TEMPERATURE °K

fig.7·3

7.3 Results

7.3.1 Temperature variation of Absorption Spectrum

The variation of the line width and second moment of CHF are shown in figures 7.2 and 7.3. All the measurements were taken as a series of increasing temperatures to avoid supercooling effects.

Below 80°K the line width and second moment of phase II attain steady values of 10.0 ± 0.2 gauss and 12.5 ± 0.3 gauss^2 respectively. Beginning at the region of the heat capacity anomaly at 82-92°K there is a continuous reduction in both quantities to new plateaux values of 2.4 ± 0.1 gauss and 0.81 ± 0.05 gauss^2. The plateaux values extend from about 130°K to the II-I transition at 154°K. At a temperature of about 145°K fine structure was observed in the absorption derivative curves. The modulation amplitude was reduced in an attempt to resolve this narrow component, but its true line width appeared to be distorted by the magnet field inhomogeneity. The apparent width of this narrow component is plotted as a separate line in figure 7.2. As the temperature was increased the resolution of the narrow component improved, but at all times its true width appeared distorted by the field inhomogeneity. At the II-I transition a slight reduction was observed in the broad component, and this continued smoothly until, at about 175°K, the observed line width of both components was governed by the field inhomogeneity. A similar variation was shown by the second moment, after the II-I phase transition its value fell from 0.6 ± 0.1 gauss^2 to less than

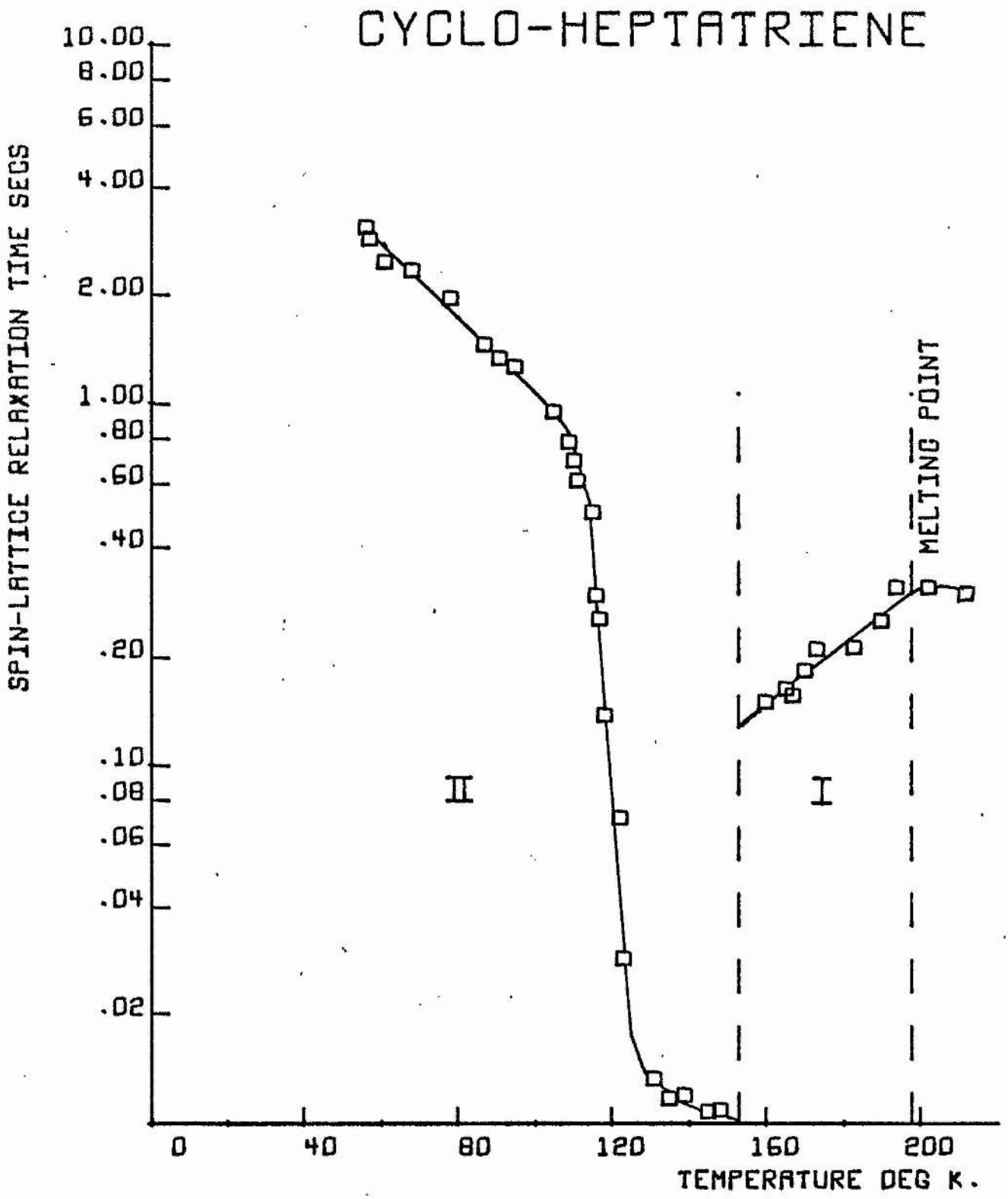
CYCLO-HEPTATRIENE
SPIN-LATTICE RELAXATION TIME SECS
10.00
8.00
6.00
4.00
2.00
1.00
.80
.60
.40
.20
.10
.08
.06
.04
.02
0
40
80
120
160
200
TEMPERATURE DEG K.
MELTING POINT
II
I

fig.7-4

0.05 gauss^2.

7.3.2 Spin Lattice Relaxation

The temperature variation of the spin lattice relaxation time T_1 is shown in figure 7.4. All of these values were obtained by the storage oscilloscope technique. To obtain sufficient amplitude of the modulation field to observe the full width of the absorption spectrum below 80°K, (line width = 10 gauss) the mains frequency of 50 c/s was used. This was coupled to the modulation coils through a variac. The relatively short values of T_1, even down to 54°K in phase II, meant that the signal was at all times sufficiently strong for oscilloscope display. The values obtained below 0.02 secs may be subject to a slight systematic error due to the finite recovery time of the receiver system from the switching transients of the r.f. attenuator. The duration of these transients was checked on a fast oscilloscope, and they appeared to have decayed to negligible proportions within 8 msec after switching the attenuator.

7.4 Discussion

7.4.1 Absorption Spectrum

(a) Rigid Lattice.

A theoretical value for the intra-molecular second moment of CHT was calculated on the basis of the molecular structure parameters given by Butcher (1965), see figure 7.1. These parameters had been obtained from a comparison of the moments of inertia of a CHT molecule, with

those calculated from the observed bands of the microwave spectrum. To simplify the analysis Butcher took only one parameter, the C-C-C bond angle, and varied this to fit a quantity which was the most sensitive function of the non-planarity of the molecule. The remaining structure parameters were then derived from this angle by assuming that the three ethylene groups were planar, and that the C = C, C-C, and C-H bond lengths were similar to those for analogous molecules.

The derived parameters are very sensitive functions of the C-C-C bond angle, and unfortunately it became apparent during the computer calculation of the carbon co-ordinates, that the values given by Butcher were slightly in error. However since the computed values were still within the uncertainties given by Butcher, they were used in the actual calculation of the intra-molecular second moment. Because of the relatively large separations between most of the hydrogen atoms, the effect on the second moment of the slight differencies between the values was found to be small. The computed values were preferred on the grounds of consistency, and a better methylene C-C-C angle a. (i.e. closer to a tetrahedral value of 109.47°)

Comparison of values for the derived angles (see figs. 7.1, 7.5)

	ϕ	θ	angle a, $C_6C_7C_8$
Butcher's values	29.5° ± 4°	50° ± 5°	105°
Computed values	31.3°	46.7°	108.18°

1,3,5-CYCLOHEPTATRIENE C_7H_8

****

ORIGIN=1 DUMMY ATOMS =1,2,3

FIRST CARBON = 4 AND 11 LAST CARBON =10

NO	DATA INPUT BOND LENGTH	BOND ANGLE	DIHEDRAL ANGLE	COMPUTED CARBON COORDINATES X	Y	Z
2	0.000	0.00	180.00	0.000	0.000	0.000
3	1.211	148.74	0.00	-1.035	.628	0.000
4	.670	90.00	90.00	-1.035	.628	-.670
5	1.470	124.50	0.00	0.000	0.000	-1.503
6	1.340	124.50	322.07	1.309	-.001	-1.215
7	1.500	124.50	0.00	1.912	.641	0.000
8	1.500	108.18	59.69	1.309	0.000	1.215
9	1.340	124.50	300.31	0.000	.001	1.503
10	1.470	124.50	0.00	-1.035	.629	.670
11	1.340	124.50	37.95	-1.035	.628	-.670

COMPUTED			HYDROGEN COORDINATES		
C-H=1·10	CCC=108·18	HCH=109·9	1.687	1.725	0.000
			3.008	.482	0.000
12	1.100	122.00	180.00	-1.833	1.113	-1.253
13	1.100	113.50	142.07	-.398	-.484	-2.407
14	1.100	122.00	180.00	2.050	-.485	-1.868
15	1.100	113.50	120.31	2.049	-.484	1.869
16	1.100	122.00	180.00	-.398	-.483	2.407
17	1.100	113.50	217.93	-1.833	1.113	1.252

INTRA-MOLECULAR SECOND MOMENT

= 6.19 GAUSS*2 FOR 8 PROTONS

table 7·2

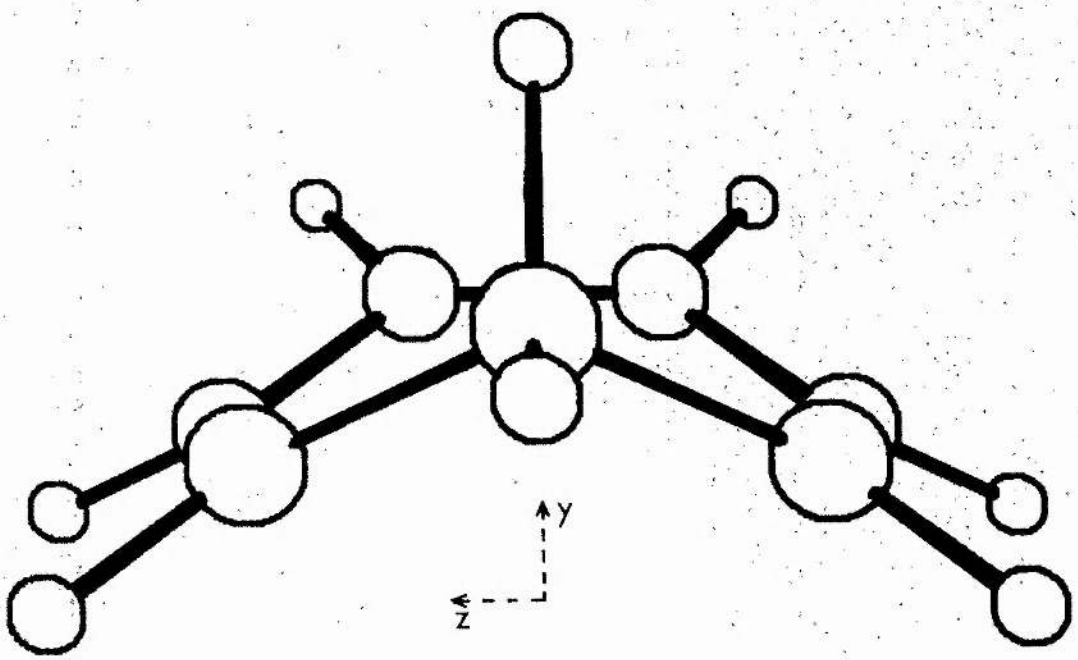

CYCLOHEPTATRIENE view a.

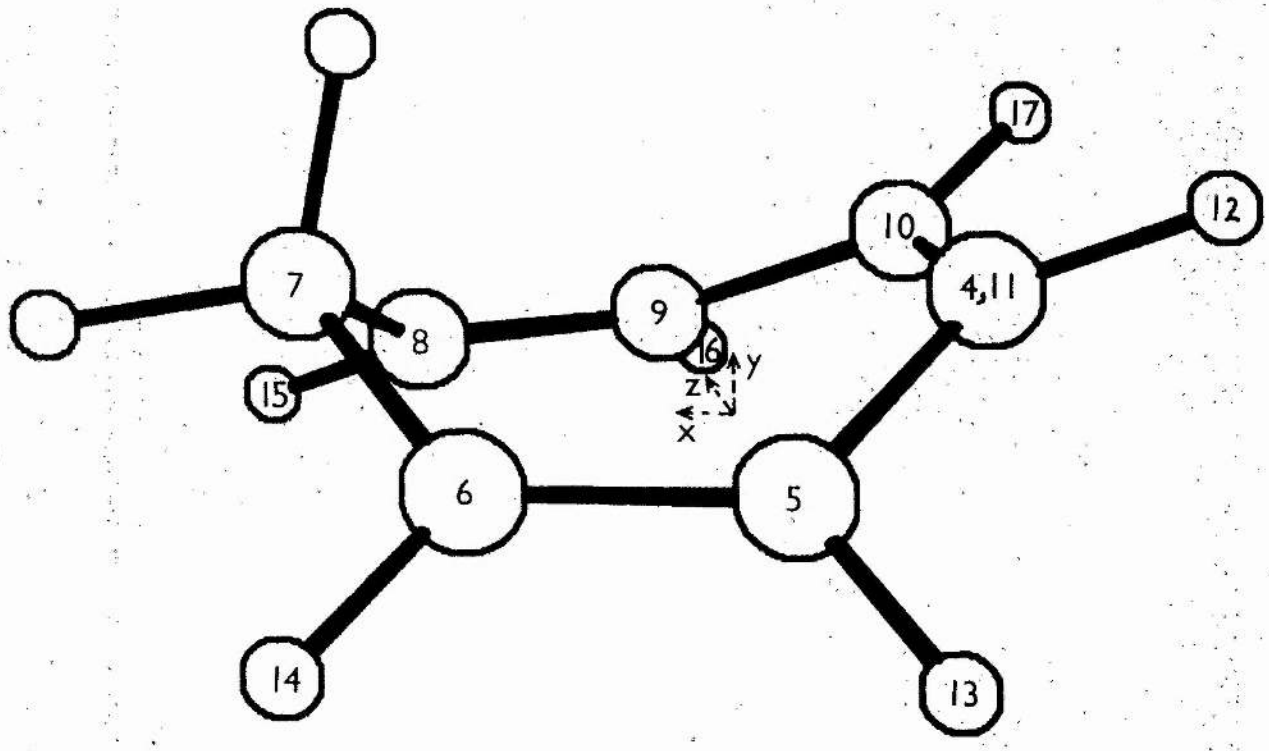

CYCLOHEPTATRIENE view b.

fig 7·5

The computer programme given in Appendix A14 was used to calculate the atomic co-ordinates and the intra second moment. The results are shown in table 7.2, and a computer drawn perspective view of these final co-ordinates is shown in figure 7.5. Two different views of the molecule are given to emphasize the atomic arrangement. View a is that seen from 10 Å along the x axis, and b is a general view from 10 Å to indicate the labelling of the atoms given in table 7.2. The origin of the co-ordinate system (dummy atom 1) is the mid point of the 5-9 bond, as shown in view b of figure 7.5. Dummy atom 2 is at the same point as 1, and dummy atom 3 is at the mid point of the 4-10 bond. No labels or data input were required for the two methylene hydrogens, since their positions were defined by the co-ordinates of carbon atoms 6, 7 and 8 using the scheme given in Appendix A3. The H-C-H bond angle obtained from this scheme 109.9°, is in fact very close to the tetrahedral value of 109.47° assumed by Butcher. From view a of figure 7.5, it can be seen that a non-planar CHT has no axis of symmetry, only a plane of symmetry containing the methylene group and the mid point of the 4-10 carbon bond, (i.e. the x,y plane).

As is to be expected, almost half of the intra-molecular second moment of 6.19 gauss^2 comes from the interaction between the two methylene protons. Of the remainder, a further third comes from the interaction between the methylene protons and their nearest neighbours.

The crystal structure of the low temperature phase II of CHT is not known, so that an exact calculation of the inter-molecular contribution for the second moment is not possible. The values obtained from n.m.r. studies of other similar cyclic hydrocarbons are shown in table 7.3. These are given in order of progressive saturation of the carbon rings.

Table 7.3

Comparison of the inter-molecular rigid lattice second moment for cyclic hydrocarbons with 8 hydrogen atoms per molecule

Name		Inter Second Moment	Reference
Cyclo-octatetraene	C_8H_8	5.0 ± 1	Lawrenson and Rushworth (1958a)
Cycloheptatriene	C_7H_8	6.0 ± 1	estimate
Cyclopentene	C_5H_8	6.6 ± 1	Lawrenson and Rushworth (1958b)
Cyclobutane	C_4H_8	6.9 ± 1	Hoch and Rushworth (1964)

(all values in gauss^2)

It seems reasonable to assume that the inter value would decrease as the proportion of hydrogen atoms per molecule became smaller. On this basis an estimated value of 6.0 ± 1 gauss^2 for CHT appears acceptable. The combined theoretical intra and inter values give a total of 12.2 ± 1 gauss^2, and this is to be compared with the experimental value of 12.5 ± 0.3 gauss^2. The latter value is only observed for temperatures below 80°K in phase II.

The good agreement between the two values indicates that below 80°K the molecules are effectively stationary in the crystal lattice. The agreement also supports the parameters obtained by Butcher for the non-planar form of CHT. Lack of knowledge of the crystal structure of CHT in phase II prevents any finer distinction to be made between possible small variations of these parameters on the basis of the n.m.r. results.

(b) Spectrum between 80°K and the II-I transition at 154°K.

The coincidence of the specific heat anomaly and the changes observed in the spectrum above 80°K suggest that they have a common origin. The very low plateau value of 0.81 ± 0.05 gauss^2 for the second moment between 130°K and 154°K indicates that considerable molecular motion is present in this region. Molecular reorientation about a symmetry axis is not possible in a non-planar CHT, since it possesses no symmetry axis. Even reorientation about the 2-fold axis of a planar model of CHT would require considerable space in the crystal lattice, and therefore appears very unlikely. An alternative possibility is general motion about a non-symmetry axis. This would be expected to be hindered by the neighbouring molecules in the lattice, but if there was co-operative motion between the molecules, quite rapid motion (greater than 10^5 changes in position per second) could be possible. From the general shape of the molecule (see figure 7.5), it would appear that motion about the y-axis would require the least "swept volume" in the crystal. The effect

of this type of motion on the intra second moment has been calculated with the aid of equation 2.13 using the computer programme described in Appendix A5. This calculation assumes that either all orientations about the axis are equally probable (i.e. free rotation), or at the least, three different positions. The result of this calculation is shown in Table 7.4, together with the values for similar motion about the x and z axes.

Table 7.4

Cycloheptatriene: reduced intra-molecular second moment for molecular motion about co-ordinate axes

Stationary molecule	Free rotation about axes given in fig. 7.5		
	x-axis	y-axis	z-axis
6.19	1.16	0.54	1.49

(all values in gauss^2)

The values for motion about the x and z axes are both greater than the experimental value without including the inter contribution, and in view of the greater "swept volume" required for these motions can probably be discounted. No exact calculation is possible for the effect on the inter contribution for motion about the y axis, since the crystal structure is not known. However an approximate value can be obtained by comparison with a similar motion which occurs in solid benzene C_6H_6. Here Andrew and Eades (1953) found that rotation about the 6-fold axis perpendicular to the plane of the molecule gave a reduction in the inter contribution from 6.52

gauss^2 to 0.91 $\pm$ 0.5 gauss^2. This value of course depends largely on the crystal structure of benzene, and while there is no reason to believe that the structure of phase II of CHT will be similar, it does suggest that the inter contribution for CHT could be reduced from 6.0 $\pm$ 1 gauss^2 to about 1 gauss^2. In view of the shape of the molecule of CHT, appreciable "rocking" might be expected to occur as the molecule rotated about the y axis. This would cause a further reduction in both the estimated intra and inter values, and permit better agreement of their combined value with the experimental value of 0.81 $\pm$ 0.05 gauss^2.

One further possibility for the molecular motion responsible for the observed reductions in line width and second moment between 80°K and 130°K is ring inversion. As mentioned in section 7.2.1, it is known from two studies of dilute solutions of CHT by high-resolution n.m.r. that above 130°K rapid ring inversion is occurring. Provided that the inter-molecular forces of the crystalline field are weak enough, a similar situation might be expected to prevail in phase II of the pure solid of CHT. The forces of the crystalline field cannot be very strong otherwise no molecular motion at all would occur.

The calculation of the effect of this type of motion on the second moment presents some difficulty. Firstly lack of knowledge of the crystal structure of CHT prevents any direct determination of the inter contribution. Secondly, although the inversion path and

the two equilibrium positions of the molecular framework are known, the relation of the atomic co-ordinates before and after the inversion, to the crystal axes is not known. This second factor prevents an exact calculation of the intra contribution. However it is possible to make a calculation under certain assumptions:

(1) that as a result of the ring inversion, the positions of the four planar carbon atoms 5, 6, 8 and 9 (see figure 7.5) remain unchanged, and all the other atoms, except the two methylene hydrogens, take up the position of their mirror image across the x-z plane.

(2) that because the methylene atoms (CH_2) invert as a composite group the relative positions of the two hydrogens are interchanged. This is easily seen from manipulation of a Dreiding model of CHT, and explains the room temperature equivalence of their n.m.r. bands.

(3) that because of the intra-molecular barrier to ring inversion, 6.3 ± 0.5 kcal./mole, the molecule spends most of its time in the two equilibrium positions.

To perform the calculation use has been made of the formulae developed by Andrew and Eades (1953) for the effect of the variation of both θ_{jk} and r_{jk} on the dipolar interaction of the second moment. These formulae are given in Appendix A6, and the computer programme given in A6 was used to compute the averages between the two equilibrium positions of the molecule, of the seven terms of the dipolar interaction for each pair of nuclear spins j and k. The answer

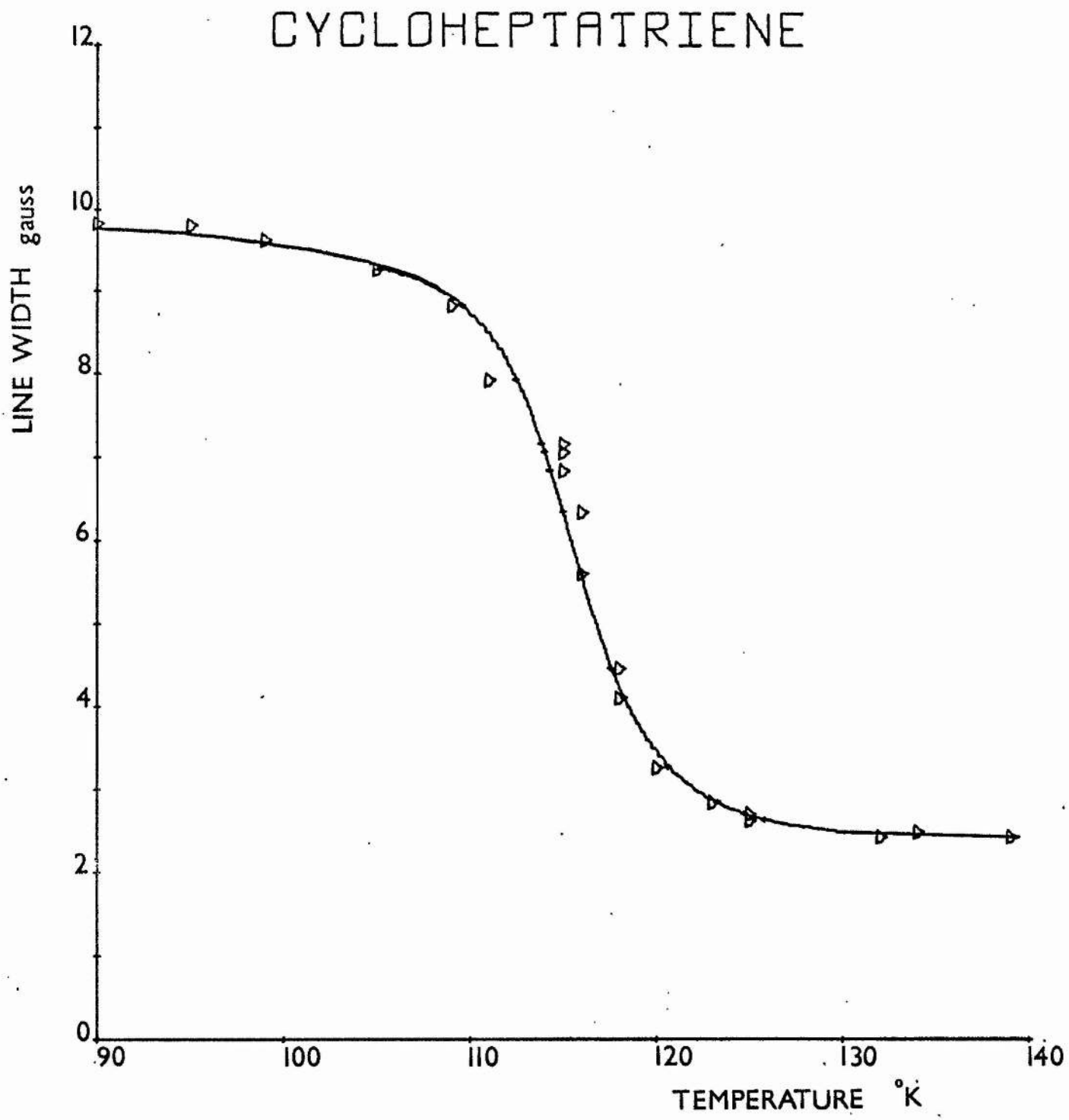
CYCLOHEPTATRIENE
LINE WIDTH gauss
12
10
8
6
4
2
0
90
100
110
120
130
140
TEMPERATURE °K

fig.7·6

obtained under the above assumptions for the effect of ring inversion on the intra-molecular contribution was a reduction from 6.19 gauss^2 to 2.61 gauss^2. This value was only reduced to about 1 gauss^2 if the plane through the four carbons 5, 6, 8 and 9 (see figure 7.5) was permitted to tilt between the inversion positions.

It is difficult to estimate the effect of this type of motion on the inter contribution, but a lower limit of about 0.5 gauss^2 would appear probable, since there is no translational motion of the molecules. On this basis an intra value much less than 1 gauss^2 is required for agreement with the experimental value of 0.81 $\pm$ 0.05 gauss^2.

The major part of the remaining intra contribution of 1 gauss^2 comes from the almost unchanged contributions to the second moment of the proton pairs 13-14, 15-16, 17-12. These contributions would be greatly reduced by any rotation about the y-axis. The molecular envelope of a rapidly inverting CHT ring is approximately "doughnut" shaped, and this would make rotation about the y-axis more facile, so that a combination of these two motions could explain the observed second moment.

Further information about the molecular motion has been obtained from an activation energy analysis of the line width reduction between 80°K and 130°K. In figure 7.6 the observed values of the line width in this temperature region are shown. The smooth curve through the experimental points was drawn by the computer digital

plotter from a computer least squares analysis of the experimental data. This analysis was based on the Kubo and Tomita (1954) relationship 2.10, and the Arhennius equation. The details of the computer programmes are given in Appendices A8 and A9. The computed activation energy from 14 data points was $6.8 \pm .5$ kcal./mole. It is interesting to note that this value is very close to the activation energy found for ring inversion in CHT 6.3 ± 0.5 kcal./mole. This gives further support to the proposal that ring inversion is the dominating molecular motion between 80°K and 154°K.

(c) Spectrum above 154°K, Phase I.

The unit cell structure of phase I of CHT is known, and so it is possible to obtain a second moment value for quasi-isotropic reorientation of the molecules on their lattice sites. This calculation is based on equation 2.15,

$$M_2 = 358.1 \, N_o \sum_{i=1} N_i R_i^{-6} \qquad 2.15$$

The calculation is very similar to that made for cyclo-octane since their unit cell structures are identical (Rudman and Post 1968). Using the value of the lattice summation computed in Appendix A12, and the CHT crystal unit cell edge $a = 10.6$ Å obtained by Reed and Lipscomb (1953), a value of 0.89 gauss^2 is obtained for the second moment. This agrees well with the experimental value of 0.8 ± 0.1

gauss^2 observed just after the II-I transition.

The smooth reduction in both the line width and second moment in phase I, to values less than 0.2 gauss and 0.05 gauss^2, is characteristic of the onset of self-diffusion of the molecules. This motion probably begins immediately after the II-I transition at a rate of the order of the line width, 10^4 jumps per second. Self-diffusion in phase II is most likely prevented by a tighter packing of the molecules in the different crystal structure. The tighter packing in phase II is suggested by the large entropy change at the II-I transition, 3.643 cal. deg.$^{-1}$ mole^{-1} (c.f. entropy of fusion, 1.402 cal. deg.$^{-1}$ mole^{-1}).

It now remains to explain the fine structure observed in the spectrum above 145°K. The most obvious answer is the presence of some hydrogen bearing impurity. The presence of such an impurity, particularly toluene an isomer of CHT, was carefully checked before sealing the samples in the glass specimen tubes. However there are certain conditions when small quantities of an impurity can escape detection by high-resolution n.m.r. A particular example occurs when the impurity spectral peaks are coincident with the main constituent peaks. The methyl peak of toluene for example occurs almost in the middle of the methylene triplet peaks of CHT, and although spectra were obtained from two samples with different 60 Mc/s spectrometers, Varian A60 and a Perkin-Elmer R-10, it is possible that small traces of toluene ($\sim 1\%$) escaped detection.

However the relative areas of the two components of the wide-line spectra seemed to indicate a greater proportion than 1% for the narrow component. The narrow line width, < 0.4 gauss, suggests the presence of a very mobile hydrogen group, and an alternative explanation is that the rapid ring inversion causes the CHT methylene proton spins to become decoupled from their surrounding interactions. Certainly the contribution of the two methylene protons to the second moment is one of those most drastically reduced by ring inversion. The narrow component could then be identified with the contribution from these two protons. It is interesting to note that the high-resolution n.m.r. studies of dilute solutions of CHT show that the methylene triplet is unchanged from room temperature to 153°K, and between 153°K and 133°K a single peak is observed. Only below 132°K is the ring inversion rate slow enough to show non-equivalence of the methylene protons by the separation of the peaks.

7.4.2 Spin Lattice Relaxation time T_1

The general variation of T_1 in the two solid phases of CHT closely mirrors the behaviour of the absorption spectrum, with significant changes associated with the heat capacity transitions at 82-92°K and 154°K, see figure 7.4. In phase II, T_1 becomes longer as the temperature is decreased. It was originally intended to follow the variation below 50°K, using the helium cryostat, to ensure that T_1 continued to increase for lower temperatures in a

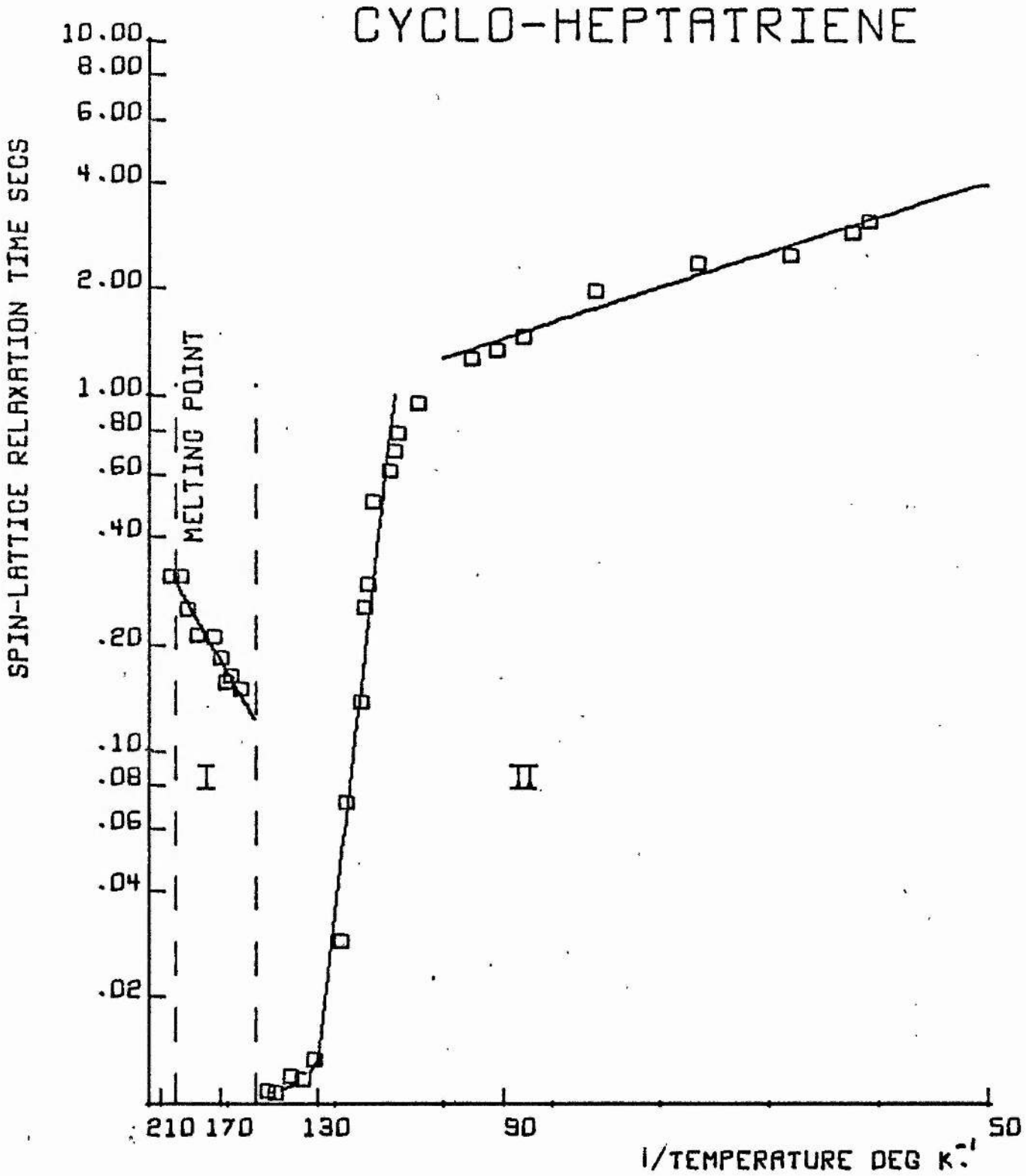
CYCLO-HEPTATRIENE
SPIN-LATTICE RELAXATION TIME SECS
10.00
8.00
6.00
4.00
2.00
1.00
.80
.60
.40
.20
.10
.08
.06
.04
.02
MELTING POINT
I
II
210
170
130
90
50
1/TEMPERATURE DEG K⁻¹

fig.7·7

manner expected for a rigid crystal lattice. But in view of the good agreement obtained for the rigid lattice second moment, it seems reasonable to assume that at these low temperatures, all the gross molecular motion has ceased.

The line width reduction observed at 100°K indicates that at this temperature the motion responsible for the narrowing of the spectrum has an average frequency of approximately 10^4 c/s. This value is less than the resonance frequency of 22 Mc/s, and from the BPP theory, one would expect the motion to cause T_1 to decrease with increasing temperature. This is observed and if it is assumed that the molecular motion can be characterized by a single correlation time τ_c, then the relation between T_1 and τ_c is given by case (1) of the BPP equation 2.17.

$$\text{i.e. for } \omega_o^2 \tau_c^2 \gg 1 \qquad T_1 = (\omega_o^2/2C_1).\tau_c$$

and if τ_c varies with temperature with the Arhennius relation, then the variation of T_1 with temperature is given by

$$T_1 = (\omega_o^2/2C_1)\tau_o \exp(E/RT)$$

where E is the activation energy for the motion. This expression implies a linear relationship for a graph of log T_1 against 1/T. This graph is shown in figure 7.7, and a least squares calculation of the slope obtained from the experimental points in the temperature interval 100-130°K yields an activation energy of 6.1 $\pm$ 0.5 kcal./mole. This temperature range includes the line width tran-

sition, which gave an activation energy of $6.8 \pm .5$ kcal./mole, and the agreement between the values suggests a common origin in the CHT ring inversion for the two processes.

The change in slope of T_1 for values below 95°K indicates that ring inversion ceases to be the dominant relaxation mechanism for these temperatures, and other processes such as lattice vibrations, and torsional oscillations determine the value of T_1. The values of T_1 above 130°K suggest the appearance of a minimum, which is interupted by the II-I phase transition. As mentioned previously the values below 0.02 seconds may be subject to a systematic instrumental error. However their magnitudes in this region are similar to other T_1 minima found for molecules containing mobile CH_2 groups. The methylene group in CHT provides the dominant dipolar interaction, and from case (3) of 2.17, it is possible to calculate a value for the T_1 minimum expected, if motion of the CH_2 group provides the major spin lattice relaxation. The value of the T_1 minimum is calculated from $T_1 = \omega_o/1.42\ C_1$, where C_1, is obtained from the expression

$$C_1 = \frac{2}{5}\ \gamma^4 h^2 I(I+1)\ b^{-6}$$

with b equal to the interproton separation of the CH_2 group. On the basis of a C-H bond length of 1.1 Å and an H-C-H angle of 109.9°, a value of 0.020 secs is found for the T_1 minimum. The reasonable agreement with the experimental values suggest that a minimum in T_1

does occur in this region, but more accurate pulse measurements of T_1, at a lower frequency, would provide a better confirmation of this proposal.

The abrupt change in T_1 at the II-I transition is consistent with the large entropy change of this transition, which implies a greater molecular freedom in phase I than phase II. T_1 is now increasing with temperature indicating motion with a frequency greater than 22 Mc/s. This motion will be the isotropic reorientation of the CHT molecules, in agreement with the value of the second moment just above the II-I transition.

The variation of T_1 in phase I plotted in figure 7.7 suggests a linear relationship. Assuming case (2) of 2.17, a least squares calculation gives an activation energy of 1.7 ± 0.2 kcal./mole for isotropic reorientation from the Arhennius relation. This value will probably be a lower limit, since the increasing rate of self-diffusion of the molecules in this phase, will begin to influence T_1 as the melting point is approached.

The two values of T_1 obtained for the liquid state of CHT, suggest that there is little change in the molecular freedom on melting.

8. SUMMARY OF RESULTS AND COMPARISON WITH THE BEHAVIOUR OF OTHER CYCLIC HYDROCARBONS

8. Summary of the results for cycloheptane, cyclo-octane and cycloheptatriene, and comparison with the behaviour of other cyclic hydrocarbons

8.1 Cycloheptane C_7H_{14} and Cyclo-octane C_8H_{16}

The results obtained for these two medium ring cycloalkanes are very similar. The long spin lattice relaxation times, and plateau values of the second moment show that the molecules of both hydrocarbons are effectively stationary in the crystal lattice of the low temperature phase (IV for C_7H_{14} and III for C_8H_{16}). This situation is slightly modified as the temperature is increased towards the solid-solid transitions. At about 20 degK before the transitions both compounds indicate the presence of molecular motion with an average frequency of 10^5 c/s. Lack of knowledge of the crystal structure, and the failure of a plateau value of the second moment to be established before the transition, prevents a clear identification of the form of molecular motion. After these energetic transitions (the IV-III for cycloheptane and III-II for cyclo-octane) a plateau value of the second moment is observed, with a value consistent with general reorientation of the molecules on their lattice sites. In view of the low energy barriers for pseudo-reorientation or inversion of the ring molecules, 5 kcal./mole for cycloheptane and 7.7 kcal./mole for cyclo-octane, Anet and Hartman (1963), it seems probable that this reorientational motion includes both internal and whole molecule motion. Because of the restricted space available in the crystal lattice, this motion

will not be free rotation of the molecules, but rapid jumps between various orientations. These orientations will be sufficiently general for the time average of the motion to be quasi-isotropic.

After the next transition the packing of the molecules in the new crystal lattice for both compounds is sufficiently modified to permit self-diffusion to occur. This commences at a rate of about 10^4 steps per second and increases rapidly towards the melting points. The X-ray study of the crystal structure of this phase of cyclo-octane shows a lattice spacing insufficient for an interstitial path for molecular self-diffusion, and so a vacancy mechanism would appear probable. The abrupt narrowing of the absorption spectrum observed at the extra solid-solid transition of cycloheptane, II-I, indicates a sudden increase in the diffusion rate caused by a further modification of the lattice.

The term 'plastic crystal' has been applied to the phases of compounds which possess rotational freedom. These crystal phases are composed of molecules with almost spherical envelopes, termed "globular", and have an unusually low entropy of fusion. The high temperature phases of cycloheptane (I, II and III) and cyclo-octane (I and II) satisfy both these conditions on the basis of the n.m.r. results, and the entropies of fusion obtained by Finke et al. (1956).

The n.m.r. results do not provide any clear evidence in favour of one molecular conformation for the two compounds, and apart from certain tetrahedral forms, the results are in agreement with the

various proposed molecular structures, Hendrickson (1961 and 1964), and Wiberg (1965). In one sense the question of any preferred conformation at ordinary temperatures is obviously meaningless, since the low barriers to internal motion imply an equilibrium mixture of rapidly interconverting forms even at quite low temperatures. An X-ray diffraction study of the low temperature crystal phase of both compounds below 100°K would appear a prerequisite to further elucidation of this problem.

8.2 Cycloheptatriene C_7H_8

The good agreement of the experimental second moment observed below 80°K with that estimated for a rigid lattice, and the increasing spin lattice relaxation in this region show the absence of any persistent motion at low temperatures in phase II. Unlike cycloheptane and cyclo-octane, this compound does show a plateau second moment in the low temperature phase, which is established about 25 degK before the first transition. The rapid rise in the heat capacity detected by Finke in this region suggests some form of anomalous behaviour in the crystal. The very low second moment implies quite general motion of the molecules, and since the molecule lacks a symmetry axis, a combination of ring inversion and reorientation about the axis normal to the general plane of the molecule appears probable. Support for ring inversion as the dominant motion is obtained from the activation energies of the line width transition and the spin lattice relaxation.

Table 8·1

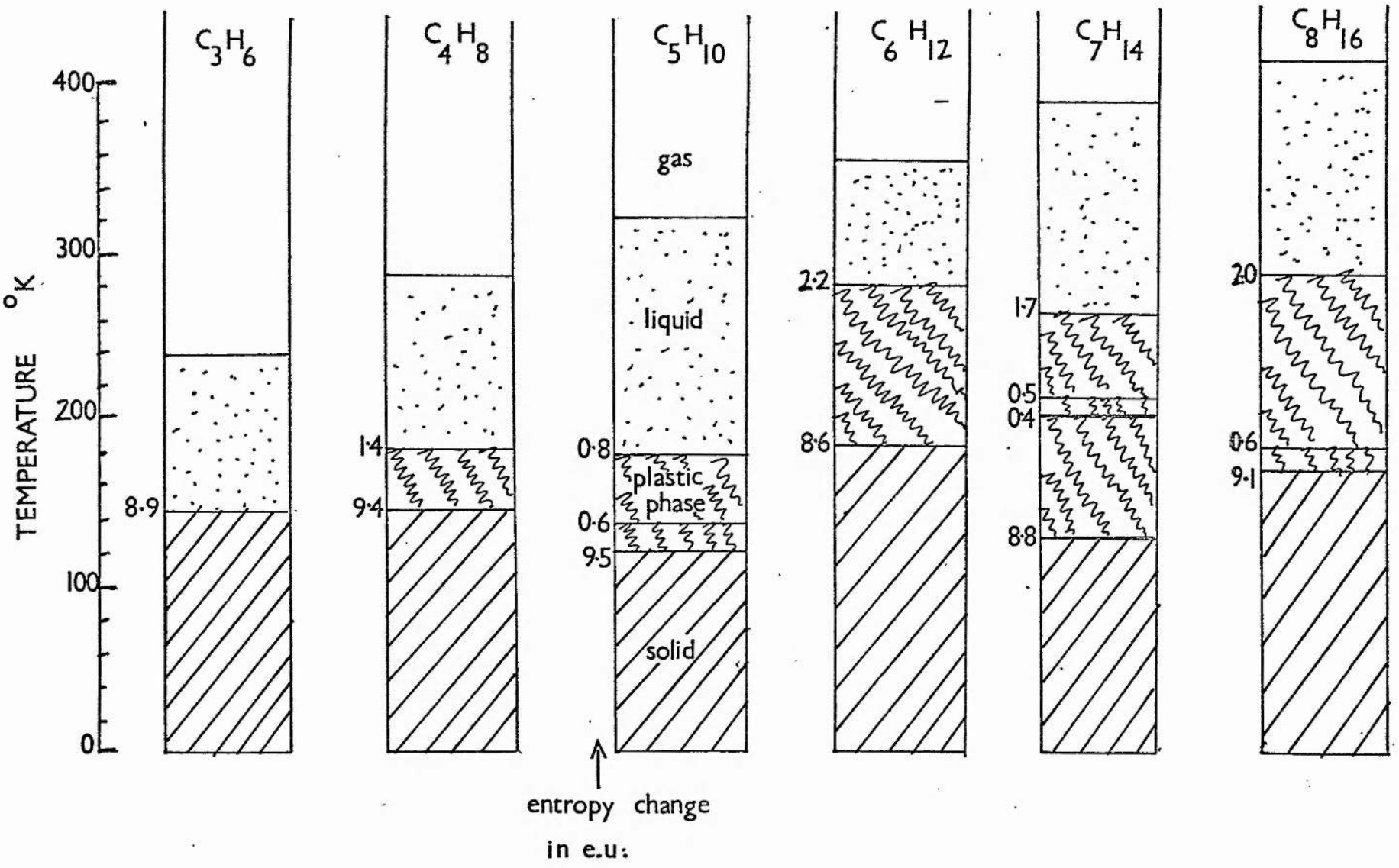
C_3H_6
C_4H_8
C_5H_{10}
C_6H_{12}
C_7H_{14}
C_8H_{16}
TEMPERATURE °K
400
300
200
100
0
gas
liquid
plastic phase
solid
8·9
1·4
9·4
0·8
0·6
9·5
2·2
8·6
1·7
0·5
0·4
8·8
2·0
0·6
9·1
entropy change in e.u.

After the single energetic solid-solid transition, self-diffusion of the molecules is revealed by further narrowing of the absorption spectrum. The low entropy of fusion and the rotational disorder imply a plastic crystal phase also for cycloheptatriene.

8.3 Comparison of Cycloheptane and Cyclo-octane with the smaller rings of the cycloalkane series $(CH_2)_n$

Six members of the cycloalkane series have now been studied by n.m.r. and their solid state behaviour is summarized in table 8.1. Apart from cyclopropane C_3H_6, they all exhibit energetic transitions in the solid state. In cyclopropane a narrowing of the n.m.r. spectrum is detected some 30 degK below the melting point, consistent with reorientation of the molecules about their three fold axes. A similar narrowing is shown in the spectrum of another four of the compounds below the lowest transition. Cyclopentane is the exception, and it is possible that motion does occur, but at a rate too slow to narrow the spectrum ($< 10^4$ c/s).

For the members n = 4 to 8 the lowest transition is the most energetic, and in all cases is followed by a plastic crystal phase in which quasi-isotropic reorientation of the molecules occurs. In some instances this motion is accompanied immediately by self-diffusion, and in others a further transition is required before diffusion is detected. It would be interesting to study the diffusion rates in this series by the ultra-slow motion technique of Allion and Slichter (1965) to measure $T_{1\rho}$, since the previous

n.m.r. measurements in cyclohexane C_6H_{12} are known to give an erroneous value for the activation energy. Another property of this series which requires more careful consideration is the effect of ring flexibility on the solid state behaviour. Cyclopropane, the only rigid molecule of the series, shows a significantly different behaviour.

Many high-resolution commercial n.m.r. spectrometers now have low temperature attachments, and these are finding increasing use in studies of ring inversions and general conformational equilibria. The results to date indicate that ring flexibility is a common feature of the cycloalkanes even at low temperature. The effect on the second moment of mobile CH_3 groups has been known for some time, but the effect of general flexing of larger groups has generally not been considered. It is interesting to note that the many measurements of ring inversion in cyclohexane C_6H_{12} (see Allerhand and Gutowsky 1965) give an activation energy, 10.3 kcal./mole, which is very similar to that found by Andrew and Eades (1953) for reorientation about the 3-fold axis of the molecule in the solid, 10.5 kcal./mole. The tight packing of the molecules in the plastic phases requires any molecular reorientation to be a co-operative process, and internal motions of the molecules would help to explain the ease with which this reorientation appears to occur. It is possible that the motion detected in the more rigid low temperature phases also has its origin in the internal

motions of the molecules, and further experiments are required to test this proposal. The very low barriers to internal motion expected for cyclobutane and cyclopentane suggest these compounds as worthy of further investigation. Cyclobutane is already known to give an anomalous fine structure in the low temperature solid phase.

8.4 General behaviour of ring hydrocarbons in the solid state

The n.m.r. studies of cycloheptatriene show that internal motion is not inhibited by the presence of double bonds in the carbon ring. In fact the introduction of a double bond into the cyclohexane ring C_6H_{12}, to form cyclohexene C_6H_{10} is known to reduce the activation energy for internal motion by half (Anet and Haq 1965). The lower energy barrier in cyclohexene might explain why this compound should have such a large high temperature plateau value of the second moment, 4.7 gauss^2, (Eades 1953). The reduction to this value from the rigid lattice value of 21.9 gauss^2 could possibly be explained on the basis of internal motion of the molecules. Further studies of the polymorphism of unsaturated ring compounds are required to provide a better picture of their solid state behaviour. One aspect which is not clearly understood is why some compounds should exhibit λ-type solid-solid transitions rather than the normal first order. Cyclobutane, cyclopentene and cycloheptatriene belong to this category, and it is interesting to note that all three show fine structure in the absorption spectrum at the

VAPOUR SNAKES

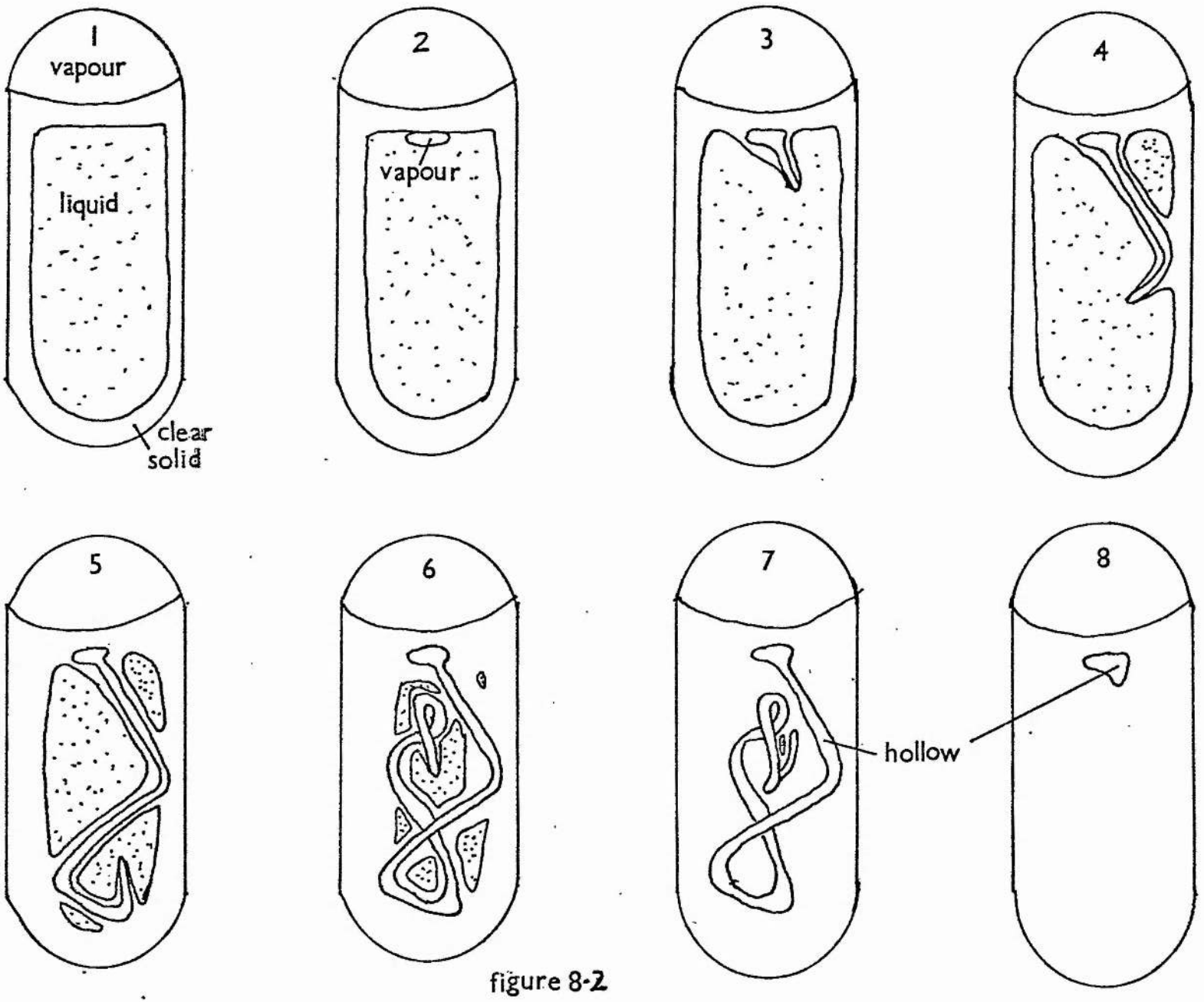

figure 8·2

λ transition. The present evidence suggests that this may originate in rapid internal motion of the molecules in this region.

It is important in any interpretation of the solid state behaviour of organic compounds to be aware of the existence of metastable solid phases. If very pure samples are used, supercooling through the transitions sometimes occurs very easily, and thermal cycling is required to obtain the equilibrium phases.

Another phenomenon associated with very pure organic samples sealed under vacuum is 'Vapour Snakes'. These were found to occur readily on cooling cycloheptane and cyclo-octane, and precautions had to be taken to prevent these hollow snake formations from seriously degrading the r.f. coil filling factor. In figure 8.2 a sequence of drawings illustrates the way the snakes are formed. The sample is sealed under vacuum in a glass tube, and on cooling from the outside three phases are seen; low pressure vapour at the top, uncooled liquid in the middle, and a plastic solid phase growing in from the outside of the tube. If the cooling is reasonably rapid a small bubble is seen to appear just beneath the solid upper crust, this is caused by contraction of the liquid as it cools. This bubble immediately fills with vapour to the vapour pressure of the liquid. The triple point vapour pressures of these compounds are high, and while their entropies of vaporization are normal, their entropies of fusion are small. The large mass transfer that occurs to the bubble therefore results in solidification at the liquid-vapour interface,

and consequently the vapour bubble becomes encased in a solid sheath. Further contraction of the liquid causes the bubble to grow at the weakest part of the sheath. This is at the bottom where the sheath formed last, and hence it grows in the form of a tubule, expanding only at its tip. It travels at a rate governed by the rate of volume contraction of the liquid until all the liquid has solidified. The sequence 1-7 of snake formation shown in figure 8.2 is typical of many snakes observed in cycloheptane and cyclo-octane. The end result is a removal of the sample from the middle of the coil, precisely where it is most required for a good filling factor. This can be avoided if the sample is cooled slowly through the melting point, when only a small bubble at the top is observed, No. 8 figure 8.2. Verschingel and Schiff (1954) have studied a number of compounds that show vapour snakes on solidification, and in each case found it to be related to a high triple point vapour pressure. Apart from degrading the filling factor, no other effects of these snakes was observed. This was to be expected since the snakes are in fact hollow.

APPENDICES

A. Computer Programmes.

B. Sample preparation.

C. Purification of Cycloheptane.

D. Mangelsdorf analysis of exponential curve.

Appendix A

Fortran IID computer programmes used in the work of this Thesis

During the course of this work extensive digital computer facilities became available through the installation in the nearby Mathematics Institute of an IBM 1620 Model II computer. This consists of a core store of 60,000 digits, floating-point arithmetic, index registers, card input and output, line printer, digital plotter and three disk drives. The disk facility was particularly useful since it enabled many library Fortran subroutines to be stored on magnetic disk and called into the working core when required. These library subroutines consisted of both general numerical analysis programmes written by the computing laboratory staff, and programmes particularly suited to n.m.r. problems written by the author. A number of the latter programmes, which are thought to be of more general application, are given in this appendix.

Many of the calculations involved in studies of molecular motion by n.m.r. are in essence simple, but require to be repeated many times, and for this reason are ideally suited to digital computer programmes. Other problems involved are amenable to solution by iterative techniques, and here the facility of digital computers for rapid arithmetic is of inestimable value. The Fortran IID computer language has the advantage that the programme statements are

constructed with symbols very similar to normal mathematical expressions. For this reason the descriptions given with each programme are restricted to the essentials of the mathematical operations, and in some instances the more simple format statements have been omitted from the programme listings. However it is hoped that sufficient information is provided to explain the operation of the programmes.

No listing is given of the programmes provided by the computing laboratory staff, these included a general least squares polynomial fitting subroutine CLFOLF, best straight line subroutine by least squares for two independent variables, solutions of a quadratic equation, and IBM library point plotting subroutines, PLOT, CHAR and POINT. The author wishes to express his thanks to the computing laboratory staff for making these subroutines available, and for their assistance with running the programmes on the computer.

Computer Programmes

A1 Main programme to calculate the co-ordinates and second moment for the cycloalkane series $(CH_2)_n$.

A2 An algorithm to compute atomic co-ordinates from molecular structure parameters.

A3 A scheme to compute the Hydrogen co-ordinates for minimum strain energy of a methylene group (CH_2)

A4 Rigid Lattice second moment.

A5 Second moment reduced by molecular reorientation.

A6 Second moment reduced by general molecular motion.

A7 Atomic co-ordinates in pseudo-reorientation itinerary.

A8 Computer analysis and plotting of line width data.

A9 Activation energy from least squares analysis of line width transition.

A10 Best straight line by least squares and standard deviation.

A11 Dihedral angle between atomic bonds.

A12 Crystal lattice summations of the form $\sum_{i=1} N_i R_i^{-6}$

A13 Experimental second moment from derivative curve.

A14 Cycloheptatriene, co-ordinates and second moment.

A15, A16 Perspective view format and "rounding off".

APPENDIX A1

```
      DIMENSION P(20,3),H1(20,3),H2(20,3),H(200,3),ANG(20,2)
      DIMENSION DATA(20,4),PR(20,3),C(20,2,3)
    4 READ 40,CHBL,LMAX,LMIN
      IF(SENSE SWITCH 1)7,8
    7 PUNCH 40,CHBL,LMAX,LMIN
    8 READ 22,(N,(DATA(N,J),J=1,4),M=2,LMAX)
      CALL RBCXYN(2,LMAX,P,PR,DATA)
      LM=LMAX-1
      DO 42 K =LMIN,LM
      IF (K-LMIN)44,43,44
   43 L1=LM
      K1=LMIN-1
      GO TO 48
   44 IF(K-LM ) 46,47,46
   47 K1=LMAX
      L1=LMIN
   48 DO 45 J=1,3
   45 P(K1,J)=P(L1,J)
   46 CALL RBHXYZ (CHBL,K,P,H1,H2,ANG,0)
      KK=K-LMIN+1
      IF (SENSE SWITCH 1)101,102
  101 CALL RBUNCH(KK,P,H1,H2,LMIN,LMAX)
  102 DO 50 J=1,3
   50 CALL RBROND(3,3,P(K,J),H1(K,J),H2(K,J),DUM,C(K,1,J),C(K,2,J))
   42 CONTINUE
   21 K1=0
      DO 301 J=LMIN,LM
      K1=K1+1
      K=K1*2
      DO 301 L=1,3
      H(K,L)=H2(J,L)
  301 H(K-1,L)=H1(J,L)
      LH=2*(LMAX-LMIN)
      CALL RBSECM(1,LH,H,SECMO,0)
      PRINT 1
      PRINT 40
      PRINT 10
      PRINT 9,LMIN,LMAX,LM
      PRINT 12,(L,(DATA(L,J),J=1,3),(PR(L,J),J=1,3),L=2,LMAX)
      PRINT 10
      PRINT 302,CHBL
      PRINT 51
      PRINT 49,(ANG(K,1),ANG(K,2),K,((C(K,M,J),J=1,3),M=1,2),K=LMIN,LM)
      PRINT 10
      PRINT 300,SECMO,LH
      PRINT 1
    5 READ 2,IC2,NFOLD,RX,RY,RZ
      IF (NFOLD) 4,4,3
    3 PRINT 6
      CALL RBSROT(1,LH,H,NFOLD,RX,RY,RZ,SECMO,1,IC2)
      GO TO 5
```

Appendix A1

Comprehensive Fortran Main Programme for studying molecular structure and motion by the method of the N.M.R. Second Moment

This programme which calls the Fortran Subroutines given in appendices A2, A3, A4, A5 will perform the following operations:

(1) Compute the cartesian co-ordinates of atomic positions from simple molecular structural data such as bond lengths and bond angles.

(2) Compute the co-ordinates of the hydrogen atoms of a methylene group (CH_2) for the minimum strain energy of an irregular tetrahedron.

(3) Provide a punched card output of the computed co-ordinates in a format suitable for drawing perspective views of the molecules on the computer digital plotter.

(4) Give a printer listing of the input data and the final co-ordinates in a standard form.

(5) Calculate the rigid lattice intra-molecular second moment for the given molecular conformation.

(6) Calculates the effect on the second moment of molecular reorientation about any given n-fold symmetry axis for n = 2, 3 or greater.

Details of the programme

The organisation of this programme is particularly arranged to suit the molecules of the cycloalkane ring series $(CH_2)_n$, however it could easily be adapted to suit other types of molecule. It is an

APPENDIX A1 CONTD.

```
 10 FORMAT(/18X,12H************)
  6 FORMAT (25X,4H ***)
  9 FORMAT  (29H  ORIGIN=1   DUMMY ATOMS =1,2/16H  FIRST CARBON =I2,4H
    1 ANDI3,3X,13HLAST CARBON =I2)
 12 FORMAT (/10X,10HDATA INPUT10X,7X,10HCOMPUTED  /1X,2HNO3X,4HBOND4X,
    14HBOND3X,8HDIHEDRAL4X,6HCARBON1X,11HCOORDINATES/5X,6HLENGTH3X,5HAN
    2GLE3X,5HANGLE7X,1HX6X,1HY6X,1HZ/12(/I3,F7.3,F9.2,F9.2,3X,3F7.3))
 51 FORMAT  (/35X,10H COMPUTED /4X,4HBOND1X,6HANGLES14X,8HHYDROGEN2X,1
    11HCOORDINATES/2X,3HCCC5X,3HHCH4X,3HNO.3X,1HX6X,1HY6X,1HZ6X,1HX6X,1
    2HY6X,1HZ/)
 40 FORMAT (64H
    1          F6.3,2I5)
  1 FORMAT (1H1///)
 22 FORMAT (I5,4F8.3)
  2 FORMAT(I1,35H                                                I1,27H
    1                F4.1,2H  F4.1,2H  F4.1)
 49 FORMAT (F6.1,F8.1,3X,I2,1X,6F7.3)
300 FORMAT(//2X,29HINTRA-MOLECULAR SECOND MOMENT//3X,1H=F6.2,14H GAUSS
    1*2  FOR I3 ,8H PROTONS)
302 FORMAT (8H   C-H =F6.3)
 20 CALL EXIT
 30 DUMMY=ABSF(ATANF(COSF(SQRTF(1.))))
    END
```

advantage where possible to make the co-ordinate axes correspond to the symmetry axes of the molecule, for this reason, as explained in A2, it is necessary to use dummy atomic positions to set up the co-ordinate axes.

Statement 4 reads the first card which gives the title of the molecule, the length in angstroms of the carbon hydrogen bond CHBL, and the labels of the first (IMIN) and last (IMAX) carbon atoms of the ring. Statement 8 reads into the array DATA(N,J) the values of the bond length, bond angle, dihedral angle and connection for each atom added to the molecular framework as required for appendix A2. The subroutine RBCXYN is then called and computes the carbon cartesian co-ordinates as described in A2. The calculated values are stored in the array P(N,J) with values rounded off to .001 angstroms stored in the array PR(N,J).

The subroutine RBHXYZ is now called and the hydrogen co-ordinates computed and stored in the arrays H1(N,J) and H2(N,J) as described in A3. The associated CCC and HCH angles are stored in the array ANG(N,K). The hydrogen co-ordinates are then rearranged into the general array H(K,J) suitable for computing the inverse sixth power summation required for the calculation of the intra-molecular rigid lattice second moment. This summation is performed by the subroutine RBSECM as described in A4.

At this point the input data and all the computed co-ordinates

CYCLOHEXANE CHAIR HENDRICKSON MODEL NO. IA

****

ORIGIN=1 DUMMY ATOMS =1,2
FIRST CARBON = 3 AND 9 LAST CARBON = 8

NO	DATA INPUT BOND LENGTH	BOND ANGLE	DIHEDRAL ANGLE	COMPUTED CARBON COORDINATES X	Y	Z
2	0.000	0.00	180.00	0.000	0.000	0.000
3	0.000	90.00	0.00	0.000	0.000	0.000
4	1.540	109.47	90.00	0.000	.513	-1.452
5	1.540	109.47	300.00	1.257	0.000	-2.178
6	1.540	109.47	300.00	2.515	.513	-1.452
7	1.540	109.47	60.00	2.515	0.000	0.000
8	1.540	109.47	300.00	1.257	.513	.726
9	1.540	109.47	60.00	0.000	0.000	0.000

****

C-H = 1.100

BOND ANGLES CCC	HCH	NO.	COMPUTED HYDROGEN COORDINATES X	Y	Z	X	Y	Z
109.5	109.5	3	-.898	.367	.519	0.000	-1.100	0.000
109.5	109.5	4	0.000	1.613	-1.452	-.898	.147	-1.971
109.5	109.5	5	1.257	.367	-3.215	1.257	-1.100	-2.178
109.5	109.5	6	2.515	1.613	-1.452	3.413	.147	-1.970
109.5	109.5	7	3.413	.367	.519	2.515	-1.100	0.000
109.5	109.5	8	1.257	1.613	.726	1.257	.147	1.763

****

INTRA-MOLECULAR SECOND MOMENT

= 17.35 GAUSS*2 FOR 12 PROTONS

table AI

are printed out in a standard form, as shown in table A1 for the example of cyclohexane C_6H_{12}. As a check on the specified structural data the co-ordinates of the first carbon of the ring are calculated twice: once as the first atom on the ring and again as an atom connected to the last atom of the ring. This ensures that the given data does provide a closed ring. In some molecular models small discrepancies were found in this check of the order of .005 angstroms; these were attributed to the lack of a second decimal figure in the specified angles of the reference structural data of Wiberg and Hendrickson. This was checked by increasing the working accuracy of the computer programmes from 8 to 16 significant figures when no change occurred in the third decimal place of the co-ordinates. The effect of these small discrepancies on the calculated second moment will be negligible.

Statement 5 of the programme now reads in cards specifying reorientation axes of n-fold symmetry, so that the reduced value of the second moment for molecular reorientation about these axes may be computed by calling the subroutine REBROT described in A5. For a given molecule, any number of reorientation axes may be specified, each on a separate card. If a blank card is read then control transfers back to statement 4 for the whole procedure to be repeated for a new set of structure data.

Switch 1 on the computer console gives the option of a punched

card output of the computed co-ordinates. If the switch is ON then the subroutine RBUNCH arranges for the co-ordinates of each atom to be punched on a separate card with an appropriate label. The format of these cards is suitable for input data to a general molecule perspective drawing programme. This programme was available through the courtesy of P. Adamson of the St. Andrews University Computing Laboratory, and all the drawings of the molecules which appear in this thesis are photographic reproductions of drawings obtained with this programme. The computer execution time of each drawing was about 4 minutes for 24 atoms, and the perspective views obtained provided a useful visual check of the structural data.

Although the various parts of this programme were checked individually as they were assembled, a final check of the whole programme was made by calculating the results for cyclohexane C_6H_{12}. The results for this molecule are already known, Andrew and Eades (1953), from calculations performed by hand on a desk calculator. The input data cards to the computer programme are punched as given in formats 40, 22 and 2, and the computed results are shown in table A1. It is to be noted that the listed values of the CCC and HCH angles are "rounded off" to one decimal place purely for simplicity in the output listing. In the computer memory core these values are stored to eight significant figures. The computer value for the rigid lattice intra-molecular second moment 17.35 $gauss^2$

compares well with the value of 17.28 gauss^2 from Andrew and Eades (1953), both calculated with the same structural data. Part of the difference, a factor of 715.9/716.2, can be attributed to the use of a more recent value for the proton gyromagnetic ratio in the computer programme. The computer value of the second moment for reorientation of the cyclohexane molecule about its triad axis is 3.65 gauss^2, this compares with a value of 3.64 gauss^2 obtained by Andrew and Eades (1953).

An example of the power of modern digital computers to perform these calculations is illustrated by the fact that it took approximately 8 minutes to manually punch the 10 data cards for this test with cyclohexane. The IBM 1620 computer then took approximately 6 minutes to perform all the calculations, a task normally requiring several days of manual calculation.

APPENDIX A2

```
      SUBROUTINE RBCXYN(N1,NL,P,PR,DATA)
      DIMENSION A(20,4,4),B(20,4),P(20,3),PR(20,3),DATA(20,4)
      PIE =.17453293E-01
      DO 1 N=N1,NL
      IF(DATA(N,4)) 13,14,13
   14 DATA(N,4)=N-1
   13 R=DATA(N,1)
      BA=PIE*DATA(N,2)
      DA=PIE*DATA(N,3)
      JCON=DATA(N,4)
      B(1,1) =-COSF(BA)
      B(1,2) =-SINF(BA)
      B(1,3) =0.0
      B(1,4) =-R*COSF(BA)
      B(2,1) =SINF(BA)*COSF(DA)
      B(2,2) =-COSF(BA)*COSF(DA)
      B(2,3) =-SINF(DA)
      B(2,4) =R*B(2,1)
      B(3,1) =SINF(BA)*SINF(DA)
      B(3,2) =-COSF(BA)*SINF(DA)
      B(3,3) =COSF(DA)
      B(3,4) =R*B(3,1)
      B(4,1) =0.0
      B(4,2) =0.0
      B(4,3) =0.0
      B(4,4) =1.0
      DO 11 J=1,4
      DO 11 I=1,4
      IF(J-I)10,9,10
    9 A(1,I,J)=1.0
      GO TO 11
   10 A(1,I,J)=0.0
   11 A(N,I,J)=0.0
      DO 5 I=1,4
      DO 5 J=1,4
      DO 5 K=1,4
    5 A(N,I,J)=A(JCON,I,K)*B(K,J)+A(N,I,J)
      DO 6 I=1,3
    6 P(N,I)=A(N,I,4)
    1 CALL RBROND(3,3,P(N,1),P(N,2),P(N,3),PR(N,1),PR(N,2),PR(N,3))
      RETURN
      END
```

Appendix A2

A Fortran Subroutine to compute atomic cartesian co-ordinates, given the bond lengths, bond angles, and dihedral angles between the atoms of a molecule.

This programme is based on an algorithm given by H. B. Thompson (1967). A base co-ordinate system is defined by the first three atoms (these may include dummy atoms to maintain the symmetry of the molecular arrangement). Then the x, y, z co-ordinates of each successive atom added to this molecular framework are calculated by matrix multiplication. Operation by a matrix B, which represents a rotational transformation and a translation, gives the co-ordinates of each new atom added, in a system with the atom to which it is attached as origin. Then operation on these co-ordinates by matrix A gives the co-ordinates of this new atom in the base co-ordinate system.

Variable identification:-

DATA (N,4)	No. of the atom on the molecular framework to which new atom no. N is connected.
DATA (N,1)	Length of bond connecting atom N to framework.
DATA (N,2)	Bond angle in degrees for atom N.
DATA (N,3)	Dihedral angle in degrees for atom N, defined clockwise looking round the framework towards the origin.
P(N,1) = A(N,1,4)	x co-ordinate of atom N.
P(N,2) = A(N,2,4)	y co-ordinate of atom N.
P(N,3) = A(N,3,4)	z co-ordinate of atom N.

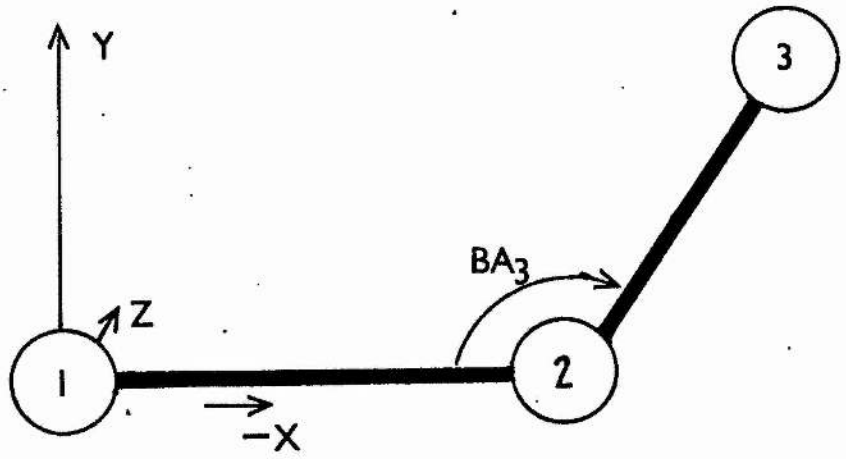

base system

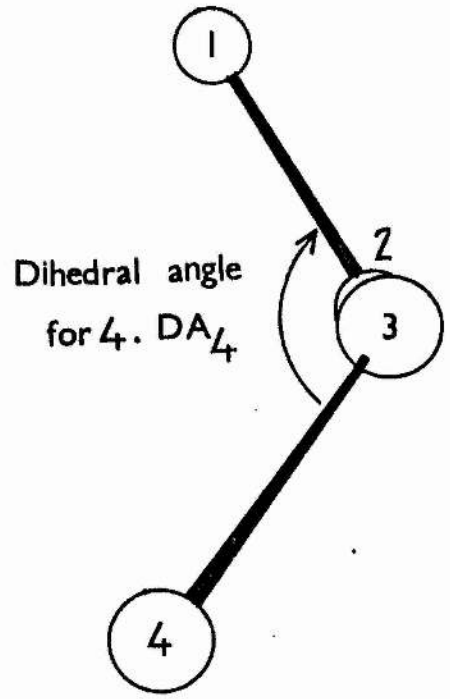

fig. A2

$PIE = \frac{2\pi}{360}$, radians per degree

For internal consistency in the matrix operation we make the following definitions for the DATA of the first three atoms.

DATA (2,2) = 0.0 DATA (2,3) = 180 DATA (3,3) = 0.0

Method of computation

1. Definition of base co-ordinate system, see figure A2.

The origin is taken as atom 1, and the direction of the bond from 1 to 2 defines the negative X axis. The XY plane is defined to pass through atoms 1, 2 and 3. The positive Y axis is enclosed in the acute angle between 3, 2 and 1, and hence the Z axis is uniquely defined too.

2. Addition of further atoms.

The matrix B_N is formed from the DATA values for the new atom N to be added. Computation of the x, y and z co-ordinates in the base system is then obtained by the matrix multiplication:-

$$B_2 \times B_3 \times \ldots\ldots B_{N-1} \times B_N$$

where we assume that atom N is connected to atom N-1. For efficient programming the 4 x 4 matrix

$$B_2 \times B_3 \times \ldots\ldots B_{N-1} \times B_N$$

is computed, and its elements stored as the matrix A(N,I,J) each time a new atom N is added to the system. Hence for the general case of atom K attached to atom N of the system, we require the matrix multiplication of

$$A(N,I,J) \times B_K(I,J) = A(K,I,J)$$

this is performed by statement 5 of the programme

From this operation we obtain the x, y and z co-ordinates in the base system of atom K as:-

$$x = A(K,1,4)$$

$$y = A(K,2,4)$$

$$z = A(K,3,4)$$

We also obtain the matrix A(K,I,J), which may be used to calculate the co-ordinates of atoms connected to atom K.

APPENDIX A3

```
      SUBROUTINE RBHXYZ(CHBL,I,P,H1,H2,ANG,IC)
      DIMENSION P(20,3),H1(20,3),H2(20,3),A(3),B(3),C(3),A4(3),S(3),T(3)
      DIMENSION ANG(20,2)
      AJ =0.0
      BJ =0.0
      AJBJ =0.0
      CJ=0.
      DO 1 J=1,3
      A(J)=P(I-1,J)-P(I,J)
      B(J)=P(I+1,J)-P(I,J)
      AJBJ =AJBJ+A(J)*B(J)
      AJ =AJ+A(J)**2
      BJ =BJ+B(J)**2
      C(J)=(A(J)+B(J))/2.
    1 CJ=CJ+C(J)**2
      PIE =.17453293E-01
      D =SQRTF(CJ)/CHBL
      SQCOS =(AJ*BJ)/AJBJ**2
      CC =180.0*PIE-ATANF(SQRTF(SQCOS-1.))
      TET =109.46667*PIE
      IF (TET-CC) 4,5,6
    4 AA =.29
      GO TO 7
    6 AA =.3
      GO TO 7
    5 AA =.0
    7 HCH =(1.+AA)*TET-AA*CC
      DO 2 J=1,3
      A4(J) =-COSF(HCH/2.)*C(J)/D
      S(J) =A(J)-A4(J)
    2 T(J) =B(J)-A4(J)
      DENOM =S(1)*T(2)-T(1)*S(2)
      B(1) =(T(3)*S(2)-S(3)*T(2))/DENOM
      B(2) =(S(3)*T(1)-T(3)*S(1))/DENOM
      B(3) =1.0
      SP =SQRTF(B(1)**2+B(2)**2+1.)/CHBL
      DO 3 J=1,3
      A(J) =SINF(HCH/2.)*B(J)/SP
      SBJ2=B(2)/ABSF(B(2))
      H1(I,J)=SBJ2*A(J)+A4(J)+P(I,J)
    3 H2(I,J)=-SBJ2*A(J)+A4(J)+P(I,J)
      HCH =HCH/PIE
      CC =CC/PIE
      CALL RBROND(2,1,CC,HCH,1.,ANG(I,1),ANG(I,2),DUM)
      IF(IC)9,10,9
    9 PRINT 8,ANG(I,1),ANG(I,2)
    8 FORMAT(5H CCC=F6.1,5H HCH=F6.1)
   10 RETURN
      END
```

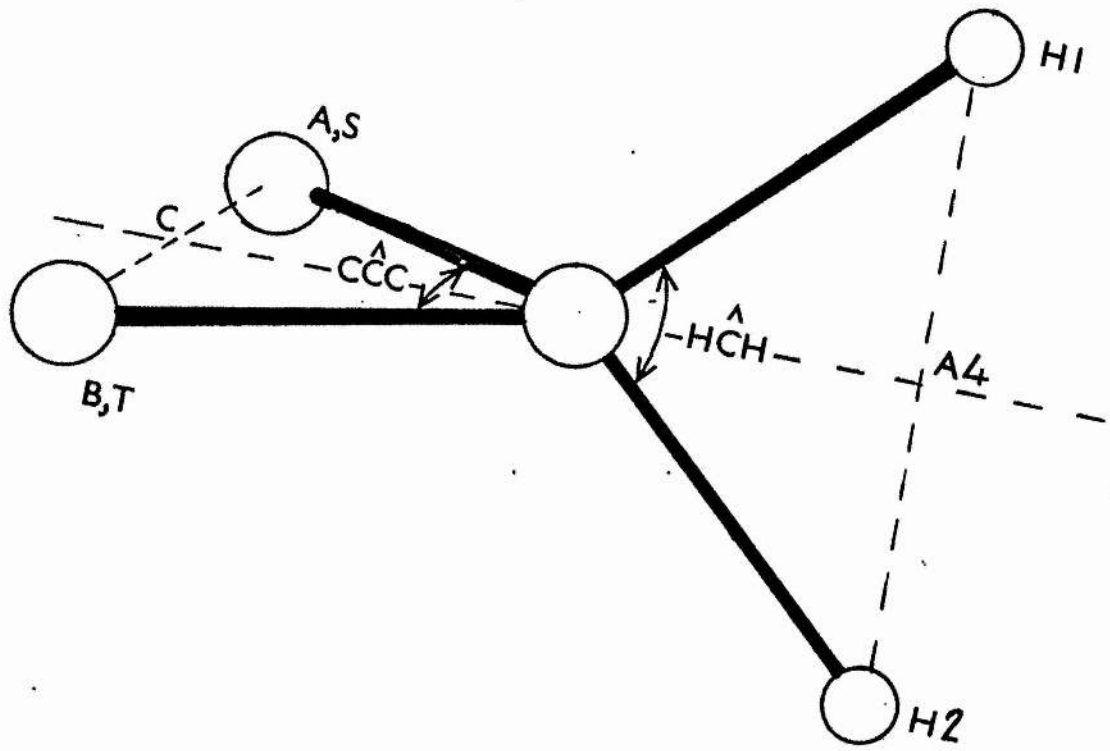

fig A·3

Appendix A3

A Fortran Subroutine to compute the cartesian co-ordinates of the Hydrogen atoms of a Methylene group, given the co-ordinates of the three associated carbon atoms.

This programme sets the HCH angle for the methylene group according to the scheme given by J. B. Hendrickson (1961). This scheme relates the HCH angle to the value of the associated CCC angle, so that if the CCC angle is different from tetrahedral, the HCH angle is set to give a minimum bond angle strain for the methylene configuration.

For departures from tetrahedral angles of less than 10 degrees, the relationship is linear and is given by:-

$$HCH = T(1 + b) - b \times CCC$$

$b = 0.30$ for $CCC < T$
$b = 0.29$ for $CCC > T$
$T = 109.47$ degrees.

The details of the computer programme are as follows:-

The co-ordinates of the carbon atoms are stored in a data matrix P(I,J), where P(I,1), P(I,2), P(I,3) are the x, y and z co-ordinates respectively, for the carbon atom I. The computed hydrogen co-ordinates associated with the carbon atom I are stored in the data matrices H1(I,J) and H2(I,J), J = 1, 2, 3 for x, y, z respectively.

Variable Identification. (See figure A3).

A(J) co-ordinates of I-1 carbon atom

B(J) co-ordinates of I + 1 carbon atom

C(J) co-ordinates of the mid. point of A(J) and B(J)

A4(J) co-ordinates of mid. point of H1(I,J) and H2(I,J) all with respect to P(I,J) as origin.

S(J) and T(J) are the co-ordinates of A(J) and B(J) with respect to A4(J) as origin.

The co-ordinates of the two hydrogen atoms are set in a plane perpendicular to the plane of the three carbon atoms by calculation of the vector product

$$\overline{A4(J)S(J)} \times \overline{A4(J)T(J)}$$

This is given by B(1), B(2), B(3), and the hydrogen atoms are then set at the required positions in this plane by knowledge of the C-H bond length CHBL, and the HCH angle. The co-ordinates are then translated back to the original cartesian base system.

APPENDIX - A4

```
      SUBROUTINE RBSECM(N,NN,H,SECMO,IC)
      DIMENSION H(200,3)
      NPROT =NN-N+1
      PPROT =NPROT
      SECMO =0.0
      LL=NN-1
      DO 2 L=N,LL
      K1=L+1
      DO 2 K=K1,NN
      AJ =0.0
      DO 1 J=1,3
    1 AJ=AJ+(H(K,J)-H(L,J))**2
    2 SECMO=SECMO+1./AJ**3
      SECMO=716.2*SECMO/PPROT
      CALL RBROND(1,2,SECMO,2.,3.,SECMO,B,C)
      IF(IC) 4,5,4
    4 PRINT 3,SECMO,NPROT
    3 FORMAT(//2X,29HINTRA-MOLECULAR SECOND MOMENT//3X,1H=F6.2,14H GAUSS
     1*2  FOR I3 ,8H PROTONS)
    5 RETURN
      END
```

Appendix A4

A Fortran Subroutine to calculate the rigid lattice Second Moment for an array of Hydrogen nuclei given the cartesian co-ordinates

The cartesian co-ordinates are stored in the data matrix H(L,J) with the nuclei labelled from L = N to NN, and the x, y, z co-ordinates as J = 1, 2, 3 respectively. The summation for the second moment of N nuclei is computed from the expression:

$$\text{SECMO} = 716.2/N \sum_{j>k}^{N} (r_{jk})^{-6} \text{ gauss}^2$$

where r_{jk} is the inter-nuclear distance in angstroms, whose square is computed by statement 1 of the programme. IC controls the print out option.

APPENDIX A5

```
      SUBROUTINE RBSROT(N,NN,H,NFOLD,RX,RY,RZ,SECMO,IC,IC2)
      DIMENSION H(200,3),A(3),R(3)
      PIE =.17453293E-01
      R(1)=RX
      R(2)=RY
      R(3)=RZ
      RR=RX**2+RY**2+RZ**2
      NPROT =NN-N+1
      PPROT =NPROT
      SECMO =0.0
      LL=NN-1
      DO 2 L=N,LL
      K1=L+1
      DO 2 K=K1,NN
      TOP=0.
      AJ =0.0
      DO 1 J=1,3
      A(J)=H(K,J)-H(L,J)
      TOP=TOP+R(J)*A(J)
    1 AJ=AJ+A(J)**2
      HHDIS=SQRTF(AJ)
      SQCOS=TOP**2/(RR*AJ)
      IF (NFOLD-2)6,6,7
    6 FACT =(1.-3.*(1.-SQCOS)*SQCOS)
      GO TO 8
    7 FACT=(3.*SQCOS-1.)**2/4.
    8 RSIX=716.2/(HHDIS**6*PPROT)
      RSIXH=RSIX*FACT
      SECMO =SECMO+RSIXH
   13 IF (IC2)2,2,10
   10 ANGLE=(ATANF(SQRTF(1./SQCOS-1.)))/PIE
      IF(TOP) 14,15,15
   14 ANGLE =180.-ANGLE
   15 PRINT 12,L,K,HHDIS,ANGLE,FACT,RSIX,RSIXH,SECMO
    2 CONTINUE
      CALL RBROND(1,2,SECMO,2.,3.,SECMO,B,C)
      IF(IC) 4,5,4
    4 PRINT 3,NFOLD,(R(J),J=1,3),SECMO,NPROT
   12 FORMAT (2I5,F8.3,I6,F8.3,3F8.4)
    3 FORMAT (51H REDUCED INTRA-MOLECULAR SECOND MOMENT
     1/20H  FOR ROTATION ABOUTI3,36H FOLD AXIS THROUGH ORIGIN AND POINT
     2F5.1,2H XF5.1,2H YF5.1,2H Z/3H  =F7.2,12H GAUSS*2 FORI4,7HPROTONS)
    5 RETURN
      END
```

Appendix A5

A Fortran Subroutine to compute the reduced intra-molecular Second Moment due to molecular reorientation about a symmetry axis

This programme is based on the two reduction factors given in equations 2.13 and 2.14 for 2-fold and 3-fold or greater symmetry axes respectively, where

$$\rho_2 = (1 - 3 \sin^2\gamma_{jk} \cos^2\gamma_{jk})$$

$$\rho_3 = (3 \cos^2\gamma_{jk} - 1)^2/4$$

γ_{jk} being the angle the inter-proton vector r_{jk} makes with the axis of reorientation. The complete expression for the reduced second moment for a molecule with N protons reorientating about an n-fold symmetry axis is

$$\text{SECMO} = 716.2/N \sum_{j\ k}^{N} \rho_n(\gamma_{jk})/r_{jk}^6$$

The cartesian co-ordinates of the protons from N to NN are stored in the data matrix H(I,J) (see Appendix A4). The value of the integer NFOLD determines which of the reduction factors, statements 6 or 7, is applied. RX, RY, RZ define the orientation of the symmetry axis with respect to the cartesian system, since the axis is assumed to pass through the origin of the co-ordinates and the point RX, RY, RZ. So that for reorientation about the Y axis we

have RX = 0, RY = 1, RZ = 0, this of course will be the same for any other axis parallel to the Y axis. The angle γ_{jk} is calculated in two steps; first the co-ordinates of proton k with proton j as origin are computed as $x_k = A(1)$, $y_k = A(2)$, $z_k = A(3)$, then $\cos^2\gamma_{jk}$ is obtained as SQCOS from the scalar product of the reorientation vector R and the inter-proton vector A where

$$\cos\gamma_{jk} = \sum_{I=1}^{3} R(I).A(I)/[R].[A]$$

The summation for the value of SECMO is then obtained in a straightforward manner as in Appendix A4.

Two print out options are available through IC, and IC2. If IC2 = 1 then statement 15 gives the details of the calculation for each j and k. IC controls the print out of the final answer.

The specification of the reorientation axes is considerably facilitated by the coincidence of the co-ordinate axes with the symmetry axes of the molecule. In the example of cyclohexane given in table A1 this is achieved by the use of two dummy atoms Nos. 1 and 2, the bond angles of 90.0° and 109.47° for atoms 3 and 4, and the dihedral angles of 90.0° and 300.0° for atoms 4 and 5. The actual molecular configuration is independent of all of these angles, they are merely required to specify the co-ordinate axes. The specification of these angles for the non-tetrahedral forms of cyclo-heptane and cyclo-octane was not so straightforward, and as the tables show an

exact coincidence of axes was not achieved in all cases. This was mainly due to the lack of a second decimal place in the other angles given by Wiberg and Hendrickson. As the tables show the residual errors were small, and their effect on the calculated second moments will be negligible.

APPENDIX A6

```
      SUBROUTINE RBMJK(N,NN,R,AMJK)
      DIMENSION A(7),A2(7),R(100,3)
      DO 4 J=1,7
    4 A(J)=0.
      DO 1 K=N,NN
      RXYSQ=R(K,1)**2+R(K,2)**2
      RXY=SQRTF(RXYSQ)
      R2=RXYSQ+R(K,3)**2
      R3=R2**(-1.5)
      SGSQ=RXYSQ/R2
      CGSQ=1.-SGSQ
      S2G =2.*R(K,3)*RXY/R2
      CT  =R(K,1)/RXY
      ST  =R(K,2)/RXY
      CTSQ=CT**2
      STSQ=ST**2
      S2T =2.*ST*CT
      A(1)=A(1)+3.0*R3*CGSQ
      A(2)=A(2)+1.5*R3*S2G*CT
      A(3)=A(3)+1.5*R3*S2G*ST
      A(4)=A(4)+3.0*R3*SGSQ*CTSQ
      A(5)=A(5)+1.5*R3*SGSQ*S2T
      A(6)=A(6)+3.0*R3*SGSQ*STSQ
    1 A(7)=A(7)+R3
      AN=NN-N+1
      DO 2 J=1,7
      A(J)=A(J)/AN
    2 A2(J)=A(J)**2
      AMJK=.2*(A2(1)+A2(4)+A2(6)+5.*A2(7))+4./15.*(A2(2)+A2(3)+A2(5))
      AMJK=AMJK+2./15.*(A(1)*A(4)+A(1)*A(6)+A(4)*A(6))
      AMJK=AMJK-2./3.*A(7)*(A(1)+A(4)+A(6))
      RETURN
      END
```

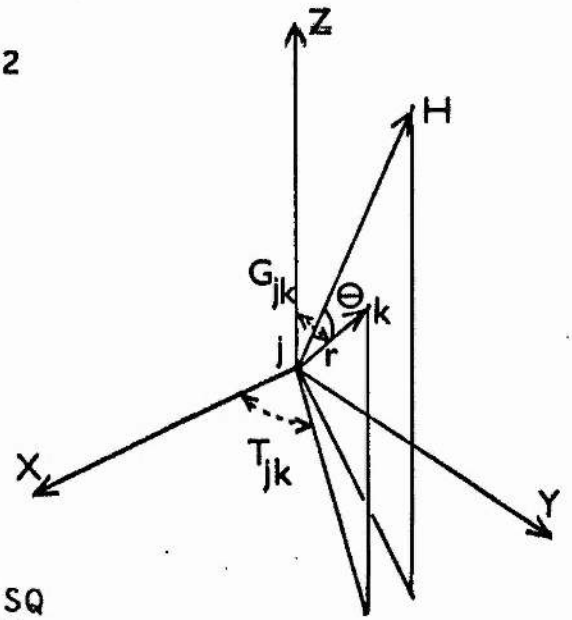

fig. A 6

Appendix A6

A Fortran Subroutine to compute the effect of general molecular motion on the Second Moment

This programme is based on the analysis of Andrew and Eades (1953) which considered the effect of the variation of both the inter-nuclear distance r_{jk}, and the angle Θ_{jk} which r_{jk} makes with the applied magnetic field. From equation 2.5 the second moment of a rigid lattice of N nuclei is given by:

$$M_2 = \frac{3}{2} I(I+1) \frac{\gamma^2 \hbar^2}{N} \sum_{j>k} (1 - 3\cos^2\theta_{jk})^2 . r_{jk}^{-6}$$

If the molecular reorientation causes each inter-nuclear vector $\bar{r}_{jk}$ to take up 'n' different orientations in the crystal lattice, then for a polycrystalline sample Andrew and Eades obtained the following expression for M_2 averaged over these 'n' orientations.

$$M_2 = \frac{3}{2} I(I+1) \frac{\gamma^2 \hbar^2}{N} \sum_{j>k} \left[\frac{1}{5}(a^2 + d^2 + f^2 + 5g^2) + \frac{4}{15}(b^2 + c^2 + e^2) + \frac{2}{15}(ad + af + df) - \frac{2}{3}g(a + d + f)\right]$$

where

$$a = \frac{3}{n} \sum_{1}^{n} r_{jk}^{-3} \cos^2\theta_{jk}$$

$$b = \frac{3}{2n} \sum_{1}^{n} r_{jk}^{-3} \sin 2G_{jk} \cos T_{jk}$$

$$c = \frac{3}{2n} \sum_{1}^{n} r_{jk}^{-3} \sin 2G_{jk} \sin T_{jk}$$

$$d = \frac{3}{n} \sum_{1}^{n} r_{jk}^{-3} \sin^2 G_{jk} \cos^2 T_{jk}$$

$$e = \frac{3}{2n} \sum_{1}^{n} r_{jk}^{-3} \sin^2 G_{jk} \sin 2T_{jk}$$

$$f = \frac{3}{n} \sum_{1}^{n} r_{jk}^{-3} \sin^2 G_{jk} \sin^2 T_{jk}$$

$$g = \frac{1}{n} \sum_{1}^{n} r_{jk}^{-3}$$

and G_{jk} and T_{jk} are the polar and azimuthal angles respectively of the inter-nuclear vector $\bar{r}_{jk}$ with respect to the Z axis of the crystal, see figure A6.

Before entering the subroutine the co-ordinate specification of the 'n' orientations of the vector $\bar{r}_{jk}$ are stored in the array R(L,I) from L = N to NN, and I = 1, 2 and 3 for the x, y and z co-ordinates of the nucleus k with nucleus j as origin. The polar and azimuthal angles are then calculated from co-ordinate geometry. e.g.

$$SGSQ = \sin^2 G = (x_k^2 + y_k^2)/(x_k^2 + y_k^2 + z_k^2)$$

$$CT = \cos T = x_k/(x_k^2 + y_k^2)^{\frac{1}{2}}$$

The a, b, c, d, e, f, g terms are summed over the n values of $\bar{r}_{jk}$ by the elements of the array A, and their accumulated sum is returned by AMJK.

APPENDIX A7

```
      SUBROUTINE RBPSYD(LH,NCONF,H,AM,LF,LL,LS,IC)
      DIMENSION H(200,3),A(16,16,3),B(3),AM(16),R(100,3)
      ALH=LH
      DO 3 L=1,LH
      DO 3 J=1,3
    3 A(1,L,J)=H(L,J)
      DO 11 L=2,NCONF
    8 DO 4 K=2,LH,2
      KL=K+2
      IF(K-LH)9,5,9
    5 KL=2
    9 DO 4 J=1,3
      A(L,K,J)=A(L-1,KL,J)
    4 A(L,K-1,J)=A(L-1,KL-1,J)
   11 CONTINUE
      DO 15 L=LF,LL,LS
   15 PRINT 10,L,(K,(A(L,K,J),J=1,3),K=1,LH)
   10 FORMAT (/I4,/(I4,3F10.3,I4,3F10.3))
      SECMO=0.
      LHM1=LH-1
      DO 2 K=1,LHM1
      KP1=K+1
      DO 2 K1=KP1,LH
      L1=0
      DO 1 L=LF,LL,LS
      L1=L1+1
      DO 1 J=1,3
    1 R(L1,J)=A(L,K1,J)-A(L,K,J)
      CALL RBMJK(1,L1,R,AM(K1))
      RSIXH=2.*358.1*(5./4.)*AM(K1)/ALH
      SECMO=SECMO+RSIXH
      IF(IC)16,2,16
   16 PRINT 13,K,K1,AM(K1),RSIXH,SECMO
   13 FORMAT (2I4,5H  AM=E10.4,F10.4,F8.4)
    2 CONTINUE
      PRINT 14,SECMO,L1
   14 FORMAT (38H REDUCED INTRA MOLECULAR SECOND MOMENT/27H  FOR PSEUDOR
     1EORIENTATION =F10.4,9H BETWEEN I3,21H EQUIVALENT POSITIONS)
      RETURN
      END
```

Appendix A7

A Fortran Subroutine to compute atomic co-ordinates in a molecular pseudo-reorientation itinerary

The form of these itineraries for a number of cycloalkanes has been described in detail by Hendrickson (1961 and 1964). The itinerary is perhaps easiest to visualize in cyclopentane C_5H_{10}. The generally accepted structure of this molecule is of four coplanar carbon atoms, with the fifth carbon slightly puckered out of the plane of the ring.

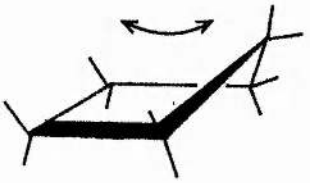

cyclopentane

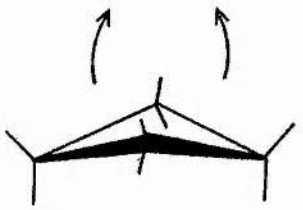

cyclobutane

This molecule can then pseudorotate by the passage of the out-of-plane pucker from carbon to carbon around the ring. The energy barrier to this form of internal motion is low, and so it is expected to occur readily. In some conformations of the series this motion is equivalent to ring inversion, the puckered form of cyclobutane C_4H_8 for example.

Unlike reorientation of a rigid molecule about a symmetry axis, there is no fixed reference axis to describe pseudoreorientation, and so it is not clear what form this motion would take in a crystal lattice. One possibility is that in the course of the internal motion, the molecule will externally reorientate to present

the same envelope to the crystal lattice. In cyclobutane for example this could be achieved by a turn through 90° as the ring inverted. Although there might be departures from this model of the motion in the actual details of the pseudo-reorientation itinerary, it was felt that it would provide a reasonable basis for an estimate of the effect on the intra-molecular second moment.

The computer programme A7 is based on this model for the molecular motion. The cartesian co-ordinates of the proton pairs of the molecule are passed to the subroutine in the data matrix H(L,J), labelled from L = 1 to LH and J = 1, 2, 3 for x, y and z. The proton co-ordinates are then rearranged into I sets of the larger matrix A(I,L,J), where I = 1 to NCONF is the number of equivalent positions each proton can take up in the course of the itinerary.

By the choice of suitable values for the integers LF, LL and LS it is possible to calculate the reduced intra-molecular second moment for reorientation between n of these equivalent positions, where n = (LL - LF + 1)/LS and LF is the first position, LL the last, and LS the interval between the positions. The subroutine REMJK, described in A6, is called to perform the averages of the dipolar interaction of the second moment for the n equivalent positions.

This programme in fact can be applied for more general molecular

motion than the particular model described above. For example, by suitable choice of LF, LL, and LS it is possible to calculate the effect of reorientation about a symmetry axis. Thus in the case of reorientation about the 3-fold axis of cyclohexane C_6H_{12}, if LF = 2, LS = 2, and LL = 6, the second moment will be averaged for the 3 equivalent positions of the proton pairs, i.e. the symmetry positions 2, 4, 6 of the ring. The value obtained for this calculation was 3.65 $gauss^2$ which agrees exactly with that obtained in Appendix A1 by the conventional 3-fold reduction factor. Similar agreement was found for 2-fold and 6-fold reorientation in appropriate molecules. This provided a useful check on the correct organisation of programmes A6 and A7.

The integer IC gives an optional print out of the details of the calculation.

```
      DIMENSION W(100,5),FNAME(4),X(4)
    8 PRINT 16
      M=0
    3 M=M+1
      READ 1,W(M,1),C,(FNAME(I),I=1,4),DMV,UMV,CHLG,W(M,3),W(M,2)
      IF(W(M,2))4,5,4
    4 W(M,4)=W(M,3)*(UMV-DMV)*.457/CHLG
      PRINT 2,M,C,(W(M,J),J=1,4),(FNAME(I),I=1,4)
      GO TO 3
    5 M=M-1
      CALL RBASH(1.,3.)
   11 CALL PLOT (7)
      READ   6,NPLOT,T1,T2,T3,T4,T5,XMIN,XMAX,XL,XD,YMAX,YL,YD,NTPTS,(X(
     1I),I=1,NTPTS)
      GO TO (7,8,9),NPLOT
    7 CALL PLOT(1,XMIN,XMAX,XL,XD,0.0,YMAX,YL,YD)
      YMIN=0.0
      XS=(XMAX-XMIN)/XL
      YS=YMAX/YL
      DO 10 K=1,M
      CALL PLOT(98,W(K,2),W(K,4))
      CALL POINT(4,0.05,1,1)
   10 CONTINUE
      DO 14 I=1,NTPTS
      DO 13 K=1,40,2
      YK=K
      CALL PLOT(99)
      IF(YMAX-YS*(2.+.2*YK))14,15,15
   15 CALL PLOT(90,X(I),YMIN+.2*YS*YK)
   13 CALL PLOT (90,X(I),YMIN+.2*YS*(YK+1.))
   14 CONTINUE
      CALL PLOT (9,XMIN,0.0)
      CALL PLOT (98,XMIN+XS,YMAX)
      CALL CHAR(5,.2,0,T1,T2,T3,T4,T5)
   12 FORMAT(5A4)
      GO TO 11
    9 CALL RBEST(W,M)
      GO TO 11
    2 FORMAT (I4,2X,A1,2I5,2F8.2,2X,4A4)
   16 FORMAT (1H1)
    6 FORMAT (I1,5A4,3F4.0,2F3.0,F4.1,F3.1,I1,4F5.1)
    1 FORMAT (F4.0,A1,6H      4A4,5H     F5.1,1X,4H    F6.1,1X,5H      F4
     1.0,11H           F5.1,1X,F5.0)
   20 CALL EXIT
      END
```

Appendix A8

A Fortran programme to compute the activation energy from a line width transition

The programme A8 reads in the experimental line width data together with a temperature for each value. All values are then converted into units of gauss by the appropriate field calibration and the results printed out. At this point a card with the control integer NPLOT is read. If NPLOT is negative a graph is drawn on the digital plotter of the line widths versus temperature together with appropriate thermal transition points, an example of this graph is shown in figure 7.2. If NPLOT is positive the subroutine RBEST given in A9 is called, and from a least squares analysis of the line width values in the transition region, a value for the activation energy is calculated as described in A9. Finally if NPLOT is zero, the programme is repeated for a new set of data.

```
      SUBROUTINE RBEST(W,M)
      DIMENSION X(50),Y(50),WT(50),W(100,5),AK(3),A(20),T(6)
      DIMENSION YDEV(50),YCALC(50)
      TANF(B)=SINF(B)/COSF(B)
      GAMMA=.267523E05
      PAG=GAMMA/(8.*LOGF(2.)*6.284)
      READ 1,TMIN,TMAX,RIGIDW,REDW,XMIN,XMAX,YMIN,YMAX,IC,(T(I),I=1,5)
      PRINT 1,TMIN,TMAX,RIGIDW,REDW,XMIN,XMAX,YMIN,YMAX,IC,(T(I),I=1,5)
      PC =(RIGIDW**2-REDW**2)*2./3.142
      DO 3 K=1,M
      X(K)=0.0
      Y(K)=0.0
      WT(K)=0.0
      IF(W(K,2)-TMIN)3,4,4
    4 IF(W(K,2)-TMAX)5,5,3
    5 W(K,5)=PAG*W(K,4)/TANF((W(K,4)**2-REDW**2)/PC)
      IF(W(K,5))3,20,20
   20 WT(K)=LOGF(W(K,5))
      X(K)=1./W(K,2)
      Y(K)=LOGF(W(K,5))
    3 CONTINUE
      CALL CLPOLF(X,Y,WT,1,M,1,AK,NORD,SMIN,A,3)
      E=-(8.315/4.184)*AK(2)/1000.
      PRINT 2,E
      IF(IC)15,14,15
   15 CALL PLOT (1,XMIN,XMAX,5.5,10.,YMIN,YMAX,6.,1.)
   14 DO 7 K=1,M
      XP=AK(2)/(Y(K)-AK(1))
      IF(WT(K))8,17,8
    8 PRINT 9,XP,W(K,4),W(K,2)
      IF(IC)16,7,16
   16 XP=PAG*W(K,4)/TANF((W(K,4)**2-REDW**2)/PC)
      IF(XP)7,22,22
   22 XP=AK(2)/(LOGF(XP)-AK(1))
      CALL PLOT(9,XP,W(K,4))
   17 IF(W(K,2)-XMIN)7,18,18
   18 IF(W(K,2)-XMAX)19,19,7
   19 IF(IC)25,7,25
   25 CALL PLOT(98,W(K,2),W(K,4))
      CALL POINT(2,.06,1,1)
    7 CONTINUE
      IF(IC)13,12,13
   13 IMAX=(RIGIDW-REDW)/.1-1.
      DO 10 I=1,IMAX
      RI=I
      RI=RI/10.
      RI=REDW+RI
      XP=PAG*RI/TANF((RI**2-REDW**2)/PC)
      XP=AK(2)/(LOGF(XP)-AK(1))
      CALL PLOT (90,XP,RI)
   10 CONTINUE
   12 RETURN
```

Appendix A9

A Fortran Subroutine to determine the correlation frequency and activation energy from the line width transition

M values of the line width are passed to this subroutine in the data matrix W, see A8. The two plateau values of the line width are read in as RIGIDW for the rigid lattice, and REDW for the reduced value after the transition. A correlation frequency v is then obtained for each line width value between the temperatures TMIN and TMAX from the Kubo and Tomita expression 2.10, and stored in the fifth column of the data matrix, i.e. W(K,5), (statement No. 5).

The library subroutine CLFOLF is now called and a least squares fit of v to the equation 2.9 obtained

i.e. $$\ln v = \ln v_0 - E/RT$$

each value of v is given an appropriate weight by the array WT(K), and the activation energy E is obtained from the coefficient AK(2) of the best fit.

If the integer IC is non-zero a graph of the experimental points versus temperature is drawn on the digital plotter, together with the best fit through the experimental points. Figure 7.6 is an example of this graph.

The above analysis may be repeated any number of times for different values of RIGIDW, REDW, TMIN and TMAX to test for their

effect on the computed activation energy E, and the standard deviation of the best fit.

```
      SUBROUTINE  RBLSQU(X,Y,W,N1,NLAST,YINCT,SLOPE,YDEV,YCALC,PSDSL,IC)
C     BEST STRAIGHT LINE BY LEAST SQUARES
C        Y(I)=YINCT +SLOPE*X(I)
      DIMENSION X(1),Y(1),W(1),YDEV(1),YCALC(1)
      N=NLAST-N1+1
      SUMX =0.0
      SUMY =0.0
      SUMX2=0.0
      SUMXY=0.0
      DO 10 I=N1,NLAST
      IF (W(I)) 11,12,11
   11 SUMX =SUMX +X(I)
      SUMY =SUMY +Y(I)
      SUMX2=SUMX2+X(I)**2
      SUMXY=SUMXY+X(I)*Y(I)
      GO TO 10
   12 N =N-1
   10 CONTINUE
      AN =N
      DENOM =AN*SUMX2-SUMX**2
      SLOPE =(AN*SUMXY-SUMX*SUMY)/DENOM
      YINCT =(SUMY*SUMX2-SUMX*SUMXY)/DENOM
      SUMD2 =0.0
      DO 16 I=N1,NLAST
      YCALC(I) =SLOPE*X(I)+YINCT
      YDEV(I) =Y(I)-YCALC(I)
   16 SUMD2 =SUMD2 +YDEV(I)**2*W(I)
      SDY =SQRTF(SUMD2/(AN-2.0))
      SDSLP =SDY*SQRTF(AN/DENOM)
      PSDSL=100.*SDSLP/ABSF(SLOPE)
      IF(IC-1)21,29,22
   22 PRINT 13
      DO 27 I=1,NLAST
      IF(W(I))28,27,28
   28 PRINT 14,X(I),Y(I),W(I),YCALC(I),YDEV(I)
   27 CONTINUE
   29 PRINT 17,SLOPE,SDSLP,PSDSL,SDY,YINCT
   17 FORMAT (///8H SLOPE =E15.8,6H S.D. E15.8,F10.3,8H PERCENT//8H S.D.
     1Y =E15.8,14H Y INTERCEPT =E15.8)
   13 FORMAT(/4H    X14X1HY14X1HW14X7HY(CALC)8X8HRESIDUAL)
   14 FORMAT (5E15.8)
   21 RETURN
      END
```

Appendix A10

A Fortran Subroutine to calculate the parameters of the best straight line by the method of least squares

This programme is based on the analysis of Macfayden and assumes that the errors in the independent variable X are negligible in comparison with the errors in the dependent variable Y. The data points are stored in the two data arrays X(I), Y(I) from I = N1 to NLAST. A simple weighting scheme can be applied to the input data by the array W(I) where W(I) = 1. or 0.0, this enables various points to be discarded if required. From the solutions of the normal equations the values of the best slope and Y intercept, YINCT, for N data points are:

$$\text{SLOPE} = \frac{N\sum xy - \sum x \sum y}{N\sum x^2 - (\sum x)^2}$$

$$\text{YINCT} = \frac{\sum y \sum x^2 - \sum x \sum xy}{N\sum x^2 - (\sum x)^2}$$

Also available are the standard deviation of a given point Y from the slope, SDY, and the standard deviation of the slope, SDSLP, obtained from the expressions:

$$\text{SDY} = \left(\sum d^2/(N-2)\right)^{\frac{1}{2}} \qquad \text{SDSLP} = \left[\frac{N\sum d^2}{(N-2)(N\sum x^2 - (\sum x)^2)}\right]^{\frac{1}{2}}$$

where $\sum d^2$ is the sum of the squares of the deviations.

Three print out options are available depending on the value of IC.

IC = 0 Values of SLOPE and YINCT are computed but no print out.

IC = 1 Print out of SLOPE, SDSLP, percentage standard deviation of slope PSDSL, SDY, and YINCT.

IC = 2 As for IC = 1 plus print out of each data point with its weight W(I), calculated value YCALC(I) for each X(I), and the deviation YDEV(I) for each Y(I).

```
      SUBROUTINE RBDANG(K,P,DA)
C     THIS SUBROUTINE RETURNS THE VALUE OF THE DIHEDRAL ANGLE *DA* IN
C     RADIANS BETWEEN THE BONDS (K-3)-(K-2)AND(K-1)-K AS VIEWED
C     CLOCKWISE ALONG THE BOND (K-1)-(K-2). THE CARTESIAN COORDINATES
C     OF ATOMS K MUST BE STORED IN MATRIX P(20,3) X=1,Y=2,Z=3
C     PROCEDURE = ALL COORDINATES TRANSLATED TO MAKE K-2 THE ORIGIN,
C     ALL COORDINATES ROTATED TO PUT K-1 ON  Z AXIS
C     DIHEDRAL ANGLE NOW SEEN AS PROJECTION ON X Y PLANE
      DIMENSION P(20,3),W(2,3)
      PIE=.17453293E-01
      DO 1 J=1,3
      W(1,J)=P(K-3,J)-P(K-2,J)
    1 W(2,J)=P(K,J)-P(K-2,J)
      X=P(K-1,1)-P(K-2,1)
      Y=P(K-1,2)-P(K-2,2)
      Z=P(K-1,3)-P(K-2,3)
      AS=Y/SQRTF(Y**2+Z**2)
      AC=Z/SQRTF(Y**2+Z**2)
      BS=-X/SQRTF(X**2+Y**2+Z**2)
      BC=SQRTF(Y**2+Z**2)/SQRTF(X**2+Y**2+Z**2)
      ANGL =0.0
      DO 24 M=1,2
      XP=W(M,1)*BC+W(M,2)*BS*AS+W(M,3)*BS*AC
      YP=W(M,2)*AC-W(M,3)*AS
      ZP= -W(M,1)*BS+W(M,2)*BC*AS+W(M,3)*BC*AC
      ANG =ABSF(ATANF(YP/XP))
      IF (XP) 21,22,22
   21 IF(YP) 29,30,30
   29 ANG =180.*PIE+ANG
      GO TO 25
   30 ANG =180.*PIE-ANG
      GO TO 25
   22 IF(YP) 23,25,25
   23 ANG =360.*PIE-ANG
   25 DA =ANG-ANGL
   24 ANGL =ANG
      DADEG=DA/PIE
      IF(DADEG) 27,28,28
   27 DADEG =360.+DADEG
   28 PRINT 26,K,DADEG
   26 FORMAT (/10H CARBON NOI4,16H DIHEDRAL ANGLE=F9.3)
      RETURN
      END
```

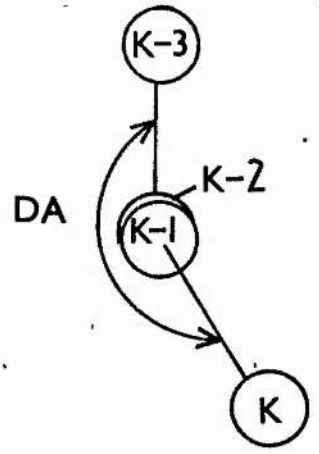

APPENDIX A12

```
      DIMENSION X(2),Y(2),Z(2)
      N1=1
      NL=20
      SUM1=0.0
      SUM2=0.0
      SUM3=0.0
      NLP1=NL+1
      DO 1 I=N1,NL
      X(1)=I-NL
      X(2)=NLP1-I
      DO 1 J=N1,NL
      Y(1)=J-NL
      Y(2)=NLP1-J
      DO 1 K=N1,NL
      Z(1)=K-NL
      Z(2)=NLP1-K
      DO 1 L=1,2
      DO 1 M=1,2
      DO 1 N=1,2
      SUM1=SUM1+1./((X(L)-.5)**2+(Y(M)-.5)**2+(Z(N)-.5)**2)**3
      SUM3=SUM3+1./((X(L)-.25)**2+(Y(M)-.5)**2+Z(N)**2)**3
      F=(X(L)-1.)**2+Y(M)**2+Z(N)**2
      IF(F)2,1,2
    2 SUM2=SUM2+1./(F*F*F)
      IF(SENSE SWITCH 3)3,1
    3 PRINT 4,I,J,K,SUM1,SUM2,SUM3
    1 CONTINUE
      SUM3=SUM3*6.
      SUM=SUM1+SUM2+SUM3
      SUMBC=SUM1+SUM2
      PRINT 4,I,J,K,SUM1,SUM2,SUM3,SUM,SUMBC
    4 FORMAT (4X,3H I=I4,3H J=I4,3H K=I4,5E14.8)
      CALL EXIT
      END
```

Appendix A12

A Fortran programme to compute general crystal lattice summations

For isotropic reorientation the second moment may be calculated by considering all the nuclear spins to be concentrated at their molecular centres on the lattice sites. From equation 2.15 we have:

$$\text{Second Moment} = 358.1\ N_o \sum_{i=1}^{\infty} N_i R_i^{-6}$$

For a cubic unit cell of side a the summation

$$\sum_{i=1}^{\infty} N_i R_i^{-6}$$

may be written as ka^{-6} where k is a constant for a given type of unit cell obtained by summing over all the significant lattice sites. Gutowsky and McGarvey (1952) give the values of k for the simpler crystal types such as b.c.c. and f.c.c.

The high temperature phases of cyclo-octane and cycloheptatriene crystallise in a unit cell similar to b.c.c., with the addition of two molecules on each face of the unit cell, see figure 6.2. If the central molecule of the cell is taken as the origin of co-ordinates, then the general co-ordinates of these two face molecules are .25a, .5a, 0, and there are three non-equivalent pairs per unit cell. Similarly the co-ordinates for the corner molecules of the b.c.c. are .5a, .5a, .5a, with the other central atoms at 1a, 0, 0. The

calculation of k for this type of cell then corresponds to the sum of three terms, each given by the general expression

$$\sum_{i=-N}^{+N} \sum_{j=-N}^{+N} \sum_{k=-N}^{+N} 1/((i-x)^2 + (j-y)^2 + (k-z)^2)^3$$

where x, y, z are the general co-ordinates for each type of lattice site, and $(2N)^3$ is the number of sites included in the summation.

The three sums are given by SUM1, SUM2, and SUM3. SUM2 and SUM1 + SUM2 correspond to the values of k for a simple cubic and b.c.c. respectively and so provide a useful check on the results obtained, since their values are already accurately known, (Gutowsky and McGarvey 1952, Jones and Ingham 1925).

Results obtained for k

	SUM2 (simple cubic)	SUM1 + SUM2 (b.c.c.)	SUM (cyclo-octane unit cell, Pm3n)
N = 5	8.38096	29.00513	468.47487
N = 15	8.40118	29.04424	468.63065
reference values	8.40192	29.045	-

Since the computed values were obtained by working to sixteen significant figures, and summing the smallest contributions first, the differences between the values can be ascribed to terms for N > 15. However only three significant figures were necessary in

the final answer, the other figures are included here for completeness.

```
C       CALCULATION OF EXPT SECOND MOMENT
      DIMENSION Y(78),CONT(80)
   18 READ 1,NCHART,TEMP,EMF
      READ 2,XO,YO,DMV,UMV,FMOD,UNIT,CHARL
      READ 3,(Y(J),J=1,78)
      SCALE= (UMV-DMV)*0.457*UNIT/CHARL
      HM=FMOD*0.025
      SUMD=0.0
      SUMD3=0.0
      SUMU=0.0
      SUMU3=0.0
      DO 12 J=1,78
      X=J
      H=(XO-X)*SCALE
      IF(H) 23,24,24
   23 Y(J)=-Y(J)
   24 CALJ =(Y(J)-YO)*H
      CONT(J) =CALJ*H**2
      IF (H)11,12,10
   10 SUMD =SUMD+CALJ
      SUMD3 =SUMD3+CALJ*H**2
      GO TO 12
   11 SUMU=SUMU+CALJ
      SUMU3 =SUMU3+CALJ*H**2
   12 CONTINUE
      L=XO
      KMAX=78.0-XO
      DO 13 K=1,KMAX
      JU=L+K
      JD=L-K
      IF (JD) 13,13,16
   16 CONTD=CONT(JD)/(SUMD*3.0)
      CONTU=CONT(JU)/(SUMU*3.0)
      PRINT 5,JD,Y(JD),CONTD,JU,Y(JU),CONTU
   13 CONTINUE
      SECMD=SUMD3/(SUMD*3.0)
      SECMU=SUMU3/(SUMU*3.0)
      CORRT=0.25*HM**2
      DIFF=SECMU-SECMD
      SECMO=(SUMD3+SUMU3)/(3.*SUMD+3.*SUMU)
      CSECM=SECMO-CORRT
      PRINT 1,NCHART,TEMP,EMF
      PRINT 2,XO,YO,DMV,UMV,FMOD,UNIT,CHARL
      PRINT 6,SECMD,SECMU,DIFF,SECMO,SCALE,HM
   14 PRINT 4,CSECM,CORRT
      PRINT 19
      GO TO 18
    1 FORMAT (35H1                                        ,I2,13H
     1 ,F6.1,F5.2)
    2 FORMAT (10H          ,2F6.2,5H       ,F7.2,5H       ,F7.2,10H
     1   ,F5.1,5H      ,F4.2,5H      ,F5.1)
```

Appendix A13

A Fortran programme to calculate the Experimental Second Moment from the derivative curve

This programme computes the value of the second moment according to the expression given in 3.4.2.

$$M_2 = \frac{1}{3}\frac{\sum h^3.f(h)}{\sum h.f(h)} - \frac{1}{4}h_m^2$$

where f(h) is the height of the derivative curve at a distance h (in gauss) from the centre of the curve. h_m is the modulation amplitude for the Andrew correction term.

The first card read contains the chart number NCHART, the temperature and the thermocouple e.m.f. The next card has the co-ordinates of the centre of the curve XO, YO, the limits of the field sweep DMV, UMV, the modulation amplitude FMOD, the interval between the points, and the chart length, CHARL. This is followed by six cards containing the curve height f(h) at regular field increments. The contributions for each half of the curve are summed separately and normalized, SECMD and SECMU, and their mean calculated SECMO.

The contributions for each point are printed out together with the totals for each half, the input data, and the finally corrected value of the second moment CSECM.

```
C                    APPENDIX  A14
C
      DIMENSION ANG(20,2)
      DIMENSION P(20,3),PR(20,3),DATA(20,4),H1(20,3),H2(20,3),H(200,3)
      READ 40,CHBL,LMAX,LMIN
      READ 2,(N,(DATA(N,J),J=1,4),M=2,17)
      CALL RBCXYN(2,17,P,PR,DATA)
   23 DO 5 L=12,17
      N=L-8
      IF(L-15) 16,17,17
   17 N=N+1
   16 CONTINUE
      DO 5 J=1,3
      H1(N,J)=P(L,J)
      H2(N,J)=0.0
    5 H(N-3,J)=P(L,J)
      CALL RBHXYZ(CHBL,7,P,H1,H2,ANG,1)
      DO 4 K=1,3
      H(4,K)=H1(7,K)
    4 H(8,K)=H2(7,K)
      DO 7 L=1,7
    7 CALL RBUNCH(L,P,H1,H2,4,11)
      LH=8
      CALL RBSECM(1,LH,H,SECMO,0)
      PRINT 19
      PRINT 40
      PRINT 10
      LM=LMAX-1
      PRINT 9,LMIN,LMAX,LM
      PRINT 12,(L,(DATA(L,J),J=1,3),(PR(L,J),J=1,3),L=2,11)
      PRINT 14
      PRINT 13,((H(I,J),J=1,3),I=4,8,4)
      PRINT 15,(L,(DATA(L,J),J=1,3),(PR(L,J),J=1,3),L=12,17)
      PRINT 300,SECMO,LH
      PRINT 19
    2 FORMAT (I5,4F8.3)
    9 FORMAT  (29H  ORIGIN=1   DUMMY ATOMS =1,2/16H  FIRST CARBON =I2,4H
     1 ANDI3,3X,13HLAST CARBON =I2)
   10 FORMAT(/18X,12H**********)
   12 FORMAT (/10X,10HDATA INPUT10X,7X,10HCOMPUTED  /1X,2HNO3X,4HBOND4X,
     14HBOND2X,8HDIHEDRAL5X,6HCARBON1X,11HCOORDINATES/5X,6HLENGTH3X,5HAN
     2GLE3X,5HANGLE7X,1HX6X,1HY6X,1HZ/10(/I3,F7.3,F9.2,F9.2,3X,3F7.3))
   13 FORMAT (2(/31X,3F7.3))
   14 FORMAT  (//10X,9H COMPUTED12X,21H HYDROGEN COORDINATES)
   15 FORMAT  (10(/I3,F7.3,F9.2,F9.2,3X,3F7.3))
   19 FORMAT (1H1///)
   40 FORMAT (64H
     1          F6.3,2I5)
  300 FORMAT(//2X,29HINTRA-MOLECULAR SECOND MOMENT//3X,1H=F6.2,14H GAUSS
     1*2  FOR I3 ,8H PROTONS)
   21 CALL EXIT
      END
```

Appendix A14

A Fortran Programme to compute the atomic co-ordinates and second moment for cycloheptatriene C_7H_8

This programme is similar to A1 and illustrates the adaptability of the subroutines A2, A3 and A4 for molecules other than the cycloalkane series. Since there is only one methylene group in cycloheptatriene the subroutine REHXYZ (A3), can only be used for the co-ordinates of this pair of hydrogens. The subroutine RBCXYN is employed to calculate the co-ordinates of the other lone hydrogens as well as the ring carbons as described in A2. The necessary bond angles and dihedral angles for the latter subroutine are read into the array DATA(N,J) with the carbons labelled from N = 4 to 10, and the lone hydrogens from 12 to 17, see table 7.2. As with programme A1, the intra-molecular second moment is computed by the subroutine RBSECM (A4), and the effect of reorientation about appropriate axes was obtained using A5.

APPENDIX A15

```
      SUBROUTINE RBUNCH(K,P,H1,H2,LMIN,LMAX)
      DIMENSION P(20,3),H1(20,3),H2(20,3)
      RADC=0.25
      RADH=0.15
      K1=K+1
      IF (K-LMAX+LMIN) 6,7,6
    7 K1=1
    6 K2=K-1
      IF(K2) 4,5,4
    5 K2=LMAX-LMIN
    4 L=K+LMIN-1
      IF (H2(L,1)+H2(L,2)+H2(L,3)) 13,14,13
   13 PUNCH 1,K,(P(L,J),J=1,3),RADC,K1,K2,K,K
      PUNCH 2,K,(H1(L,J),J=1,3),RADH,K
      PUNCH 3,K,(H2(L,J),J=1,3),RADH,K
      GO TO 16
   14 PUNCH 15,K,(P(L,J),J=1,3),RADC,K1,K2,K
      PUNCH 2,K,(H1(L,J),J=1,3),RADH,K
   15 FORMAT(1HCI1,2X,3F8.4,F5.2,3H  CI1,3H  CI1,3H HAI1)
    1 FORMAT(1HCI1,2X,3F8.4,F5.2,3H  CI1,3H  CI1,3H HAI1,3H HBI1)
    2 FORMAT (2HHAI1,1X,3F8.4,F5.2,3H  CI1)
    3 FORMAT (2HHBI1,1X,3F8.4,F5.2,3H  CI1)
   16 RETURN
      END
```

APPENDIX A16

```
      SUBROUTINE RBROND(N,K,R1,R2,R3,RN1,RN2,RN3)
      DIMENSION R(3),RN(3)
      R(1) =R1
      R(2) =R2
      R(3)=R3
      DO 1 I=1,N
      IF (R(I)) 2,3,3
    2 IR=R(I)*10.**K-.55555
      GO TO 4
    3 IR=R(I)*10.**K+.55555
    4 RR=IR
    1 RN(I)=RR/10.**K
      RN1=RN(1)
      RN2=RN(2)
      RN3=RN(3)
      RETURN
      END
```

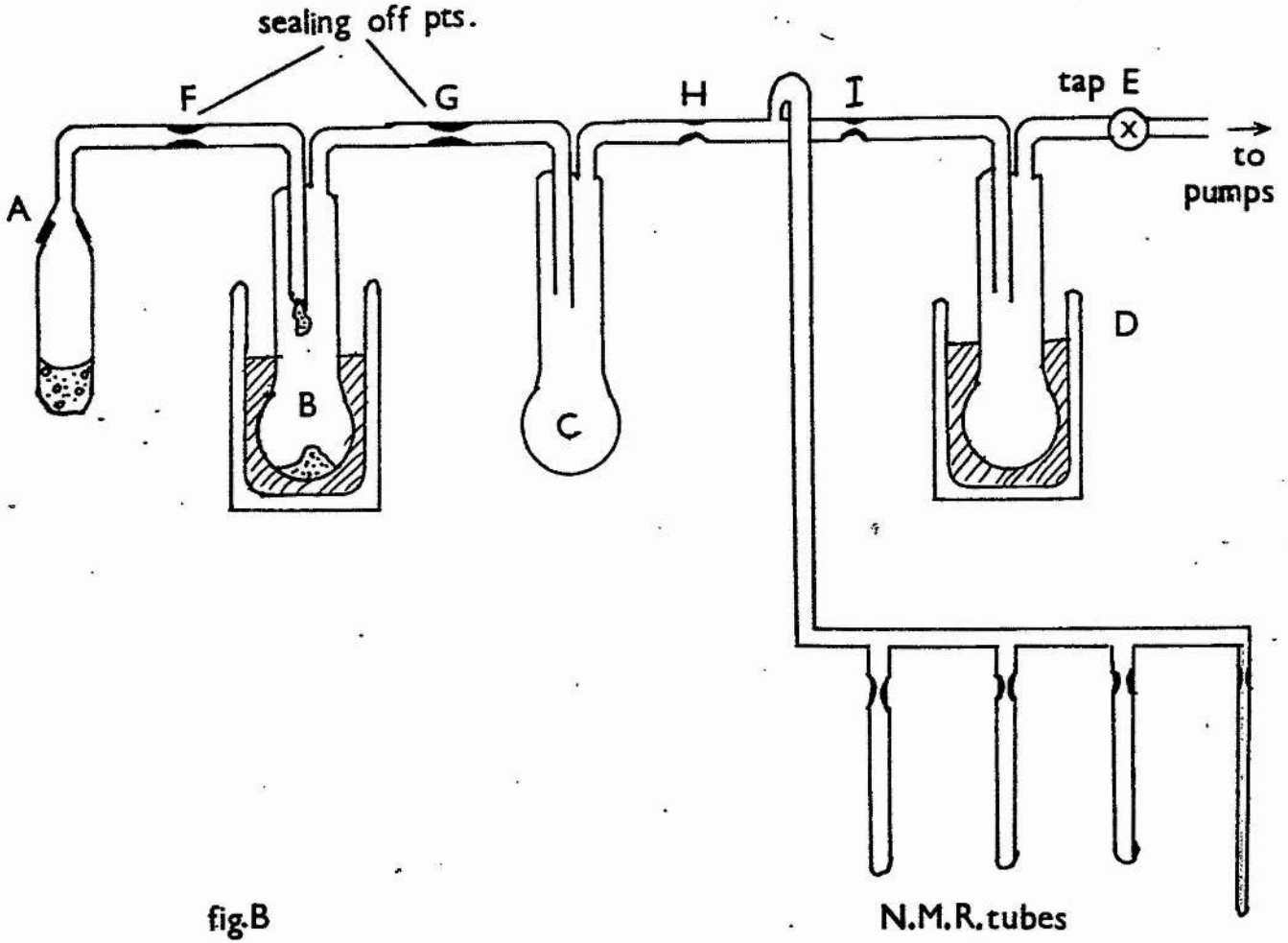

fig.B

Appendix B

Freeze-pump-thaw sample preparation to remove dissolved oxygen.

The glass system in figure B was assembled and a blank sample tube was fitted to the greased ground glass joint at A. Tap E to the mercury diffusion pump was opened and the entire system was evacuated and torched until a steady pressure of 10^{-5} m.m. Hg was indicated on a Penning gauge. Tap E was then closed, a flexible tape heater wrapped around the glassware, and the system baked overnight. In the morning tap E was re-opened and the system was again pumped to less than 10^{-5} m.m. Hg, and all the sealing off joints and sample tubes carefully torched.

With tap E once more closed, the blank sample tube was quickly exchanged for one containing about 10 c.c.'s of the sample to be bottled. Liquid nitrogen was placed around trap D, and shortly afterwards also around the sample. Tap E was now opened and the system was once more pumped. Liquid nitrogen was placed around B, and the sample was then slowly allowed to reach room temperature, evaporating over into trap B in the process. Strong fluctuations in pressure indicated copious effusion of dissolved gases; these had passed out of the system through trap D. The last fraction of the sample was left behind, and seal F was made.

At this stage the system is free of greased joints, which was considered important because of possible sample contamination. The transfer process was now repeated for trap C, and again the last fraction

was discarded by sealing off at G. Very little gas effusion was indicated for this transfer, and it was easy to maintain an indicated pressure of 10^{-4} m.m. Hg on the vacuum gauge.

Careful adjustment of the liquid nitrogen dewar levels enabled these transfers to take place with neither blocking of the narrow tubes, nor undue loss of the sample to trap D. The portion of the sample collected in trap C was now allowed to warm to a liquid state, and then refrozen, with no indication of gas effusion. Seal I was now made.

A portion of the remaining sample was then transferred by a similar process to each of the N.M.R. sample tubes, which were sealed off in turn.

Appendix C

Purification of Cycloheptane by Gas Chromatography

The sample of Cycloheptane was bought from Shell Thornton Research Centre. A purity check by gas chromatography revealed three detectable impurities, the largest of which gave a peak area of approximately 0.1 percent of the main material, on a flame detector chart output.

The reasonable separations of the impurity peaks from the Cycloheptane peak suggested that a purification attempt by gas chromatography might be successful. This was performed using a Wilkens Autoprep. A column of 15 percent Carbo wax 400, on an 80 to 100 mesh silo cell was used, and 0.6 c.c. of the sample was injected each time and collected over ice. The material corresponding to the impurity peaks was discarded for each injection.

A total of approximately 5 c.c.'s of the purified sample was collected. The impurity peaks for this material were now less than 0.04 percent. A 60 Mc/s high resolution nuclear magnetic resonance spectrum of this material showed no detectable impurity bands.

Appendix D

Calculation of the time constant of an exponential recovery curve by the method of Mangelsdorf (1959)

The exponential recovery of the longitudinal magnetization $M_z(t)$ from a saturation radio frequency pulse is described by the equation

$$M_z(t) = M_o \ (1 - \exp(-t/T_1))$$

where M_o is the equilibrium magnetization. The usual procedure adopted for the calculation of T_1 from a recovery curve of this form, is to measure $M_z(t)$ for a sufficiently long time ($t > 5T_1$) so that $M_z(t) \doteq M_o$, and then to plot the quantity $(M_o - M_z(t))$ against time on a semi-log graph and obtain the time constant of the recovery T_1 from the slope.

Mangelsdorf (1959) has suggested a procedure to obtain the time constant T_1 without prior knowledge of M_o. This has a great advantage for both the experimental methods employed to measure T_1. For very long T_1 values with the direct recovery method, the time necessary to wait for the condition $t > 5T_1$ is prohibitive. Similarly for the storage oscilloscope technique, where the width of the oscilloscope screen (8 cms) would make it necessary to have the sweep speed set very slow to ensure that $M_z(t) \doteq M_o$ by the end of the trace, and at the same time cause the major part of the exponential recovery to be recorded in the first 2 or 3 cms of the screen only.

Essentially the procedure suggested by Mangelsdorf consists of

a linear graph of alternate peak heights measured at a regular time interval τ, plotted one against the other. The value of T_1 is then obtained from the slope of the plot as shown in the following analysis.

At time t we have $M_z(t) = M_o(1 - \exp.(-t/T_1))$ 1.

and time $t + \tau$ $M_z(t + \tau) = M_o(1 - \exp.(-(t + \tau)/T_1))$ 2.

and upon rearranging and dividing 1. by 2. we obtain

$$M(t) = M(t + \tau)\exp(\tau/T_1) + M_o(1 - \exp(\tau/T_1))$$

so that a linear plot of $M(t)$ against $M(t + \tau)$ has a slope of $\exp(\tau/T_1)$. The value of τ was usually chosen to be of the order of T_1.

Another advantage of this method is that it requires only a linear graph plot, and the determination of one exponential to obtain a value for T_1, a useful point for quick calculation in the laboratory. The actual values of T_1 used in the analysis of the results were calculated by a computer least squares programme, in which both the variables were assumed to have equal errors, i.e. the perpendicular distance of the points to the line was minimised.

For the direct recovery method about 15 points were usually taken for each T_1, and an error of about 1% was found for the value of the slope, giving an error of about 10% in the value of T_1. Similarly for the storage oscilloscope technique, the slope error was about 3% giving an error of about 7% in T_1.

REFERENCES

Abragam, A. (1961) The Principles of Nuclear Magnetism (O.U.P.)

Ailion, D. C. and Slichter, C. P. (1965) Phys. Rev. 137 A235

Allerhand, A. and Gutowsky, H. S. (1964) J. Chem. Phys. 41 2115

Almenningen, A., Bastiansen, O. and Jensen, H. (1966) Acta Chem. Scand. 20 2689

Anet, F. A. L. and Hartman, J. S. (1963) J. Am. Chem. Soc. 85 1205

Anet, F. A. L. (1964) J. Am. Chem. Soc. 86 458

Anet, F. A. L. and Haq, M. Z. (1965) J. Am. Chem. Soc. 87 3147

Anet, F. A. L. and Jacques, M. (1966) J. Am. Chem. Soc. 88 2585

Anderson, H. L. (1949) Phys. Rev. 76 1460

Anderson, J. E., Steele, J. and Warnick, A. (1967) Rev. Sci. Inst. 38 1139

Andrew, E. R. (1950) J. Chem. Phys. 18 607

Andrew, E. R. and Bersohn, R. (1950) J. Chem. Phys. 18 159; 20 924

Andrew, E. R. and Eades, R. G. (1953) Proc. Roy. Soc. A216 398

Andrew, E. R. and Eades, R. G. (1953) Proc. Roy. Soc. A218 537

Andrew, E. R. (1955) Nuclear Magnetic Resonance, Cambridge Univ. Press

Andrew, E. R. and Rushworth, F. A. (1955) Electrical J. 155 1344

Andrew, E. R. and Finch, N. D. (1957) Proc. Phys. Soc. 70 980

Andrew, E. R., Bradbury, A. and Eades, R. G. (1958) Nature 182 1659

Andrew, E. R., Swanson, K. M. and Williams, B. R. (1961) Proc. Phys. Soc. 77 36

Andrew, E. R. and Tunstall, D. P. (1963) Proc. Phys. Soc. 81 986

Bellis, H. E. and Slowinski, E. J. (1959) Spectrochim. Acta 12 1103

Bersohn, R. and Gutowsky, H. S. (1954) J. Chem. Phys. 22 651

Bloembergen, N., Purcell, E. M. and Pound, R. V. (1948) Phys. Rev. 73 679

Butcher, S. S. (1965) J. Chem. Phys. 42 1833

Clough, S. (1968) Proc. Phys. Soc. Ser. 2 1 265

Darmon, I. and Brot, C. (1967) Mol. Cryst. 2 301

Das, T. P. (1957) J. Chem. Phys. 27 763

Deeley, C. M. and Richards, R. E. (1954) Trans. Farad. Soc. 50 560

Dimitrieva, L. V. and Moskalev, V. V. (1964) Soviet Phys. Solid State 5 1623

Eades, R. G. (1953) Thesis St. Andrews University

Eliel, Allinger, Angyal and Morrison (1965) Conformational Analysis (Interscience)

Evans, M. V. and Lord, R. C. (1960) J. Am. Chem. Soc. 82 1876

Finke, Scott, Gross, Messerly and Waddington (1956) J. Am. Chem. Soc. 78 5469

Frenkel, J. (1935) Acta Physica Chimica 555 R, 3 No. 123

Gheorghiu, D. and Valeriu, A. (1962) Nuclear Inst. and Methods 16 313

Gutowsky, H. S. and Pake, G. E. (1950) J. Chem. Phys. 18 162

Gutowsky, H. S. and McGarvey, B. R. (1952) J. Chem. Phys. 20 1472

Hansen, J. W., Grimes, C. C. and Libchaber, A. (1967) Rev. Sci. Inst. 38 895

Hendrickson, J. B. (1961) J. Am. Chem. Soc. 83 4537

Hendrickson, J. B. (1964) J. Am. Chem. Soc. 86 4854

Herzfeld, C. M. (1962) Temperature Vol. 3 Part 2, Reinhold

Hoch, M. J. R. (1963) Thesis St. Andrews University

Hoch, M. J. R. and Rushworth, F. A. (1964) Proc. Phys. Soc. 83 949

Hood, G. M. and Sherwood, J. N. (1966) J. Chim. Phys. 63 121

Itoh, Kusaka, Yamagata, Kiriyama and Ibamoto (1952) J. Chem. Phys. 20 1503

Jensen, F. R. and Smith, L. A. (1964) J. Am. Chem. Soc. 86 956

Kubo, R. and Tomita, K. (1954) J. Phys. Soc. Japan 9 888

Lau, C. and Ruyter, H. (1963) Spectrochim. Acta 19 1559

Lawrenson, I. J. and Rushworth, F. A. (1958a) Nature 182 391

Lawrenson, I. J. and Rushworth, F. A. (1958b) Proc. Phys. Soc. 72 791

Mangelsdorf, P. C. (1959) J. Appl. Phys. 30 443

McCullough, J. P. (1961) Pure and Appl. Chem. 2 221

Pake, G. E. (1948) J. Chem. Phys. 16 327

Pake, G. E. (1956) Solid State Physics 2 1

Read, P. L. (1963) Vacuum 13 271

Redfield, A. G. (1955) Phys. Rev. 98 1787

Reed, T. B. and Lipscomb, W. N. (1953) Acta Cryst. 6 108

Resing, H. A., Corke, N. T. and Sherwood, J. N. (1968) Phys. Rev. Lett. 20 1227

Richards, R. E. and White, J. W. (1964) Proc. Roy. Soc. A.279 474

Roberts, J. D. (1966) Chemistry in Britain December 529

Robinson, F. N. H. (1962) Noise in Electrical Circuits (O.U.P.)

Rushworth, F. A. (1954) Proc. Roy. Soc. A.222 526

Rudman, R. and Post, B. (1968) Mol. Cryst. 3 325

Sands, D. E. and Day, W. V. (1965) Acta Cryst. 19 278

Sandu, H. S., Lees, J. and Bloom, M. (1960) Can. J. Chem. 38 493

Slichter, C. P. (1964) Principles of Magnetic Resonance, Harper and Row

Smith, W. G. (1965) J. Chem. Phys. 42 4229

Solomon, I. (1955) Phys. Rev. 99 559

Thompson, H. B. (1967) J. Chem. Phys. 47 3407

Van Vleck, J. H. (1948) Phys. Rev. 74 1168

Verschingel, R. and Schiff, H. I. (1954) J. Chem. Phys. 22 723
Waugh and Fedin (1963) Soviet Phys. Solid State 4 1633
Waugh, Humphrey and Yost (1953) J. Chem. Phys. 57 486

Wiberg, K. B. (1965) J. Am. Chem. Soc. 87 1070

Woodhams, F. W. D., Carlow, J. S. and Meads, R. E. (1966) J. Sci. Instrum. 43 333